Supporting Information for

No-wash fluorogenic labeling of proteins for reversible photoswitching in live cells

Kenji Torii,[a] Sam Benson,[b,c] Yuichiro Hori,*[d] Marc Vendrell,*[b,c] and Kazuya Kikuchi*[a,e]

[a]*Graduate School of Engineering, Osaka University, Suita, Osaka 565-0871, Japan*

[b]*Centre for Inflammation Research, The University of Edinburgh, Edinburgh EH16 4UU, UK*

[c]*IRR Chemistry Hub, Institute for Regeneration and Repair, The University of Edinburgh, Edinburgh EH16 4UU, UK*

[d]*Faculty of Science, Kyushu University, Fukuoka, Fukuoka 819-0395, Japan*

[e]*Immunology Frontier Research Center, Osaka University, Suita, Osaka 565-0871, Japan*

*To whom correspondence should be addressed.

E mails: hori@chem.kyushu-univ.jp, marc.vendrell@ed.ac.uk and kkikuchi@mls.eng.osaka-u.ac.jp

Contents

1. Experimental Methods **2**
2. Supporting Figures **13**
3. Supporting Tables **35**
4. Synthetic Schemes **37**
5. Synthetic Procedures **39**
6. NMR spectra **54**
7. References **90**

1. Experimental Methods

1-1. Materials and instruments

All chemical reagents for the synthesis were purchased from Tokyo Chemical Industries Co., Ltd. (Tokyo, Japan), Wako Pure Chemical Corp. (Osaka, Japan), or Sigma-Aldrich Chemicals Pvt., Ltd. (St. Louis, MO, USA) and used as received. Thin-layer chromatography (TLC) was performed to judge the reaction completion using aluminum 60F254 silica gel sheets (Merck Co., Inc., Kenilworth, NJ, USA). The microwave reactions were completed using a microwave synthesizer (Initiator; Biotage). The purification and purity analysis of Trp-BODIPY, Trp-BODIPY-FF, and HTL-Trp-BODIPY-FF were carried out using a high-performance liquid chromatography (HPLC) system composed of a reversed-phase column (Inertsil ODS-3, 250 × 10 mm (for semi-prep), 250 × 4.6 mm (for analysis); GL Sciences, Inc., Tokyo, Japan), a detector (MD-4010; JASCO Corp., Tokyo, Japan), and a pump (PU-2080; JASCO Corp.). For HPLC analysis, samples were eluted through a column with a linear gradient of acetonitrile/water containing 0.1% formic acid. ^{1}H (500 MHz) and ^{13}C (125 MHz) nuclear magnetic resonance (NMR) spectroscopic data were recorded and analyzed using an AVANCE III HD 500 (Bruker Corp., Billerica, MA, USA) with a software (TopSpin 4.3.0; Bruker Corp.). Mass spectra (MS) were collected using an electrospray ionization (ESI) (LCT-Premier XE; Waters Corp., Milford, MA, USA), a fast atom bombardment (FAB), a electron ionization (JMS-700; JOEL Ltd., Tokyo, Japan), or a matrix assisted laser desorption ionization (MALDI) spectrometry (JMS-S300; JOEL Ltd.). Absorption and fluorescence spectroscopic data were recorded on a V-650 (JASCO Corp.) and an F-4500 spectrometer (Hitachi High-Tech Science Corp., Tokyo, Japan).

1-2. Light irradiation setup for in vitro analysis

Light irradiation of samples in a cuvette was conducted by a home-built system using a MAX-302 xenon light source (Asahi Spectra Co., Ltd., Tokyo, Japan) equipped with two band-pass filters LX0365 (Asahi Spectra Co., Ltd.) for 365 nm irradiation and LX0530 (Asahi Spectra Co., Ltd.) for 530 nm irradiation. The light was irradiated to the orthogonal side of the cuvette from the detector in the V-650 or F-4500 spectrometer. The concentration of Trp-BODIPY-FF or HTL-Trp-BODIPY-FF was optimized at 10 μM to obtain absorption spectra and extinction coefficients and at 1.0 μM to obtain fluorescence spectra and intensities. Each spectroscopic data was recorded in 100 mM phosphate buffer (pH 7.4), *n*-octanol and glycerol containing 1% dimethyl sulfoxide (DMSO) at 37 °C. The photoswitching performance of Trp-BODIPY-FF including 5.0 eq. BSA, or HTL-Trp-BODIPY-FF with 2.0 eq. Halo-tag (previously incubated for 20 minutes at 37 °C to complete labeling) were also evaluated in this system.

1-3. Measurement of fluorescence quantum yields and brightness of Trp-BODIPY, Trp-BODIPY-FF, and HTL-Trp-BODIPY-FF

Fluorescence quantum yields of Trp-BODIPY, Trp-BODIPY-FF, and HTL-Trp-BODIPY-FF were measured in 100 mM phosphate buffer (pH 7.4), *n*-octanol, and glycerol containing 1% DMSO at 37 °C. Fluorescence quantum yields of Trp-BODIPY and Trp-BODIPY-FF in 100 mM phosphate buffer (pH 7.4) including 5 μM BSA were also measured. The fluorescence quantum yield of Halo-tag binding HTL-Trp-BODIPY-FF was measured by incubating with a 2 μM

Halo tag at 37 °C for 20 min beforehand. We selected fluorescein in basic ethanol (Φ_{ref}= 0.92[S1]) as a reference. Fluorescence measurements were performed at 470 nm excitation. Fluorescence quantum yields (Φ_{FL}) were determined following Eq. 1.

$$\Phi_{FL} = \Phi_{ref}\frac{A_{ref}F_s n_s^2}{A_s F_{ref} n_{ref}^2}$$

Equation 1

Here, A_s and A_{ref} are the absorbances at the excitation wavelength, F_s and F_{ref} are the relative fluorescence intensities, and n_s and n_{ref} are the solvent refractive indices of the sample and reference, respectively. Brightness is calculated as the product of the fluorescence quantum yield (Φ_{FL}) and extinction coefficient at the maximum absorption wavelength (ε_{max}) (Eq. 2).

Brightness = $\Phi_{FL} \times \varepsilon_{max}$ [$M^{-1}cm^{-1}$]

Equation 2

1-4. Determination of photon flux

For determining photoconversion quantum yields and kinetics of FF, Trp-BODIPY-FF, and HTL-Trp-BODIPY-FF in various conditions, we used 4,4'-dimethylazobenzene in acetonitrile and Aberchrome 540 in toluene as chemical actinometers. The photon flux at 365 nm was determined from the *E*-to-*Z* photoisomerization kinetics of 1,4-dimethyl azobenzene at 365 nm irradiation following a previous report (see ref. S2). The photon flux at 530 nm was determined from the cycloreversion reaction kinetics of Aberchrome 540 at 530 nm irradiation following our previous report[S3].

1-5. Determination of photoconversion quantum yield

To measure the photoconversion quantum yield, the time courses of absorption change of 50 μM FF (at 530 nm), 10 μM Trp-BODIPY-FF (at 550 nm), and 10 μM HTL-Trp-BODIPY-FF (at 550 nm) in each condition (described in Experimental Methods 1-2) upon 365 or 530 nm photoirradiation were recorded as seen in Figure S1, S5, and S11. Judging from these results of measurement, both the cyclization and cycloreversion reactions of FF, Trp-BODIPY-FF, and HTL-Trp-BODIPY-FF proceed by first-order kinetics. The cyclization reaction rate constants (k_{oc}) and the cycloreversion reaction rate constants (k_{co}) were determined by following Eq. 3 and 4, respectively.

$$A(t) = A_{PSS\ at\ 530\ nm} - (A_{PSS\ at\ 365\ nm} - A_{PSS\ at\ 530\ nm})\exp(-k_{oc}t)\ [s^{-1}]$$

Fquation 3

$$A(t) = A_{PSS\ at\ 365\ nm} - (A_{PSS\ at\ 530\ nm} - A_{PSS\ at\ 365\ nm})\exp(-k_{co}t)\ [s^{-1}]$$

Equation 4

The $A(t)$ is recorded absorbance at 530 nm (FF) and 550 nm (Trp-BODIPY-FF and HTL-Trp-BODIPY-FF). $A_{PSS\ at\ 365\ nm}$ and $A_{PSS\ at\ 530\ nm}$ is the absorbance in the photostationary state at 365 and 530 nm, respectively. The value of $A_{PSS\ at\ 365\ nm}$, $A_{PSS\ at\ 530\ nm}$, k_{oc} and k_{co} was approximated from the collected data of $A(t)$.

In principle, the cyclization and cycloreversion reaction rate are defined as following Fq. 5 and 6, respectively.

$$\frac{\mathrm{d[O]}}{\mathrm{d}t} = -\frac{\phi_{\mathrm{oc}} q_{\lambda_i}}{V} \frac{\varepsilon_{\mathrm{o},\lambda_i}[\mathrm{O}] f}{\varepsilon_{\mathrm{c},\lambda_i}[\mathrm{C}] + \varepsilon_{\mathrm{o},\lambda_i}[\mathrm{O}]} + \frac{\phi_{\mathrm{co}} q_{\lambda_i}}{V} \frac{\varepsilon_{\mathrm{c},\lambda_i}[\mathrm{C}] f}{\varepsilon_{\mathrm{c},\lambda_i}[\mathrm{C}] + \varepsilon_{\mathrm{o},\lambda_i}[\mathrm{O}]}$$

Equation 5

$$\frac{\mathrm{d[C]}}{\mathrm{d}t} = -\frac{\phi_{\mathrm{co}} q_0}{V} \frac{\varepsilon_{\mathrm{c},\lambda_i}[\mathrm{C}] f}{\varepsilon_{\mathrm{c},\lambda_i}[\mathrm{C}] + \varepsilon_{\mathrm{o},\lambda_i}[\mathrm{O}]} + \frac{\phi_{\mathrm{oc}} q_0}{V} \frac{\varepsilon_{\mathrm{o},\lambda_i}[\mathrm{O}] f}{\varepsilon_{\mathrm{c},\lambda_i}[\mathrm{C}] + \varepsilon_{\mathrm{o},\lambda_i}[\mathrm{O}]}$$

Equation 6

Here, [C], [O], ϕ_{co}, ϕ_{oc}, q_{λ_i}, V, and ε_{λ_i} are the concentration of the closed-ring and open-ring form, cyclization and cycloreversion reaction quantum yield, photon flux determined using chemical actinometers, the sample volume, and the molar absorption coefficient at the irradiation wavelength (λ_i =365 and 530 nm). f is a fraction of light absorbed by a sample, estimated from the absorbance at 365 and 530 nm (Eq. 7).

$$f = 1 - 10^{-(\varepsilon_{\mathrm{c},\lambda_i}[\mathrm{C}] + \varepsilon_{\mathrm{o},\lambda_i}[\mathrm{O}])l}$$

Equation 7

In the initial stage of the cyclozation reaction, when the absorbance of the closed-ring form is 20 times lower than that of the open-ring form (Eq. 8), Equation 5 and 7 can be reduced and convened in Eq. 9.

$$\varepsilon_{\mathrm{o},\lambda_i}[\mathrm{O}] \geq 20\varepsilon_{\mathrm{c},\lambda_i}[\mathrm{C}]$$

Equation 8

$$\frac{\mathrm{d[O]}}{\mathrm{d}t} = -\frac{\phi_{\mathrm{oc}} q_{\lambda_i}}{V}(1 - 10^{-\varepsilon_{\mathrm{o},\lambda_i}[\mathrm{O}]l})$$

Equation 9

The integral of Eq .9 gives Eq. 10.

$$\ln\left(10^{\varepsilon_{\mathrm{o},\lambda_i}[\mathrm{O}]l} - 1\right) = \ln\left(10^{\varepsilon_{\mathrm{o},\lambda_i}[\mathrm{O}]_0 l} - 1\right) - \frac{\phi_{\mathrm{oc}} q_{\lambda_i} \varepsilon_{\mathrm{o},\lambda_i} l \ln 10}{V} t$$

Equation 10

Following Lambert-Beer equation, Eq. 11 is described.

$$\ln\left(10^{A_{\lambda_i}(t)} - 1\right) = \ln\left(10^{A_{\lambda_i}(0)} - 1\right) - \frac{\phi_{\mathrm{oc}} q_{\lambda_i} \varepsilon_{\mathrm{o},\lambda_i} l \ln 10}{V} t$$

Equation 11

Since the cyclization reaction follows the first-order kinetics (Eq. 3), $A_{\lambda_i}(t)$ are calculated following Eq. 12.

$$A_{\lambda_i}(t) = A_{\lambda_i}(\infty) - (A_{\lambda_i}(\infty) - A_{\lambda_i}(0)) \exp(-k_{\mathrm{oc}} t)$$

Equation 12

Here, $A_{\lambda_i}(\infty)$ and $A_{\lambda_i}(0)$ is the absorbance at λ_i =365 nm in the photostationary state at 365 and 530 nm, respectively. Here, the linear relation between $\ln\left(10^{A_{\lambda_i}(t)} - 1\right)$ and t provides the slope m and determines the quantum yield for the cyclization reaction.

$$\phi_{\mathrm{oc}} = -\frac{mV}{q_{\lambda_i} \varepsilon_{\mathrm{o},\lambda_i} l \ln 10}$$

Equation 13

In the initial stage of the cycloreversion reaction, when the absorbance of the open-ring form is 20 times lower than that of the closed-ring form (Eq. 14), Equation 6 and 7 can be reduced and convened in Eq. 15.

$$\varepsilon_{c,\lambda_i}[C] \geq 20\varepsilon_{o,\lambda_i}[O]$$

Equation 14

$$\frac{d[C]}{dt} = -\frac{\phi_{co} q_{\lambda_i}}{V}(1 - 10^{-\varepsilon_{c,\lambda_i}[C]l})$$

Equation 15

The integral of Eq.15 gives Eq. 16.

$$\ln\left(10^{-\varepsilon_{c,\lambda_i}[C]l} - 1\right) = \ln\left(10^{-\varepsilon_{c,\lambda_i}[C]_0 l} - 1\right) - \frac{\phi_{co} q_{\lambda_i} \varepsilon_{c,\lambda_i} l \ln 10}{V} t$$

Equation 16

Following Lambert-Beer equation, Eq. 17 is described.

$$\ln\left(10^{A_{\lambda_i}(t)} - 1\right) = \ln\left(10^{A_{\lambda_i}(0)} - 1\right) - \frac{\phi_{co} q_{\lambda_i} \varepsilon_{c,\lambda_i} l \ln 10}{V} t$$

Equation 17

Since the cycloreversion reaction follows the first-order kinetics (Eq. 4), $A_{\lambda_i}(t)$ are measured or calculated following Eq. 18.

$$A_{\lambda_i}(t) = A_{\lambda_i}(\infty) - (A_{\lambda_i}(\infty) - A_{\lambda_i}(0)) \exp(-k_{co} t)$$

Equation 18

Here, $A_{\lambda_i}(\infty)$ and $A_{\lambda_i}(0)$ is the absorbance at λ_i =530 nm in the photostationary state at 365 and 530 nm, respectively. Here, the linear relation between $\ln\left(10^{A_{\lambda_i}(t)} - 1\right)$ and t provides the slope m and determines the quantum yield for the cycloreversion reaction.

$$\phi_{co} = -\frac{mV}{q_{\lambda_i} \varepsilon_{c,\lambda_i} l \ln 10}$$

Equation 19

1-6. Quenching efficiency calculation

We have quantified the quenching efficiency of 1.0 μM Trp-BODIPY-FF and 1.0 μM HTL-Trp-BODIPY-FF in 100 mM phosphate buffer (pH 7.4) (PB), glycerol, *n*-octanol, PB including 5.0 μM BSA (for Trp-BODIPY-FF), and PB including 2 μM Halo-tag (for HTL-Trp-BODIPY-FF) using following Eq. 20.

$$\text{Quenching efficiency, } E(n) = \frac{I_{Fl,on}(n) - I_{Fl,off}(n)}{I_{Fl,on}(n)}$$

Equation 20

Here, $I_{Fl,on}(n)$ and $I_{Fl,off}(n)$ are the fluorescence intensity before and after the nth 365 nm irradiation.

1-7. Preparation of Trp-BODIPY-FF-BSA bioconjugate

A solution of Trp-BODIPY-FF (10 mM) in DMSO (2 μL) was added to 200 mM 2-(*N*-morpholino)ethanesulfonic acid (MES) buffer (pH 6.0) (200 μL) containing *N*-hydroxysulfosuccinimide sodium salt (50 mM) and 1-ethyl-3-(3-dimethylaminopropyl)-carbodiimide hydrochloride (5 mM) and shook vigorously at 25 °C for 1 h. The mixture was then incubated with BSA (A0281; Sigma-Aldrich Chemicals Pvt., Ltd.) (10 μM) in MES buffer (pH 6.0) (200 μL) at 37 °C for 1 h. Unconjugated Trp-BODIPY-FF was excluded using Nanosep® centrifugal devices with an Omega™ membrane 30 K (OD030C34; Pall Corp., Port Washington, NY, USA). After ultrafiltration, the conjugates were dissolved in 100 mM phosphate buffer (pH 7.4) (200 μL). An aliquot of the solution (10 μL) was added to the loading buffer including 100 mM dithiothreitol (10 μL), heated at 103 °C for 3 min, and subsequently analyzed using sodium dodecyl sulfate-polyacrylamide gel electrophoresis (SDS-PAGE). The molecular marker (Precision Plus Protein Unstained Standards; BioRad Laboratories, Inc., Hercules, CA, USA) was also loaded onto the same gel plate. After the fluorescent gel images were obtained using a Typhoon FLA 9500 (GE Healthcare, Chicago, IL, USA), the gel was stained with Coomassie Brilliant Blue. The BSA concentration was determined using the Bradford assay on a multilabel counter (ARVOTM MX; PerkinElmer, Waltham, MA, USA) with BSA as a standard reagent.

1-8. Analysis of the affinity of Trp-BODIPY-FF and HTL-Trp-BODIPY-FF with BSA

Scatchard plot for Trp-BODIPY-FF and HTL-Trp-BODIPY-FF vs BSA in 100 mM phosphate buffer is analyzed from the fluorescence intensities with increasing the concentration of BSA ($[\mathrm{BSA}]_0$) varied from 0 to 2000 μM. The concentrations of the BSA-probe complex (x) were estimated from the fluorescent intensity at 520 nm using Eq. 21. The value of *n* represents the binding ratio of the probe to BSA. In the Scatchard plot, we estimate $n = 1$. The probe concentration ($[\mathrm{probe}]_0$) is fixed at 1.0 μM. F is the fluorescence intensity at 520 nm of probe containing BSA of each concentration. F_{max} is the approximated maximum fluorescence intensity at 520 nm of probe using the quadratic equation (Eq. 22) which is derived from Eq. 23. F_{min} was defined as to be 1. Both plots do not give a proper linear approximation, and show a downward convex-like curve, suggesting the presence of multiple different binding sites.

$$x = \frac{[\mathrm{probe}]_0}{n}\frac{F - F_{\mathrm{min}}}{F_{\mathrm{max}} - F_{\mathrm{min}}}$$

Equation 21

$$F = F_{\mathrm{min}} + \frac{F_{\mathrm{max}} - F_{\mathrm{min}}}{2[\mathrm{probe}]_0}\left(([\mathrm{probe}]_0 + [\mathrm{BSA}]_0 + K_{\mathrm{D}}) - \sqrt{([\mathrm{probe}]_0 + [\mathrm{BSA}]_0 + K_{\mathrm{D}})^2 - 4n[\mathrm{probe}]_0[\mathrm{BSA}]_0}\right)$$

Equation 22

$$x = \frac{([\mathrm{probe}]_0 + [\mathrm{BSA}]_0 + K_{\mathrm{D}}) - \sqrt{([\mathrm{probe}]_0 + [\mathrm{BSA}]_0 + K_{\mathrm{D}})^2 - 4[\mathrm{probe}]_0[\mathrm{BSA}]_0}}{2}$$

Equation 23

Although the dissociation constant (K_{D}) was also approximated by Eq. 22, we have determined K_{D} using the modified Hill plot. When the binding ratio is unknown, the Hill plot is more appropriate because Eq. 22 assumes that the binding ratio of the probe to BSA (n) is 1 (Eq. 24).

$$K_{\mathrm{D}} = \frac{([\mathrm{probe}] - x)([\mathrm{BSA}] - x)}{x}$$

Equation 24

Job's plot for Trp-BODIPY-FF and HTL-Trp-BODIPY-FF vs BSA in 100 mM phosphate buffer (pH 7.4) was analyzed by monitoring the fluorescence intensity at 520 nm. The concentration of the probe varied from 100 to 900 nM as the BSA concentration decreased from 900 to 100 nM. Both Job's plots exhibited maximum mole fractions $[\mathrm{probe}]_0/([\mathrm{probe}]_0+[\mathrm{BSA}]_0)$) around 0.70 (Trp-BODIPY-FF) and 0.64 (HTL-Trp-BODIPY-FF), implicating that the binding ratio of the probe to BSA is 2. To analyze the affinity with BSA, we measured the fluorescence intensity of both probes (1.0 μM) in 100 mM phosphate buffer (pH 7.4) containing varying concentrations of BSA (from 1 to 100 μM). When the binding ratio is unknown, the dissociation constant (K_{D}) was defined as Equation 25.

$$K_{\mathrm{D}} = \frac{[\mathrm{probe}]^n[\mathrm{BSA}]}{x}$$

Equation 25

Herein, the [probe] and [BSA] are the concentration of probe and BSA at equilibrium. The value of *n* represents the binding ratio of the probe to BSA (equivalent to Hill coefficient). Eq. 26 is provided by taking the logarithm of Eq. 25.

$$\log\frac{1}{[\mathrm{probe}]} = \frac{1}{n}\log\frac{[\mathrm{BSA}]}{x} - \frac{1}{n}\log K_{\mathrm{D}}$$

Equation 26

The initial concentration of the probe is fixed at 1.0 μM (Eq. 27).

$[\mathrm{probe}] = 1 - nx$ (μM)

Equation 27

The combination of Eq 21, 26 and 27 gives Equation for linear plot (modified Hill plot). (Eq. 28).

$$\log\frac{F_{\max} - F_{\min}}{F_{\max} - F} = \frac{1}{n}\log\frac{[\mathrm{BSA}](F_{\max} - F_{\min})}{F - F_{\min}} - \frac{1}{n}\log\frac{K_{\mathrm{D}}}{n}$$

Equation 28

Here, the linear relation between $\log\frac{F_{\max}-F_{\min}}{F_{\max}-F}$ and $\log\frac{[\mathrm{BSA}](F_{\max}-F_{\min})}{F-F_{\min}}$ provides the slope $\frac{1}{n}$ and the intercept $-\frac{1}{n}\log\frac{K_{\mathrm{D}}}{n}$. In this plot, [BSA] is approximated to $[\mathrm{BSA}]_0$. The modified Hill plot of Trp-BODIPY-FF vs BSA gives $n = 2.3 \pm 0.2$ and $K_{\mathrm{D}} = 6.9 \pm 2.8$ μM, and HTL-Trp-BODIPY-FF vs BSA gives $n = 2.6 \pm 0.2$ and $K_{\mathrm{D}} = 11.8 \pm 3.9$ μM, respectively.

1-9. Computational simulation of HTL-Trp-BODIPY-FF with Halo-tag

Computational simulation study on HTL-Trp-BODIPY-FF with Halo-tag was carried out using MacroModel (Schrödinger Maestro v13.1). The protein data bank (PDB ID: 6u32) was used for determining the protein structure and Halo-tag ligand (HTL) binding mode. The conformational structure of HTL-Trp-BODIPY-FF was searched and optimized using OPLS4 as a force field (solvent: water, maximum iterations: 2500, convergence threshold: 0.05) followed by torsional sampling MCMM (energy window for saving structures: 21 kJmol^{-1}, maximum atom deviation

cut off: 0.5 Å). The energy-minimized structure of HTL-Trp-BODIPY-FF was manually docked with Halo-tag and optimized the structure of the complex by OPLS4 (solvent: water, maximum iterations: 5000, convergence threshold: 0.1). The range of minimization was set to all atoms within 5 Å of HTL-Trp-BODIPY-FF.

1-10. Protein expression and purification

Escherichia coli BL21 (DE3) (Novagen) was transformed with pET21b (+)-Halo-His and cultured in Luria-Bertani (LB) medium containing 100 ng/μL ampicillin at 37 °C. The recombinant Halo-tag protein was expressed and purified according to the previously reported protocol.[S4] The purified Halo-tag protein was stored in a pH 7.4 phosphate buffered saline buffer (prepared using PBS Tablets; Takara Bio Inc., Shiga, Japan) at -80 °C by flash freezing. The assay of Halo-tag protein was performed by dissolving the appropriate solutions after thawing the stock solution on ice.

1-11. Protein labeling assay using SDS-PAGE

To confirm the labeling of HTL-Trp-BODIPY-FF with Halo-tag, SDS-PAGE analysis was performed. HTL-Trp-BODIPY-FF (1.0, 2.0, and 4.0 μM) were incubated with Halo-tag (2.0, 4.0, and 8.0 μM), respectively, in 100 mM phosphate buffer (pH 7.4) at 37°C for 1 h. After incubation, each solution (10 μL) was added to loading buffer containing 100 mM dithiothreitol (10 μL), heated at 103°C for 3 min, and then analyzed by SDS-PAGE. The molecular marker (Precision Plus Protein Unstained Standards) was also loaded onto the same gel plate. The fluorescence image was obtained using a Typhoon FLA 9500, and the gel was then stained with Coomassie Brilliant Blue.

1-12. Labeling kinetics analysis

To determine the labeling kinetics of HTL-Trp-BODIPY-FF to Halo-tag, we monitored the time course of the fluorescence intensity of 1.0 μM HTL-Trp-BODIPY-FF incubated with 2.0 μM Halo-tag in 100 mM phosphate buffer (pH 7.4) at 37 ℃. The rate of formation of Halo-tag and probe conjugate follows second-order kinetics and is defined as the rate constants k_2 using Eq. 29.

$$-\frac{d[\mathrm{probe}]}{dt} = k_2[\mathrm{probe}][\mathrm{protein}]$$

Equation 29

The value of $[\mathrm{probe}]$ and $[\mathrm{protein}]$ is the concentration of probe (HTL-Trp-BODIPY-FF) and protein (Halo-tag), respectively (Here, $[\mathrm{probe}]_0$ =1.0 μM, $[\mathrm{protein}]_0$ =2.0 μM). Additionally, when determining the value of $[\mathrm{probe}]_0$ and $[\mathrm{protein}]_0$ as the initial concentration of HTL-Trp-BODIPY-FF and Halo-tag respectively, the concentration of conjugate $[\mathrm{conjugate}]$ was expressed (Eq. 30).

$$[\mathrm{conjugate}] = [\mathrm{probe}]_0 - [\mathrm{probe}] = [\mathrm{protein}]_0 - [\mathrm{protein}]$$

Equation 30

The combination of Eq. 29 and 30 provides Eq. 31.

$$[\mathrm{probe}] = \frac{[\mathrm{probe}]_0([\mathrm{probe}]_0 - [\mathrm{protein}]_0)}{[\mathrm{probe}]_0 - [\mathrm{protein}]_0 \exp(([\mathrm{protein}]_0 - [\mathrm{probe}]_0)k_2 t)}$$

Equation 31

When the initial concentration of HTL-Trp-BODIPY-FF is lower than that of Halo-tag ($[\mathrm{probe}]_0 < [\mathrm{protein}]_0$), the concentration of conjugate [conjugate] was described using the fluorescence intensity of the reaction mixture as Eq. 32.

$$[\mathrm{conjugate}] = \frac{F(t)-F(0)}{\Delta F}[\mathrm{probe}]_0$$

Equation 32

$F(t)$ is the fluorescence intensity of the reaction mixture and ΔF is the difference in fluorescence intensity between the initial and final state (Eq. 33).

$$\Delta F = F(\infty) - F(0)$$

Equation 33

The combination of Eq. 30, 31, 32, and 33 provides Eq. 34.

$$F(t) = \left(\frac{[\mathrm{protein}]_0 - [\mathrm{protein}]_0 \exp(([\mathrm{protein}]_0 - [\mathrm{probe}]_0)k_2 t)}{[\mathrm{probe}]_0 - [\mathrm{protein}]_0 \exp(([\mathrm{protein}]_0 - [\mathrm{probe}]_0)k_2 t)}\right)\Delta F + F(0)$$

Equation 34

The value of k_2 was approximated using the recorded data of $F(t)$ following Eq.34.

1-13. Construction of plasmid

pcDNA3.1(+)-MBP-Halo-mCherry

The DNA fragment of MBP was separately prepared from pcDNA3.1(+)-MBP-PYP-NLS[S5] by PCR amplification using a forward primer 5′-GCACTCGCTAGCCACCATGAAAATCGAAGAAG-3′ and a reverse primer 5′-TCATCCGGATCCCCTTCCCTCGATCCCG -3′. The fragments were digested using restriction enzymes *Nhe*I and *BamH*I and were separately ligated into pcDNA3.1(+)-4xCox8-Halo-mCherry plasmid that underwent similar restriction enzyme digestion to generate the title plasmid.

*pcDNA3.1(+)-Tom20-Halo-mCherry

The DNA fragment of Tom20 was separately prepared from pcDNA3.1(+)-Tom20-BL which was gifted from Prof. Miyawaki's group by PCR amplification using a forward primer 5′-GCATTCGCTAGCCACCATGGTG-3′ and a reverse primer 5′-TCATAGGGATCC TTCCACATCATCTTCAGCC-3′. The fragments were digested using restriction enzymes *Nhe*I and *BamH*I and were separately ligated into pcDNA3.1(+)-4xCox8-Halo-mCherry plasmid that underwent similar restriction enzyme digestion to generate the title plasmid.

*pcDNA3.1(+)-4xCox8-Halo-mCherry

The DNA fragment of 2xCox8 was separately prepared from pKmc-2xCox8-Halo by PCR amplification using a forward primer 5′-GTAATTGGATCCGCCACCATGTCCGTCCTG-3′ and a reverse primer 5′-TGTTAAGGATCCCCCGAGCTTC-3′. The fragments were digested using a single restriction enzyme *BamH*I and were separately ligated into pcDNA3.1(+)-2xCox8-Halo-mCherry plasmid that underwent similar restriction enzyme digestion to generate the title plasmid.

*pcDNA3.1(+)-2xCox8-Halo-mCherry

The DNA fragment of 2xCox8-Halo was separately prepared from pKmc-2xCox8-Halo[S6] by PCR amplification using a forward primer 5′-GTACTTGCTAGCGCCACCATGTCCGTCCTGACGCC-3′ and a reverse primer 5′-TGTTAACTCGAGACCGGAAATCTCCAGAGTAGACC-3′. The fragments were digested using restriction enzymes *Nhe*I and *Xho*I and were separately ligated into pcDNA3.1(+)-Halo-mCherry[S7] plasmid that underwent similar restriction enzyme digestion to generate the title plasmid.

pET21b (+)-Halo-His

The DNA fragment of Halo was separately prepared from pcDNA3.1(+)-Halo-NLS[S6] by PCR amplification using a forward primer 5′-GATTCGGCTAGCATGTCCGAAATCGGTACTGG-3′ and a reverse primer 5′-GATTCGGCTAGCATGTCCGAAATCGGTACTGG-3′. The fragments were digested using a single restriction enzyme *Nhe*I and were separately ligated into pET21b (+) (Novagen) plasmid that underwent similar restriction enzyme digestion to generate the title plasmid.

pcDNA3.1(+)-Halo-EGFR-mCherry

The DNA fragment of Halo was separately prepared from pcDNA3.1 (+)-Halo-NLS[S6] by PCR amplification using a forward primers 5'-GATCGTGCTAGCATGTCCGAAATCGGTACTGG-3' and a reverse primer 5'-TGTTAAGCTAGCACCGGAAATCTCCAGAGTAGAC-3'. The fragments were digested using restriction enzyme *NheI* and were separately ligated into pcDNA3.1-BL(wt)-EGFR-mCherry plasmid that underwent similar restriction enzyme digestion to generate the title plasmid.

pcDNA3.1(+)-BL(wt)-EGFR-mCherry

The DNA fragment of mCherry was separately prepared from pcDNA3.1(+)-Halo-mCherry[S7] by PCR amplification using a forward primers 5'-CTCGAGATGGTGAGCAAGGGCGAG-3' and a reverse primer 5'-GGACGAGCTGTACAAGTAATCTAGA-3'. The fragments were digested using restriction enzyme *Xho*I and *Xba*I, and were separately ligated into pcDNA3.1-BL-EGFR[S8] plasmid that underwent similar restriction enzyme digestion to generate the title plasmid.

***Supplementary note to the construction of plasmids**

We prepared pcDNA3.1(+)-2xCox8-Halo-mCherry and pcDNA3.1(+)-4xCox8-Halo-mCherry for another study and performed mitochondrial imaging using pcDNA3.1(+)-Tom20-Halo-mCherry.

1-14. Live-cell imaging

HeLa or HEK293T cells were incubated in Dulbecco's Modified Eagle's Medium (DMEM) containing 10% fetal

bovine serum (FBS) and transfected with 2500 ng of each plasmid or pcDNA3.1(+) (for negative control) plasmid using Lipofectamine 3000 transfection reagent (L3000015; Thermo Fisher Scientific) dissolved in Opti-MEM (Thermo Fisher Scientific) following the manufacturer's protocol. After transfection, the cells were incubated for 5 h, replaced medium with a new DMEM (only HeLa cells), and then incubated for 18 h at 37 °C with a continuous supply of 5% CO_2. The cells were then washed twice with Hank's balanced salt solution (HBSS), incubated in DMEM including 1.0 μM HTL-Trp-BODIPY-FF (0.1% DMSO) for 20 min, and captured images using confocal fluorescence microscopies (FV10i; Olympus Corporation and Ti2-E; Nikon Corporation). FV10i recorded images with excitation/emission at 473/490–540 nm for HTL-Trp-BODIPY-FF detection and at 559/570–620 nm for mCherry detection. Ti2-E recorded images with excitation/emission at 488/499–551 nm for HTL-Trp-BODIPY-FF detection and at 561/571–625 nm for mCherry detection.

1-15. Light irradiation setup for live cell imaging

Light irradiation on living cells was conducted using a LED light source (CL-1501, Asahi Spectra Co., Ltd.) equipped with a timer (CL-TCN1, Asahi Spectra Co., Ltd.), a filter (CL-H1-365-9-1-B, Asahi Spectra Co., Ltd.), and a collective lens (CL-H1LCB02, Asahi Spectra Co., Ltd.) for repetitive 365 nm irradiation (Light intensity: 10 mW/cm^2, Irradiation time: 10 s per one cycle). Ti2-E equipped with a Plan Apochromat Lambda S 40XC silicon oil objective lens (NA 1.25, Nikon Corporation) or Plan Apo Lambda S 60XC silicone oil objective lens (NA 1.4, Nikon Corporation) and micro scanning stage was used to observe fluorescence images in living cells maintained at 37°C with a continuous supply of 5% CO_2 by using a stage-top incubator (STXG-WSKMX-SET, Tokai Hit). After each cycle of 365 nm irradiation, images were taken at the rate of 1.01 (40X lens) or 1.76 (60X lens) fps with a quality of 0.86 (40X lens) or 0.58 (60X lens) μm/pixel for 20 s (20 (40X lens) or 11 (60X lens) images were captured per one cycle) by confocal laser scanning microscopy (AX-R, Nikon Corporation). All the images are recorded in a single z-stack plane. During the imaging, the fluorescence intensity of HTL-Trp-BODIPY-FF was recovered upon 488 and 561 nm excitation light stimulation. 365 nm irradiation (10 s) and 488 and 561 nm excitation (20 s) were repeated 10 times with a 1 s waiting time per each irradiation event. Figure S21 may help this description more readable.

1-16. Image analyses

Image analyses were completed with commercial software ImageJ (Fiji) and NIS-Elements (Nikon Corporation). The fluorescence images were processed with the ImageJ software. Ratiometric images were obtained using both ImageJ (for image generation) and NIS-Elements software (for extracting signal intensites). Ratiometric images were generated using recorded images without background subtraction and masking. Before the analysis, all images were not processed with any contract and brightness, because it may change the original signal intensities. For each experiment, we analyzed a random selection of 10 cells in three different cell plates (the number of replicates: N=3). The signal intensities of green (I_{Green}) and red channel (I_{Red}) were measured using NIS-Elements software and calculated the ratio of green to red channel following Eq. 35.

$$\text{Ratio intensity}, I_{\text{Ratio}} = \frac{I_{\text{Green}}}{I_{\text{Red}}}$$

Equation 35

For measurement and analysis of the signal intensities, individual cells were automatically selected and defined as regions of interest (ROIs) using NIS-Elements software. The quenching efficiency in each cell was calculated using Eq. 36.

$$\text{Quenching efficiency}, E(n) = \frac{I_{\text{Ratio,on}}(n) - I_{\text{Ratio,off}}(n)}{I_{\text{Ratio,on}}(n)}$$

Equation 36

Here, $I_{\text{Ratio,on}}(n)$ and $I_{\text{Ratio,off}}(n)$ are the fluorescence ratio intensity before and after the nth 365 nm irradiation.

2. Supporting Figures

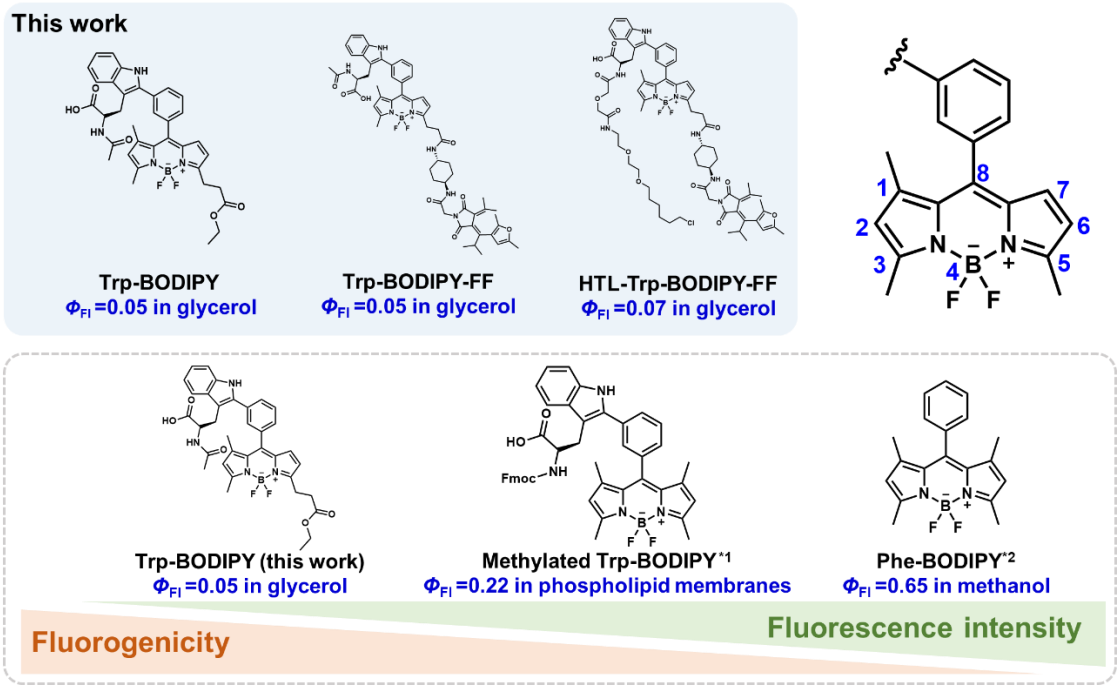

Figure S1. The comparison of photophysical properties of each BODIPY derivative. The introduction of tryptophan or the absence of a methyl group at 1 or 7 position in the BODIPY core improves the fluorogenicity because the transition energy barrier to access non-radiative decay is decreased. On the other hands, it facilitates non-radiative decay instead of the radiative decay as fluorescence. This tendency has already investigated in our previous report[S9]. Φ_{Fl}: fluorescence quantum yield *1: the value of Φ_{Fl} was cited from ref S10. *2: the value of Φ_{Fl} was cited from ref S11.

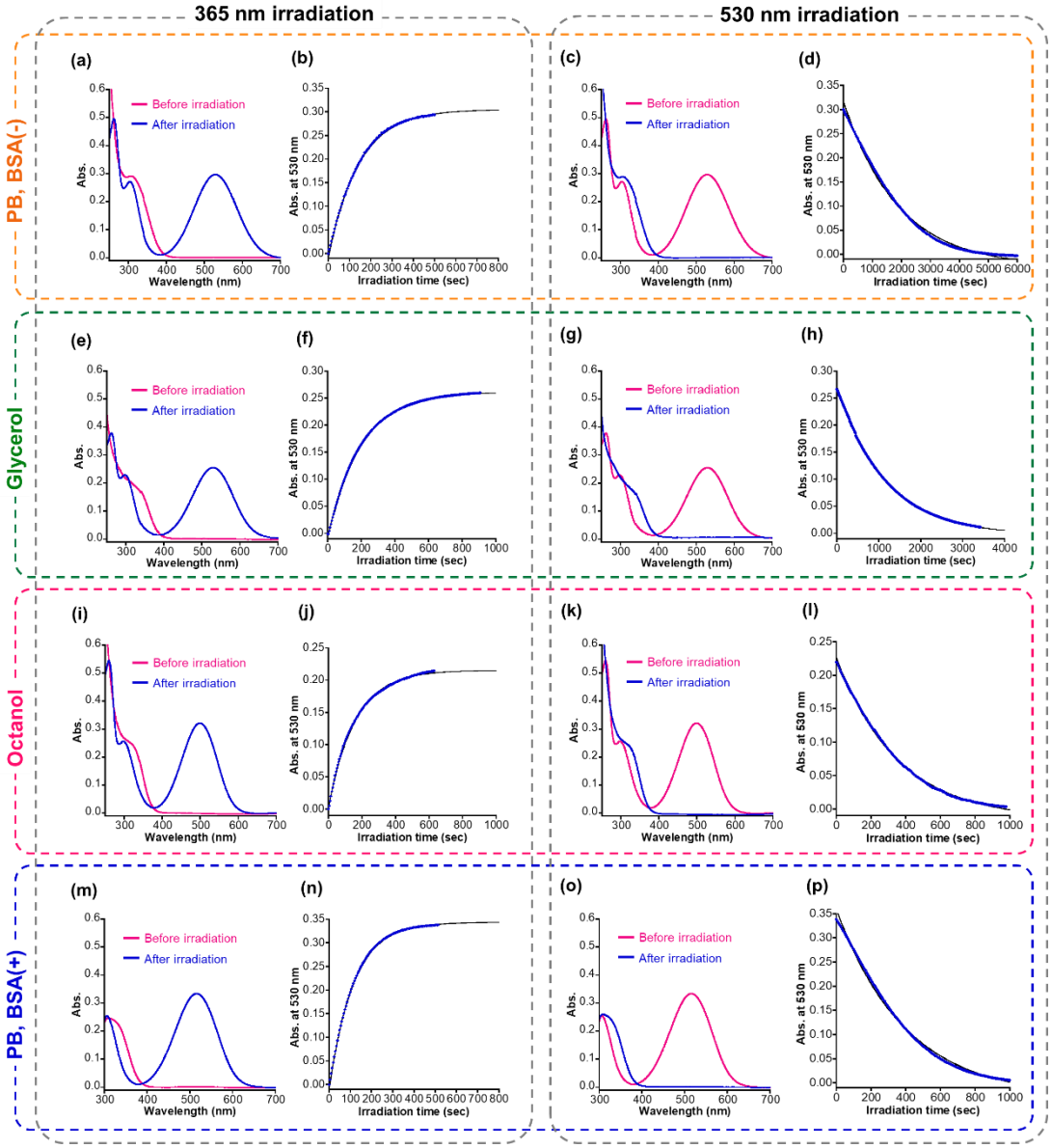

Figure S2. Absorption spectra and time courses of absorbance of 50 μM FF dissolved in **(a-d)** 100 mM phosphate buffer (pH 7.4), **(e-h)** glycerol, **(i-l)** *n*-octanol, and **(m-p)** 100 mM phosphate buffer (pH 7.4) with 250 μM (5 eq.) BSA including 0.5% DMSO. **(a,e,i,m)** The spectra before and after 365 nm (10 mW/cm^2, 10 min) irradiation are shown by the magenta and blue lines, respectively. **(c,g,k,o)** The spectra before and after 530 nm (10 mW/cm^2, 10 min) irradiation are shown by the magenta and blue lines, respectively. Time courses of absorbance at 530 nm were recorded upon **(b,f,j,n)** 365 nm (**(b,j,n)** 1.47 mW, **(f)** 0.98 mW) and **(d,h,l,p)** 530 nm (**(d)** 6.33 mW, **(h)** 4.22 mW, **(l,p)** 2.98 mW) irradiation. Temperature: 37 °C.

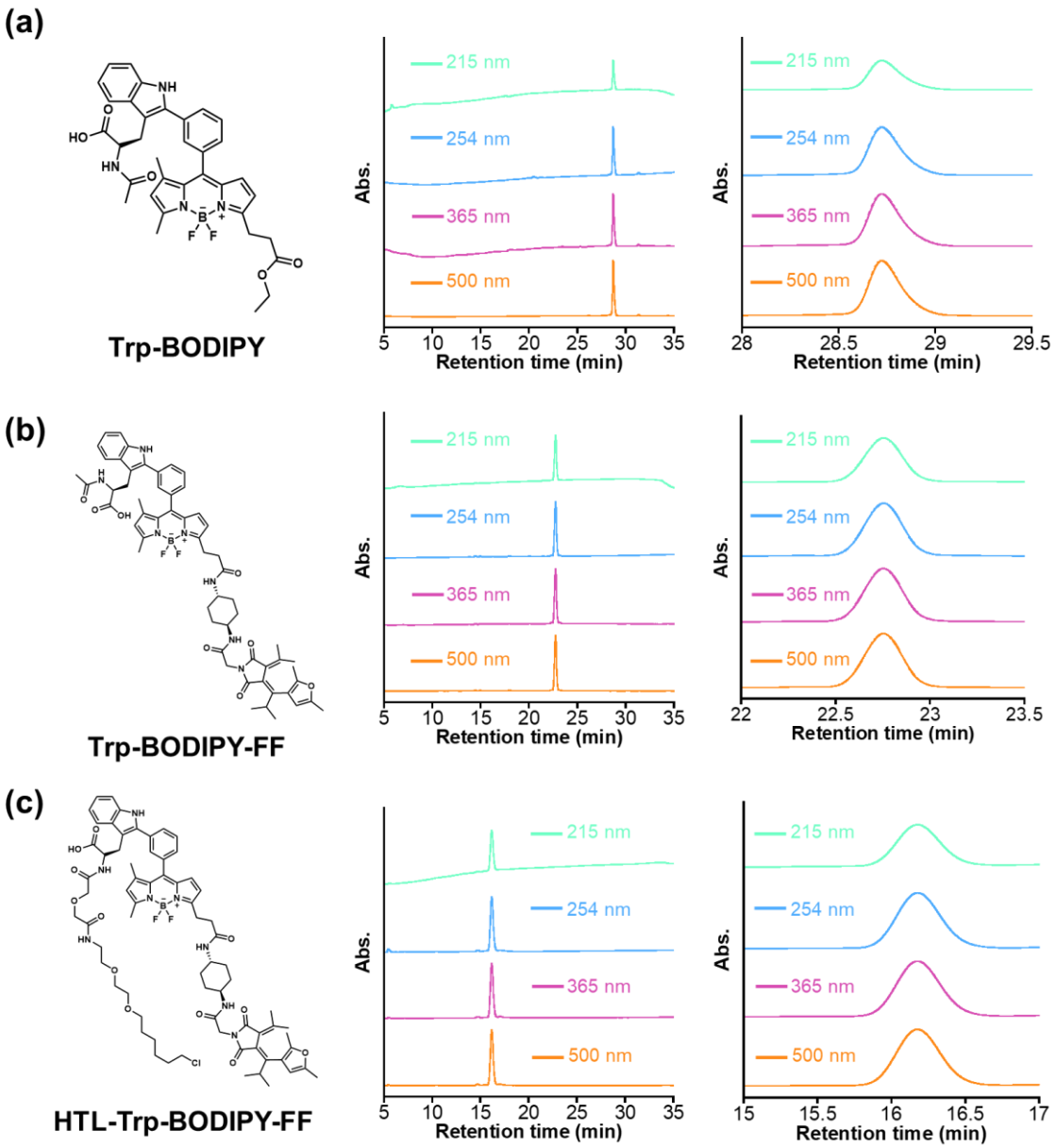

Figure S3. Purity analysis of **(a)** Trp-BODIPY, **(b)** Trp-BODIPY-FF, and **(c)** HTL-Trp-BODIPY-FF using HPLC. Each samples were dissolved 0.1% formic acid acetonotrile/water solution. Samples were eluted through a column with a linear gradient of acetonitrile/water containing 0.1% formic acid ((a) 5/95 to 95/5, (b) 50/50 to 95/5, (c) 65/35 to 95/5) monitoring by absorption at 215 (light green) , 254 (sky bule), 365(purple), and 500 nm (orange).

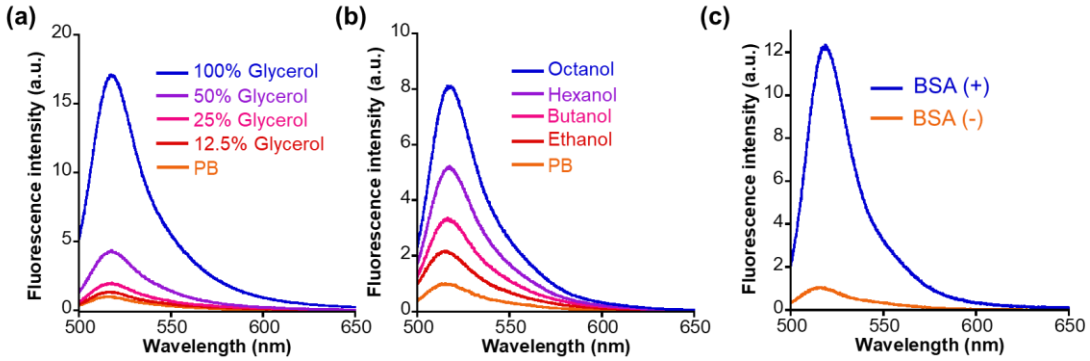

Figure S4. Fluorescence spectra of 1.0 μM Trp-BODIPY in **(a)** 100 mM phosphate buffer (PB) (pH 7.4) with increasing glycerol concentration (from top to bottom: 100, 50, 25, 12.5, and 0%), in **(b)** *n*-octanol (blue line), *n*-hexanol (purple line), *n*-butanol (magenta line), ethanol (red line), and PB (orange line) in **(c)** 100 mM PB (pH 7.4) with/without 5.0 μM BSA (blue/orange line). λ_{ex}: 470 nm, 37 ºC.

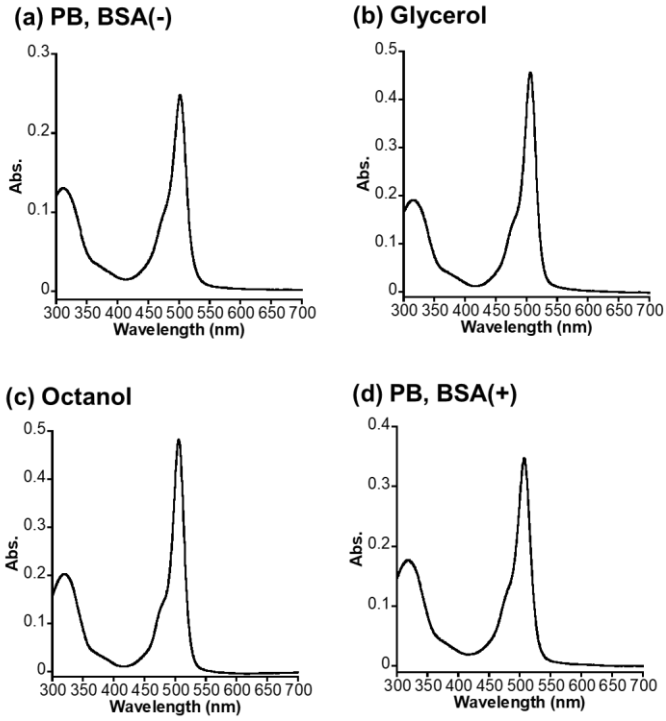

Figure S5. Absorption spectra of 10 μM Trp-BODIPY dissolved in **(a)** 100 mM phosphate buffer (pH 7.4), **(b)** glycerol, **(c)** *n*-octanol, and **(d)** 100 mM phosphate buffer (pH 7.4) with 250 μM BSA including 1% DMSO. Temperature: 37 °C.

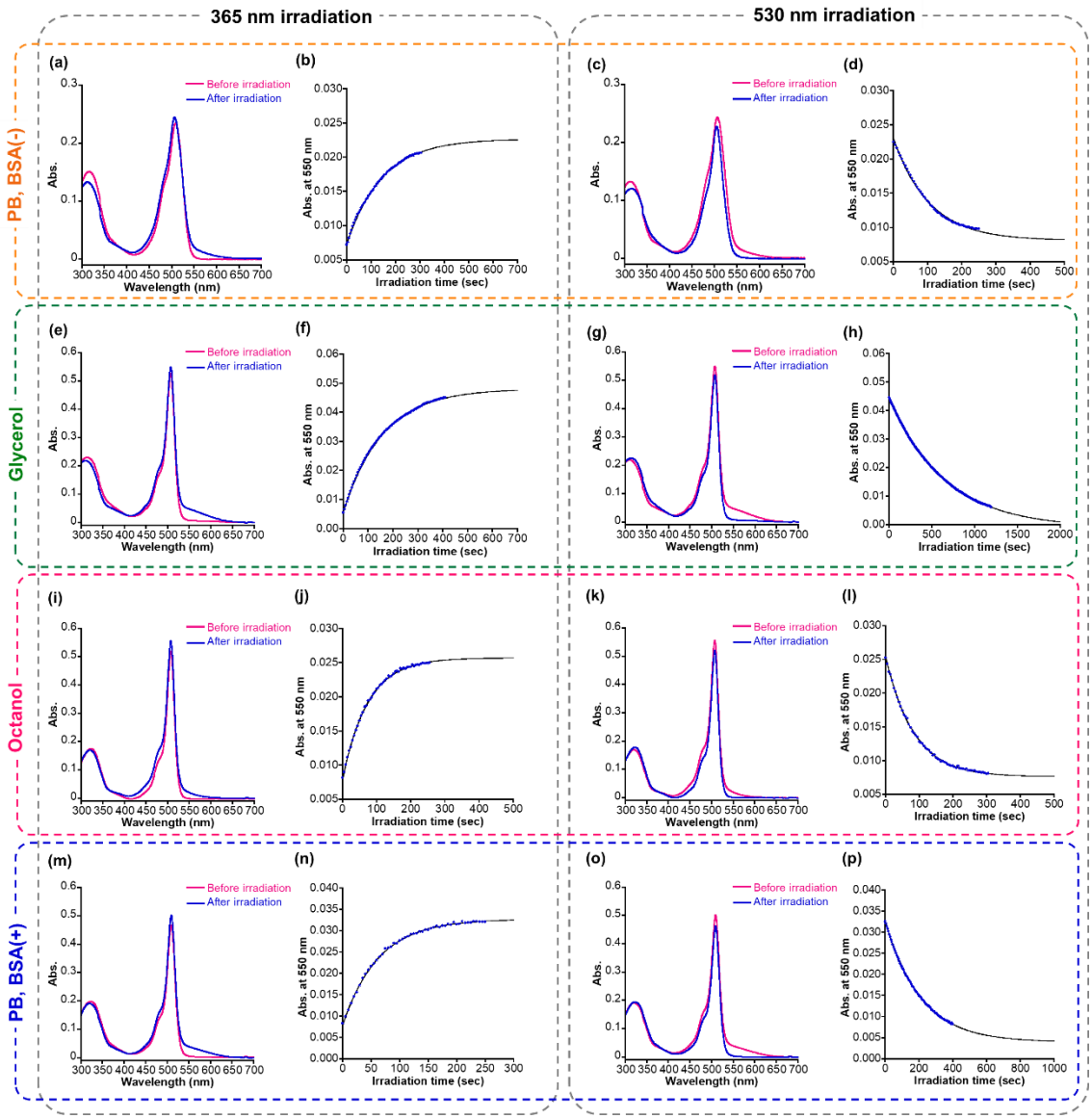

Figure S6. Absorption spectra and time courses of absorbance of 10 μM Trp-BODIPY-FF dissolved in **(a-d)** 100 mM phosphate buffer (pH 7.4), **(e-h)** glycerol, **(i-l)** *n*-octanol, and **(m-p)** 100 mM phosphate buffer (pH 7.4) with 250 μM (5 eq.) BSA including 1% DMSO. **(a,e,i,m)** The spectra before and after 365 nm (10 mW/cm^2, 3 min) irradiation are shown by the magenta and blue lines, respectively. **(c,g,k,o)** The spectra before and after 530 nm (10 mW/cm^2, 3 min) irradiation are shown by the magenta and blue lines, respectively. Time courses of absorbance at 550 nm were recorded upon **(b,f,j,n)** 365 nm (**(b,f)** 0.98 mW, **(j,n)** 1.47 mW) and **(d,h,l,p)** 530 nm (**(d,h)** 4.22 mW, **(l,p)** 2.98 mW) irradiation. Temperature: 37 °C.

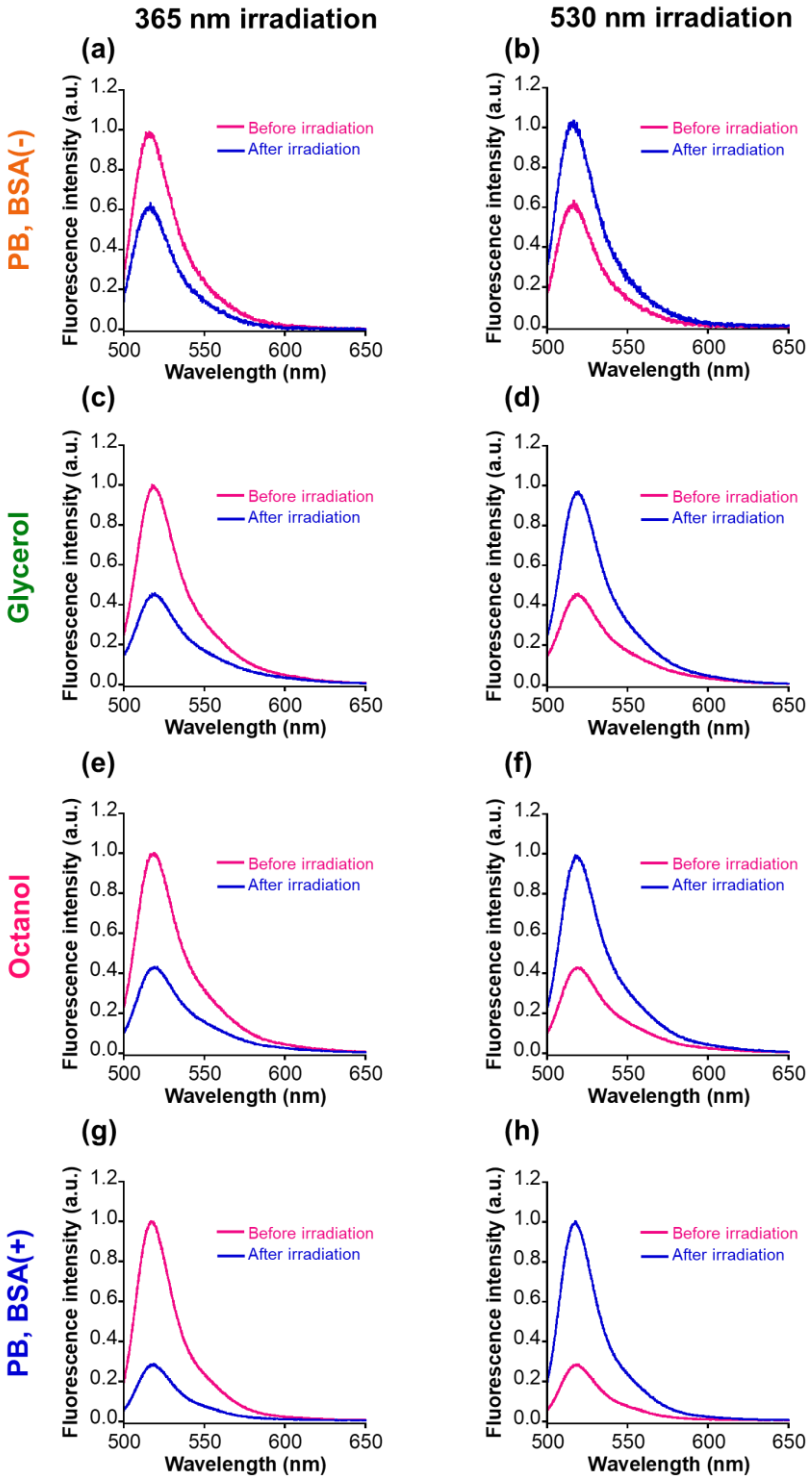

Figure S7. Fluorescence spectra of 1.0 μM Trp-BODIPY-FF dissolved in **(a,b)** 100 mM phosphate buffer (pH 7.4), **(c,d)** glycerol, **(e,f)** *n*-octanol, and **(g,h)** 100 mM phosphate buffer (pH 7.4) with 5.0 μM (5 eq.) BSA including 1% DMSO. **(a,c,e,g)** The spectra before and after 365 nm (10 mW/cm^2, 3 min) irradiation are shown by the magenta and blue lines, respectively. **(b,d,f,h)** The spectra before and after 530 nm (10 mW/cm^2, 3 min) irradiation are shown by the magenta and blue lines, respectively. λ_{ex}: 470 nm, 37 ºC.

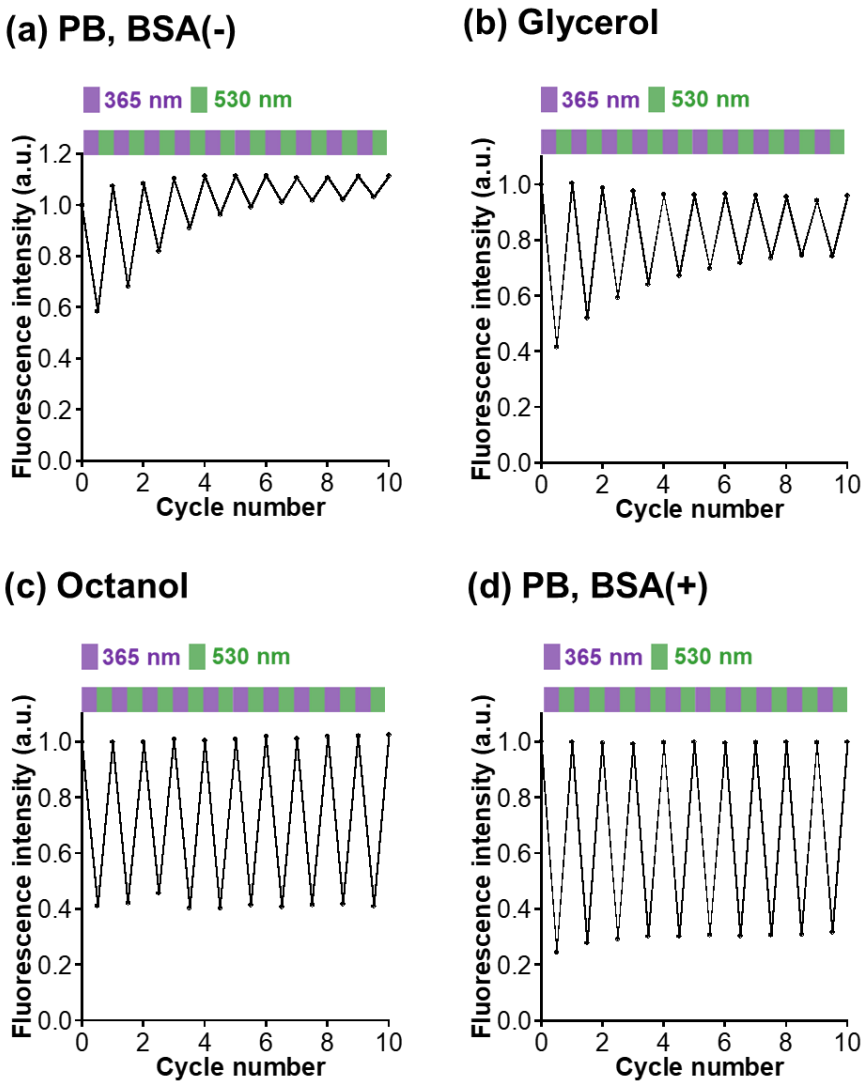

Figure S8. Fluorescence photoswitching reversibility of 1.0 μM Trp-BODIPY-FF in **(a)** PB (pH 7.4), **(b)** glycerol, **(c)** *n*-octanol, and **(d)** PB (pH 7.4) including 5.0 μM BSA. $\lambda_{ex/em}$: 490/520 nm, 37 ºC. 365/530 nm irradiations are indicated by purple/green shades, respectively.

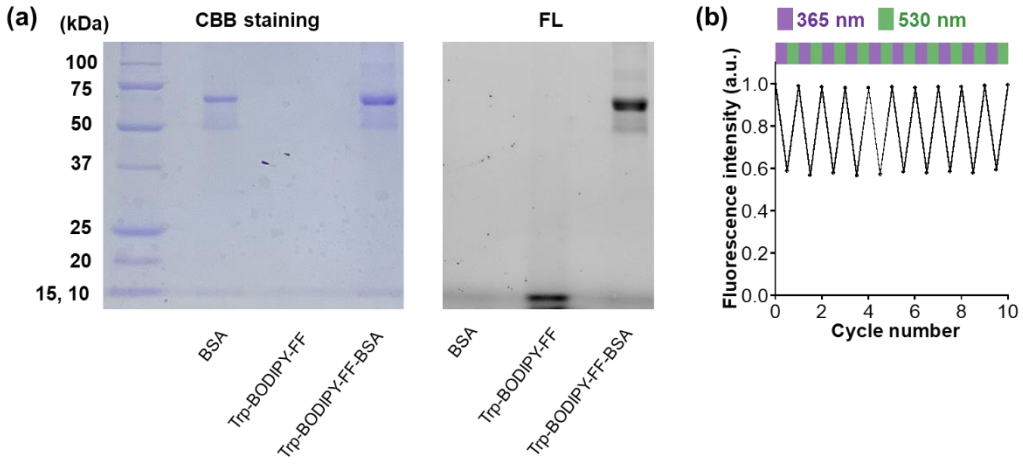

Figure S9. (a) The results of SDS-PAGE of Trp-BODIPY-FF-BSA. The left and right image shows CBB-stained and fluorescence images, respectively. The first column at the left represents a ladder to comfirm protein size (BSA: 66.5 kDa). Fluorescence images were obtained with excitation at 488 nm. **(b)** Fluorescence reversibility of 1.0 μM Trp-BODIPY-FF-BSA in PB (pH 7.4), $\lambda_{ex/em}$: 490/520 nm, 37 °C. 365/530 nm irradiations are indicated by purple/green shades, respectively.

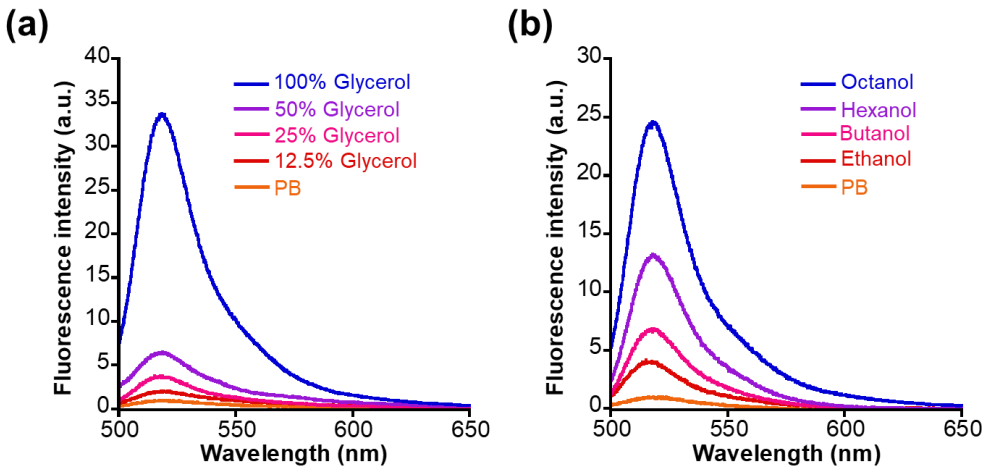

Figure S10. Fluorescence spectra of 1.0 μM HTL-Trp-BODIPY-FF in **(a)** 100 mM phosphate buffer (PB) (pH 7.4), increasing glycerol/sample volume (from top to bottom: 100, 50, 25, 12.5, and 0%), in **(b)** *n*-octanol (blue line), *n*-hexanol (purple line), *n*-butanol (magenta line), ethanol (red line), and 100 mM PB (pH 7.4) (orange line), respectively. λ_{ex}: 470 nm, 37 ºC.

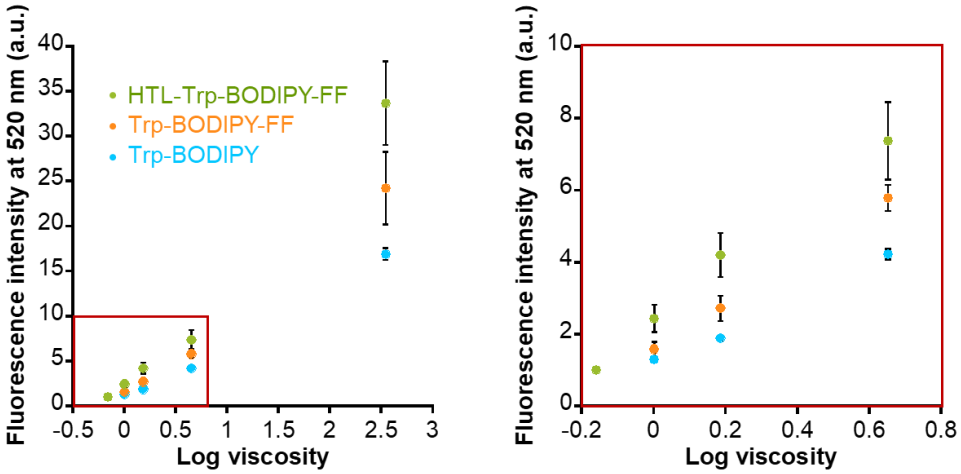

Figure S11. The relationship between the fluorescence intensity of HTL-Trp-BODIPY-FF (green), Trp-BODIPY-FF (orange), and Trp-BODIPY (sky blue) and Log viscosity. The area that is surrounded by a rad rectangle is enlarged in the right side. *N*=3. Dynamic viscosity was calculated using the equations described in the paper of ref S12. $\lambda_{ex/em}$: 470/520 nm, 37 ºC.

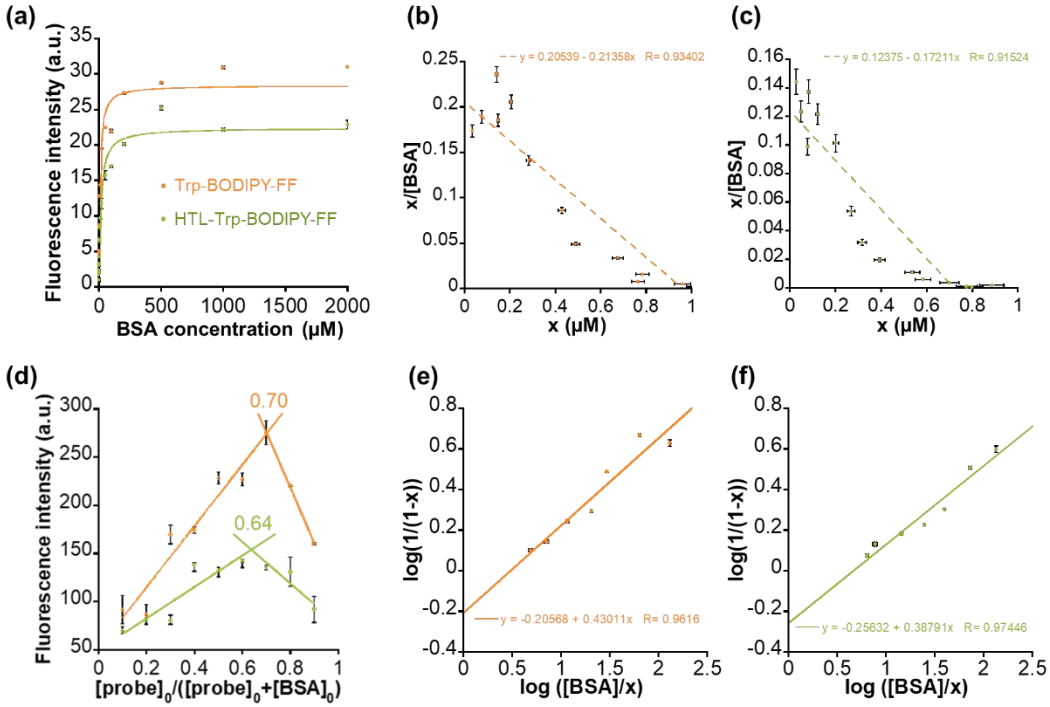

Figure S12. (a) Fluorescence intensity at 520 nm of 1.0 μM Trp-BODIPY-FF (orange) or 1.0 μM HTL-Trp-BODIPY-FF (green) in 100 mM phosphate buffer (pH 7.4) containing varying concentrations of BSA (from 0 to 2000 μM). *N*=3. **(b,c)** Scatchard plot for **(b)** Trp-BODIPY-FF or **(c)** HTL-Trp-BODIPY-FF vs BSA in 100 mM phosphate buffer. x is concentrations of BSA-probe complex estimated from fluorescent intensity at 520 nm using Eq. 21. The probe concentration is fixed at 1.0 μM. *N*=3. Both plots do not give a proper linear approximation, and show a downward convex-like curve, suggesting the presence of multiple different binding sites. **(d)** Job's plot for Trp-BODIPY-FF (orange) or HTL-Trp-BODIPY-FF (green) vs BSA in 100 mM phosphate buffer (pH 7.4) monitoring the fluorescence

intensity at 520 nm. The concentration of the probe varied from 100 to 900 nM as the BSA concentration decreased from 900 to 100 nM. *N*=3. Both Job's plots exhibited maximum mole fractions ($[probe]_0/([probe]_0+[BSA]_0)$) around 0.70 (Trp-BODIPY-FF) and 0.64 (HTL-Trp-BODIPY-FF), implicating that the binding ratio of the probe to BSA is 2. **(e,f)** The modified Hill plot for **(e)** Trp-BODIPY-FF or **(f)** HTL-Trp-BODIPY-FF vs BSA in 100 mM phosphate buffer (pH 7.4) monitoring the fluorescence intensity at 520 nm. The concentration of the probe is fixed at 1.0 μM. BSA concentration varied from 1.0 to 100 μM. *N*=3. The plot of Trp-BODIPY-FF vs BSA gives K_D = 6.9±2.8 μM, and HTL-Trp-BODIPY-FF vs BSA gives K_D = 11.8 ±3.9 μM, respectively.

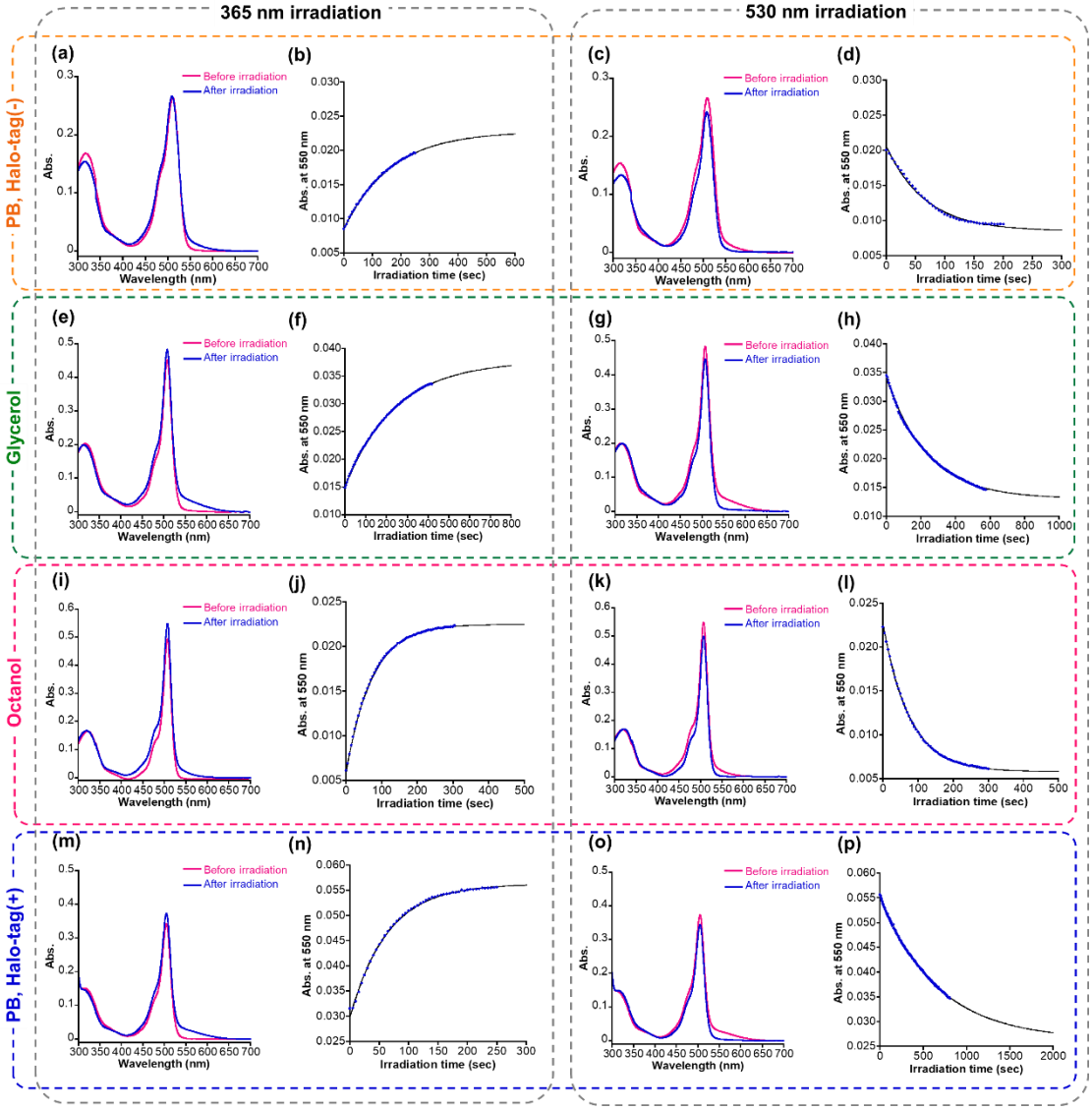

Figure S13. Absorption spectra and time courses of absorbance of 10 μM HTL-Trp-BODIPY-FF dissolved in **(a-d)** 100 mM phosphate buffer (pH 7.4), **(e-h)** glycerol, **(i-l)** *n*-octanol, and **(m-p)** 100 mM phosphate buffer (pH 7.4) with 50 μM (5 eq.) BSA including 1% DMSO. **(a,e,i,m)** The spectra before and after 365 nm (10 mW/cm^2, 3 min) irradiation are shown by the magenta and blue lines, respectively. **(c,g,k,o)** The spectra before and after 530 nm (10 mW/cm^2, 3

min) irradiation are shown by the magenta and blue lines, respectively. Time courses of absorbance at 550 nm were recorded upon **(b,f,j,n)** 365 nm ((b,f) 0.98 mW, (j,n) 1.47 mW) and **(d,h,l,p)** 530 nm ((d,h) 4.22 mW, (l,p) 2.98 mW) irradiation. Temperature: 37 °C.

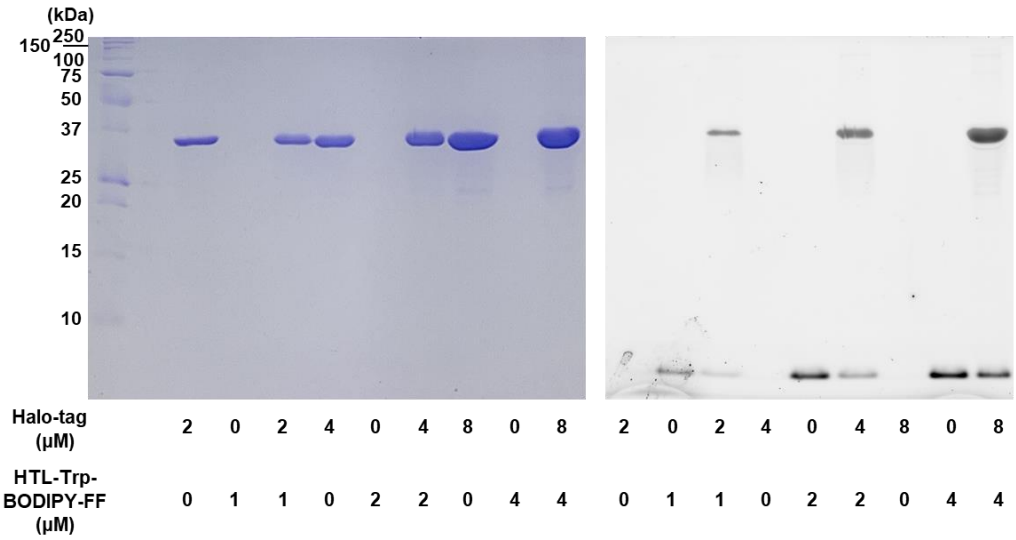

Figure S14. The results of SDS-PAGE of HTL-Trp-BODIPY-FF with Halo-tag. The left and right image shows CBB-stained and fluorescence images, respectively. 1.0, 2.0, and 4.0 μM HTL-Trp-BODIPY-FF was incubated with 2.0, 4.0, 8.0 μM Halo-tag at 37 ºC for 1 h, respectively. The first column at the left represents a ladder to comfirm protein size (Halo-tag: 34 kDa). Fluorescence images were obtained with excitation at 488 nm.

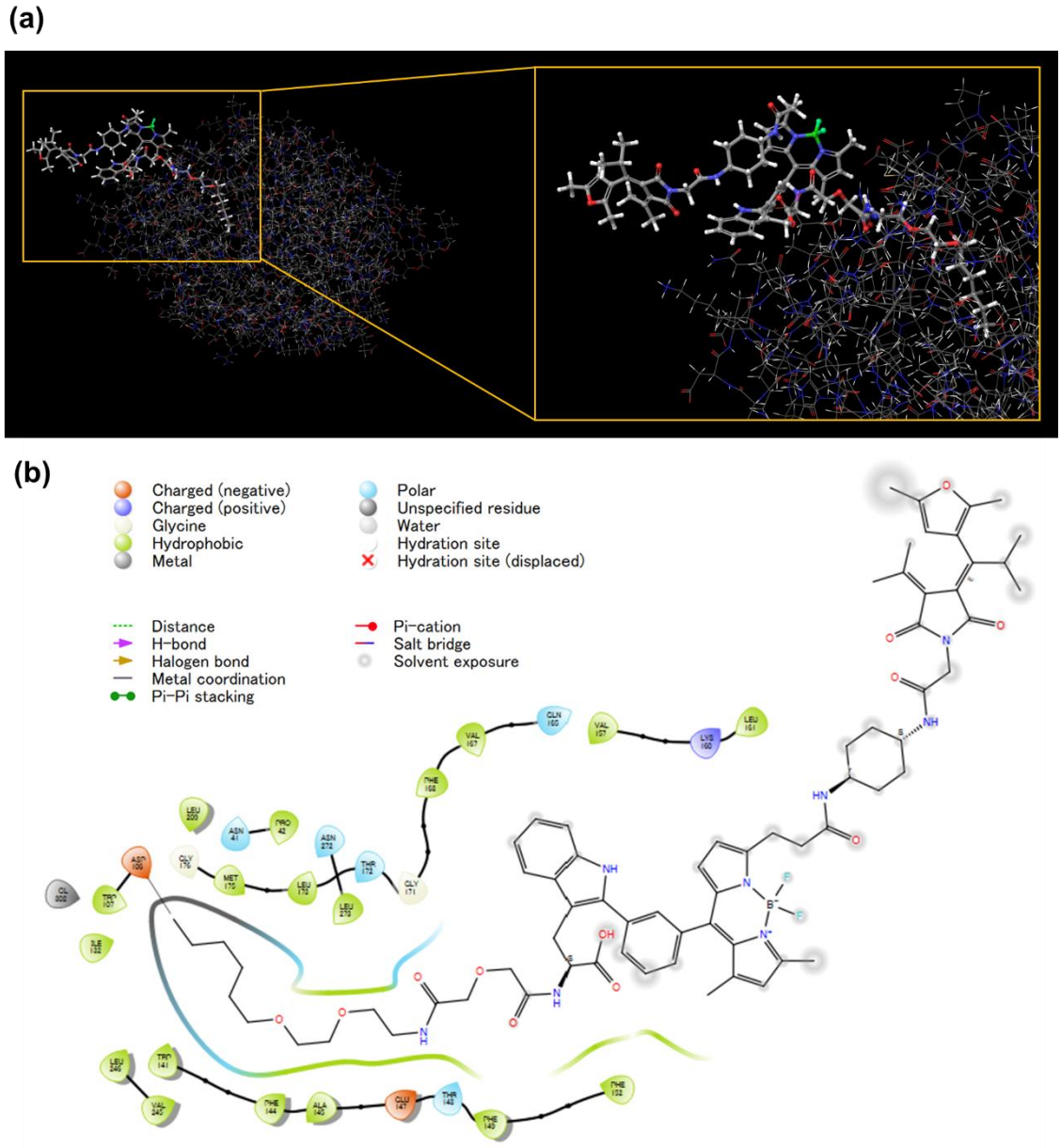

Figure S15. (a) Optimized three-dimensional (3D) structure on HTL-Trp-BODIPY-FF with Halo-tag (PDB ID: 6u32) using MacroModel software. **(b)** The two-dimensional (2D) ligand interaction map of HTL-Trp-BODIPY-FF with Halo-tag created from **(a)**.

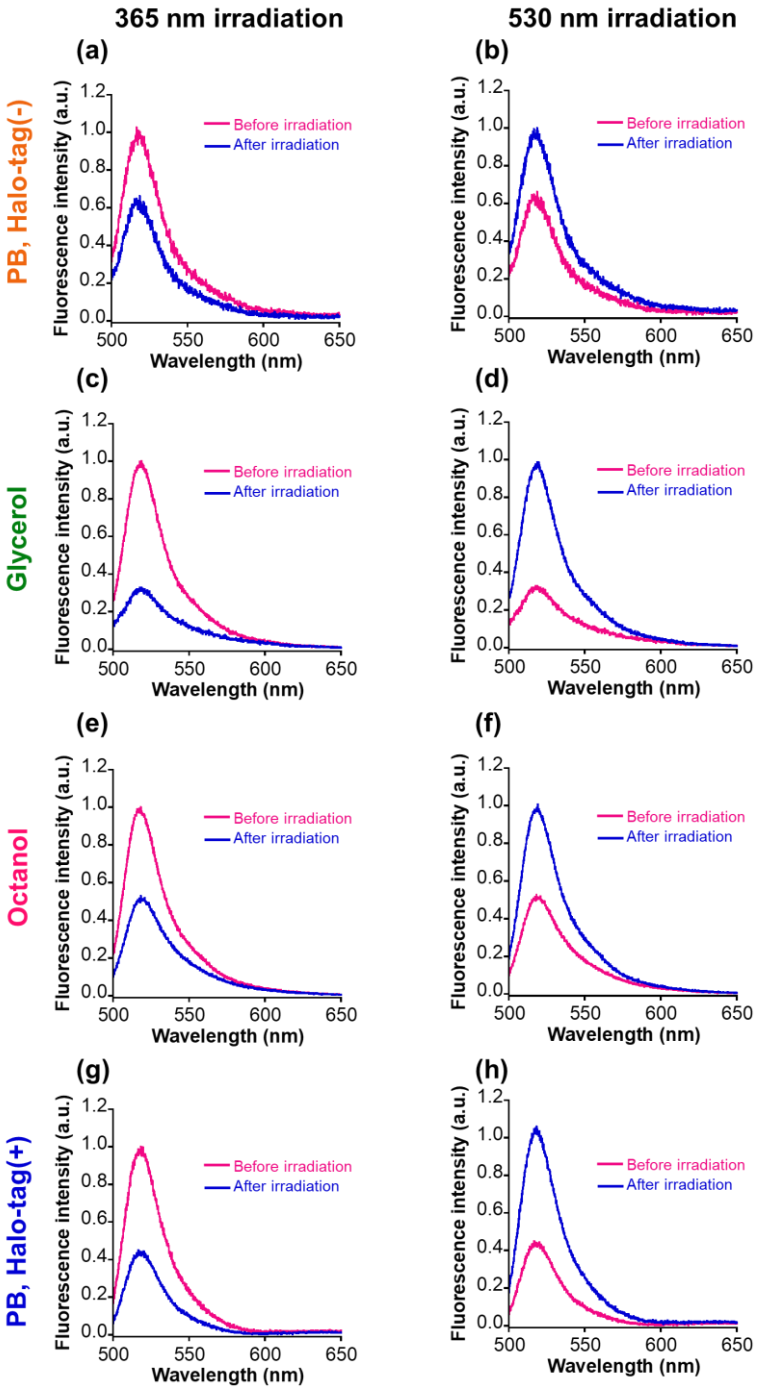

Figure S16. Fluorescence spectra of 1.0 μM HTL-Trp-BODIPY-FF dissolved in **(a,b)** 100 mM phosphate buffer (pH 7.4), **(c,d)** glycerol, **(e,f)** *n*-octanol, and **(g,h)** 100 mM phosphate buffer (pH 7.4) after incubating with 2.0 μM (2 eq.) Halo-tag for 30 min. All samples contain 1% DMSO. **(a,c,e,g)** The spectra before and after 365 nm (10 mW/cm^2, 3 min) irradiation are shown by the magenta and blue lines, respectively. **(b,d,f,h)** The spectra before and after 530 nm (10 mW/cm^2, 3 min) irradiation are shown by the magenta and blue lines, respectively. λ_{ex}: 470 nm, 37 ºC.

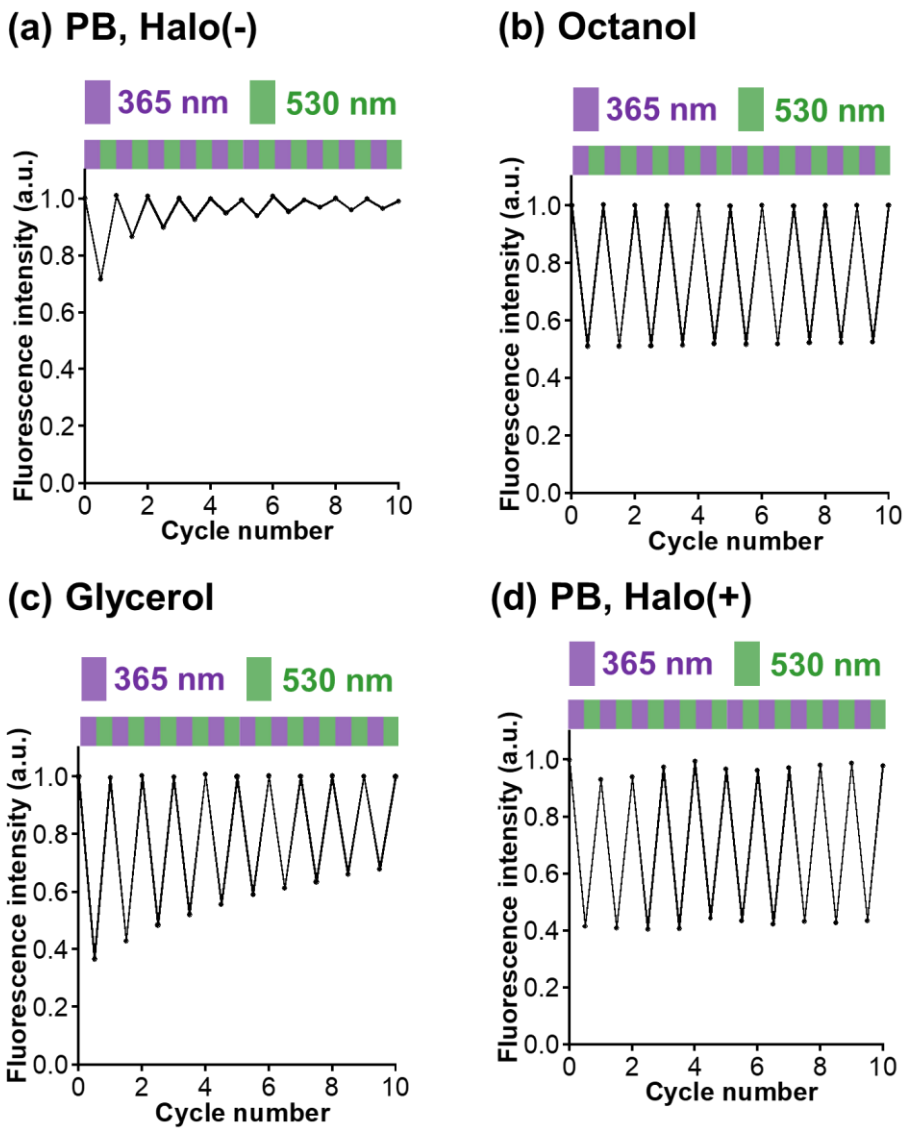

Figure S17. Fluorescence photoswitching reversibility of 1.0 μM HTL-Trp-BODIPY-FF in **(a)** PB (pH 7.4), **(b)** glycerol, **(c)** *n*-octanol, and **(d)** PB (pH 7.4) after incubating with 2.0 μM (2 eq.) Halo-tag for 30 min. All samples contain 1% DMSO. $\lambda_{ex/em}$: 490/520 nm, 37 ºC. 365/530 nm irradiations are indicated by purple/green shades, respectively.

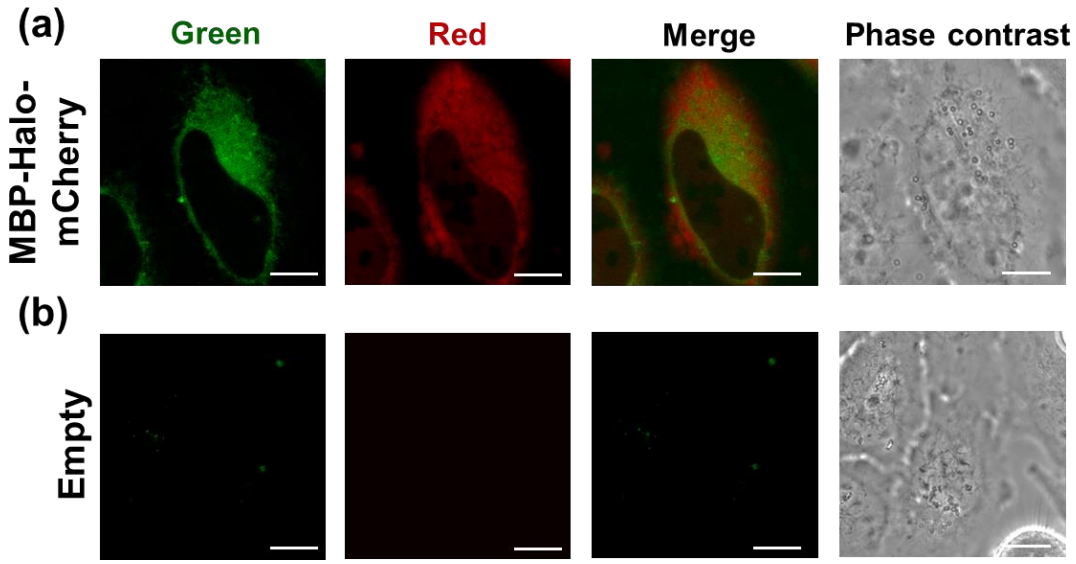

Figure S18. Live cell imaging using HTL-Trp-BODIPY-FF. **(a)** pcDNA3.1(+)-MBP-Halo-mCherry and **(b)** empty vector (pcDNA3.1(+)) fused HeLa cells. Before observation, 1.0 μM HTL-Trp-BODIPY-FF (0.1% DMSO) was added into the cell culture for 20 min. Scale bar 25 μm. Green channel: $\lambda_{ex/em}$: 473/490-540 nm; Red channel: $\lambda_{ex/em}$: 559/570-620 nm.

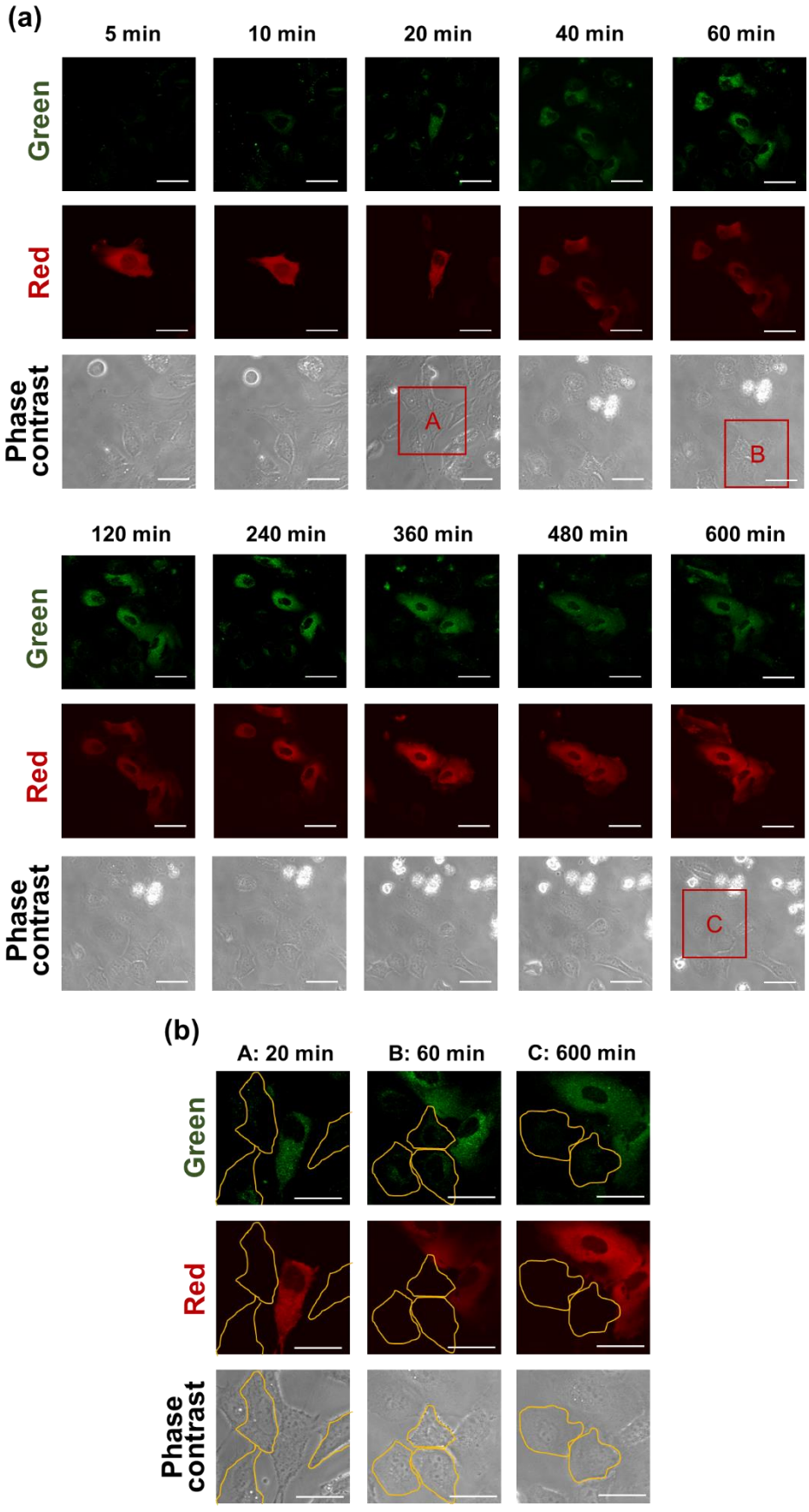
(a)
5 min
10 min
20 min
40 min
60 min
Green
Red
Phase contrast
A
B
120 min
240 min
360 min
480 min
600 min
Green
Red
Phase contrast
C
(b)
A: 20 min
B: 60 min
C: 600 min
Green
Red
Phase contrast

Figure S19. (a) Extended long time live cell imaging using HTL-Trp-BODIPY-FF. HeLa cells were transfected with pcDNA3.1(+)-MBP-Halo-mCherry. Before observation, 1.0 μM HTL-Trp-BODIPY-FF (0.1% DMSO) was added into the cell culture for 5, 10, 20, 40, 60, 120, 240, 360, 480, and 600 min, respectively. Scale bar 50 μm. Green channel: $\lambda_{ex/em}$: 473/490-540 nm; Red channel: $\lambda_{ex/em}$: 559/570-620 nm. **(b)** The enlarged images of A, B, and C are marked as red squares in **(a)**. The non-transfected cells, which do not show any expression of mCherry, are surrounded by yellow circles. Scale bar 25 μm.

(a)

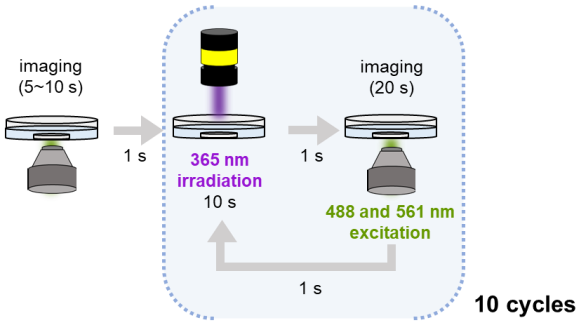

(b)

Duration time	Status	Number of acquired images
5~10 s	Imaging (488, 561 nm stimulation)	5
1 s	Waiting	
10 s	365 nm stimulation	
1 s	Waiting	
20 s	Imaging (488, 561 nm stimulation)	20 (40x lens) 11 (60x lens)
1 s	Waiting	
10 s	365 nm stimulation	
1 s	Waiting	
20 s	Imaging (488, 561 nm stimulation)	20 (40x lens) 11 (60x lens)

9x

Figure S20. (a) Schematic illustration and **(b)** time course of light irradiation experiment on living cells.

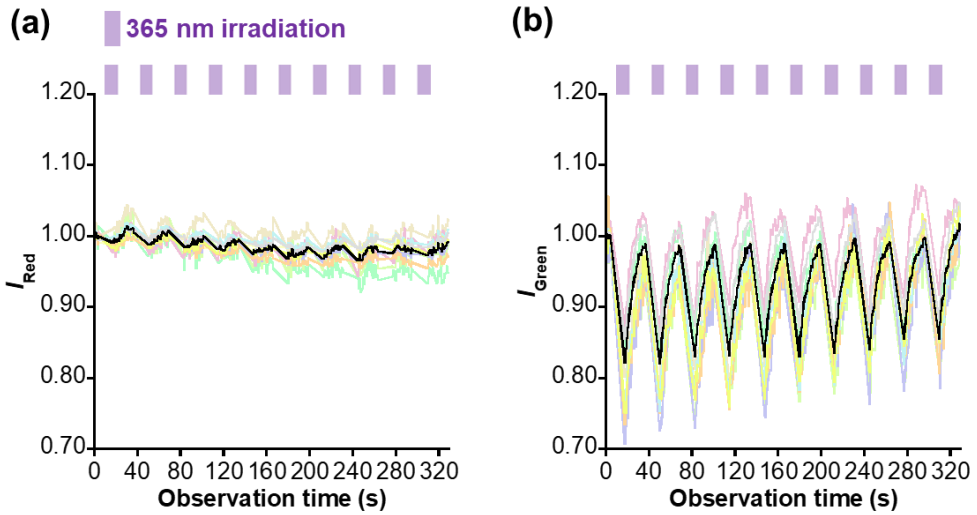

Figure S21. Time course of the fluorescence intensities of **(a)** red and **(b)** green channel with 365 nm irradiation (10 cycles). HeLa cells were transfected with pcDNA3.1(+)-MBP-Halo-mCherry. 1.0 μM HTL-Trp-BODIPY-FF (0.1% DMSO) was added into the cell culture for 20 min. The black line represents the average intensity from a random selection of 10 cells in three different cell plates (the number of replicates: *N*=3). Other pale-colored lines describe the intensity from each cell.

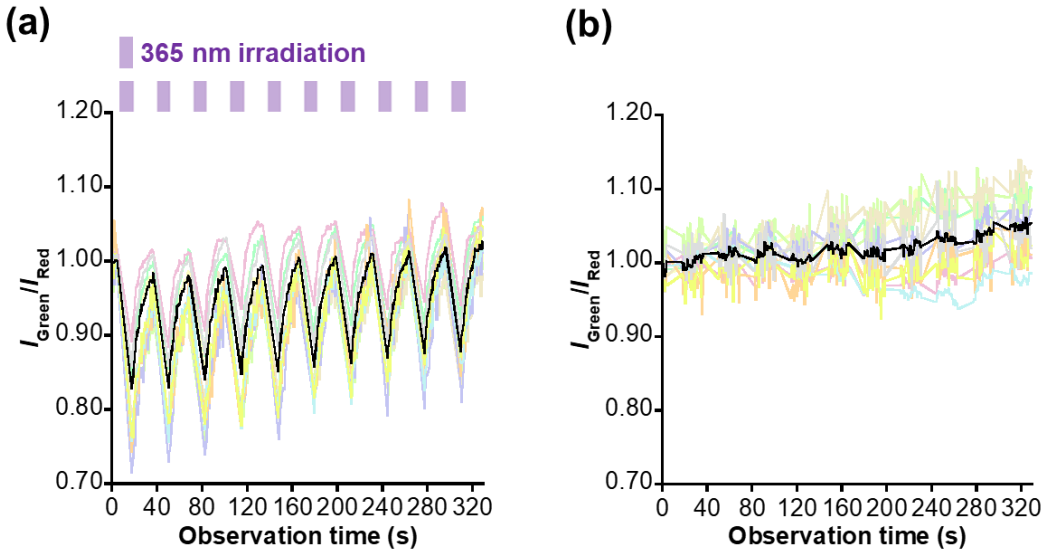

Figure S22. Time course of the ratio for fluorescence intensities of green channel to red channel **(a)** with/**(b)** without 365 nm irradiation (10 cycles). HeLa cells were transfected with pcDNA3.1(+)-MBP-Halo-mCherry. 1.0 μM HTL-Trp-BODIPY-FF (0.1% DMSO) was added into the cell culture for 20 min. The fluorescence intensity ratio (I_{Green}/I_{Red}) was obtained from a random selection of 10 cells in three different cell plates (the number of replicates: *N*=3). The black line represents the average ratio intensity from ten different cells. Other pale-colored lines describe each ratio intensity from each cell. Each ratio intensity was normalized as 1 in the first snapshot. **(a)** is a replication of Figure 4b.

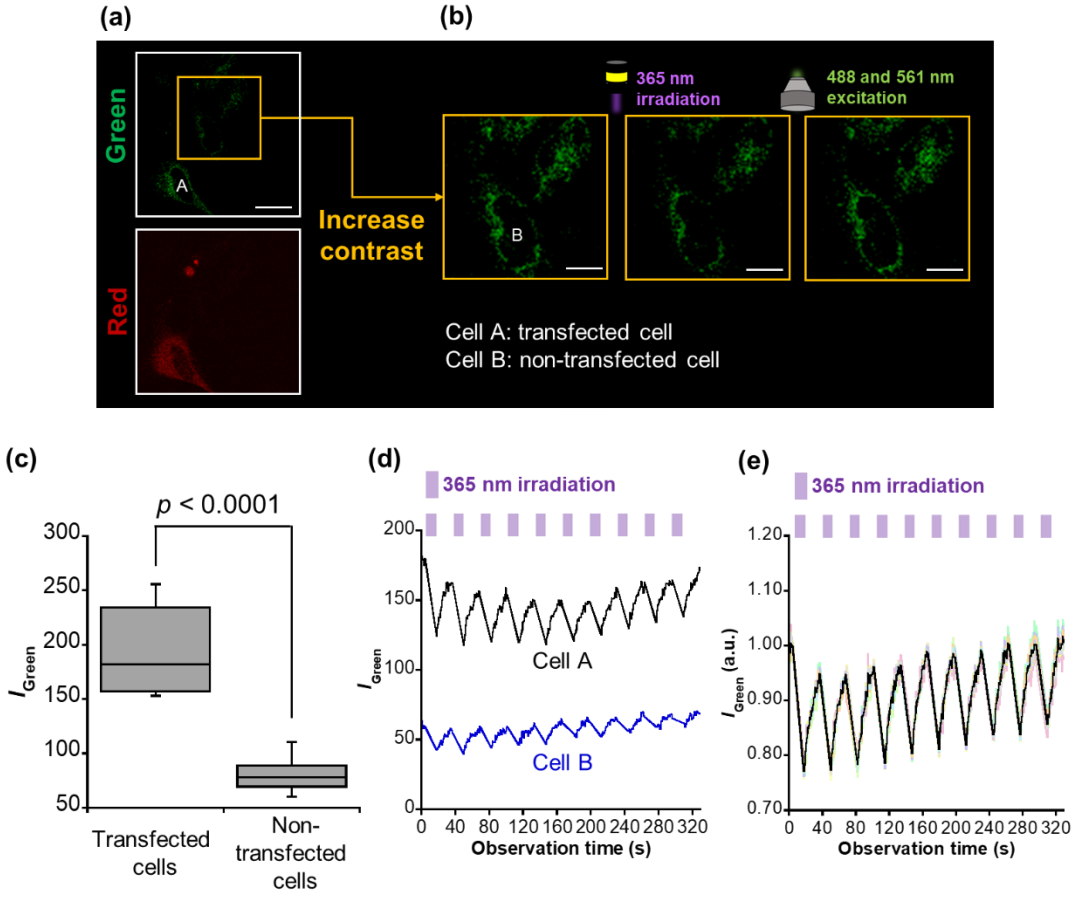

Figure S23. (a) Live cell imaging of non-transfected and MBP-Halo-mCherry transfected HeLa cells using a confocal microscope (Ti2-E). After adding 1.0 μM, HTL-Trp-BODIPY-FF (0.1% DMSO), cells were incubated for 20 min. Scale bar 50 μm. **(b)** Enlarged images of **(a)** that show fluorescence signals from non-transfected cells are modified for visualization by increasing image contrast. Scale bar 25 μm. Samples were alternately irradiated at 365 nm (10 mW/cm^2 for 10 s) and 488 and 561 nm excitation light exposure (20 s). Scale bar: 10 μm. Green channel: λ_{ex} = 488 nm, λ_{em} = 499-551 nm. Red channel: λ_{ex} = 561 nm, λ_{em} = 571-625 nm. **(c)** Comparison of green fluorescence intensity between transfected and non-transfected cells. Data presents as box plot (N=10). P values were obtained from two-tailed t tests. **(d,e)** Time course of the fluorescence intensity of green channel with 365 nm irradiation (10 cycles) of transfected cells (cell A in **(a)**) and non-transfected cells (cell B in **(b)**), **(d)** a random selection of 10 non-transfected cells in three different cell plates (the number of replicates: N=3). The black line represents the average intensity from 10 different cells. Other pale-colored lines describe the intensity of each cell.

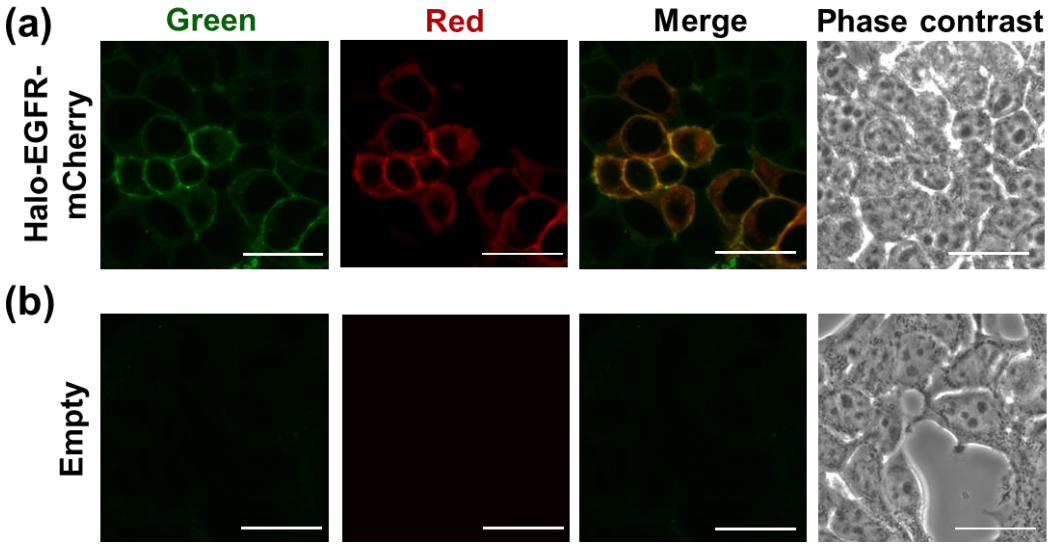

Figure S24. Live cell imaging using HTL-Trp-BODIPY-FF. **(a)** pcDNA3.1(+)-Halo-EGFR-mCherry and **(b)** empty vector (pcDNA3.1(+)) fused HEK293T cells. Before observation, 100 nM HTL-Trp-BODIPY-FF (0.1% DMSO) was added into the cell culture for 20 min. Scale bar 25 μm. Green channel: $\lambda_{ex/em}$: 473/490-540 nm; Red channel: $\lambda_{ex/em}$: 559/570-620 nm.

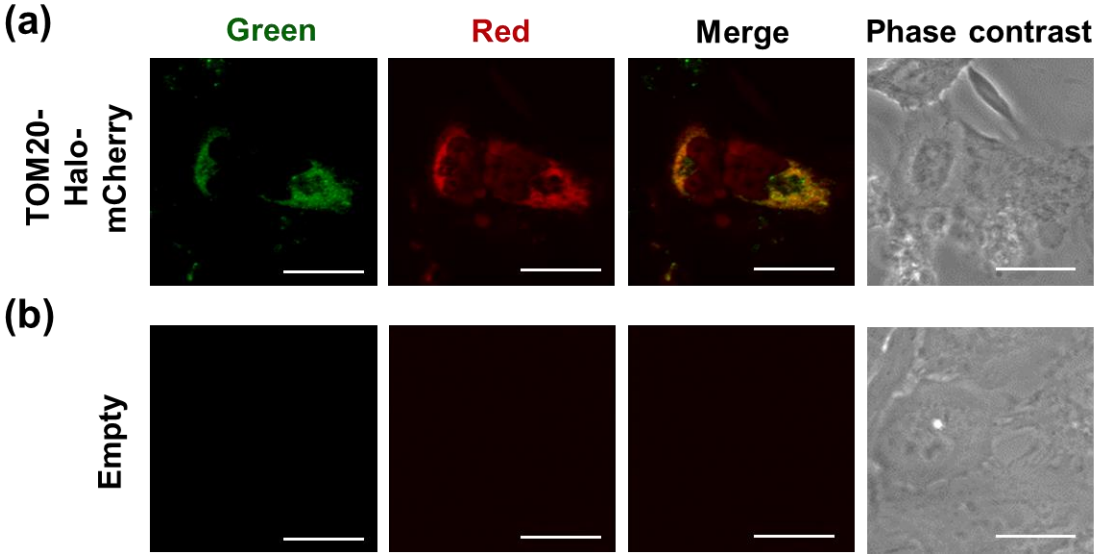

Figure S25. Live cell imaging using HTL-Trp-BODIPY-FF. **(a)** pcDNA3.1(+)-TOM20-Halo-mCherry and **(b)** empty vector (pcDNA3.1(+)) fused HeLa cells. Before observation, 1.0 μM HTL-Trp-BODIPY-FF (0.1% DMSO) was added into the cell culture for 20 min. Scale bar 25 μm. Green channel: $\lambda_{ex/em}$: 473/490-540 nm; Red channel: $\lambda_{ex/em}$: 559/570-620 nm.

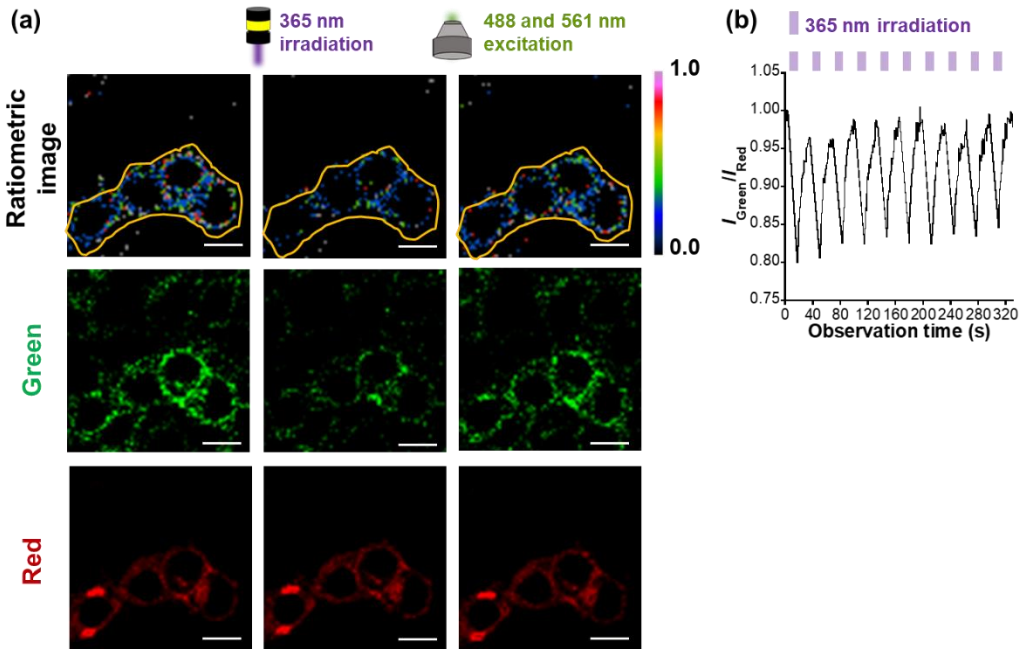

Figure S26. (a) Ratiometric imaging of living HEK293T cells transfected with pcDNA3.1(+)-Halo-EGFR-mCherry, using confocal microscope (Ti2-E). After adding 100 nM, HTL-Trp-BODIPY-FF (0.1% DMSO), cells were incubated for 20 min. Samples were alternately irradiated at 365 nm (10 mW/cm^2 for 10 s) and 488 and 561 nm excitation light exposure (20 s). Scale bar: 10 μm. Green channel: λ_{ex} = 488 nm, λ_{em} = 499-551 nm. Red channel: λ_{ex} = 561 nm, λ_{em} = 571-625 nm. Ratiometric images were generated by dividing the intensity of green channel by that of red channel in each pixel. Maximum ratio: 0.8; minimum ratio: 0.1. **(b)** Time course of the ratio for fluorescence intensities of green channel to red channel with 365 nm irradiation (10 cycles). The fluorescence intensity ratio (I_{Green}/I_{Red}) was obtained from the selected region of Interest (ROI) surrounded by the yellow circle.

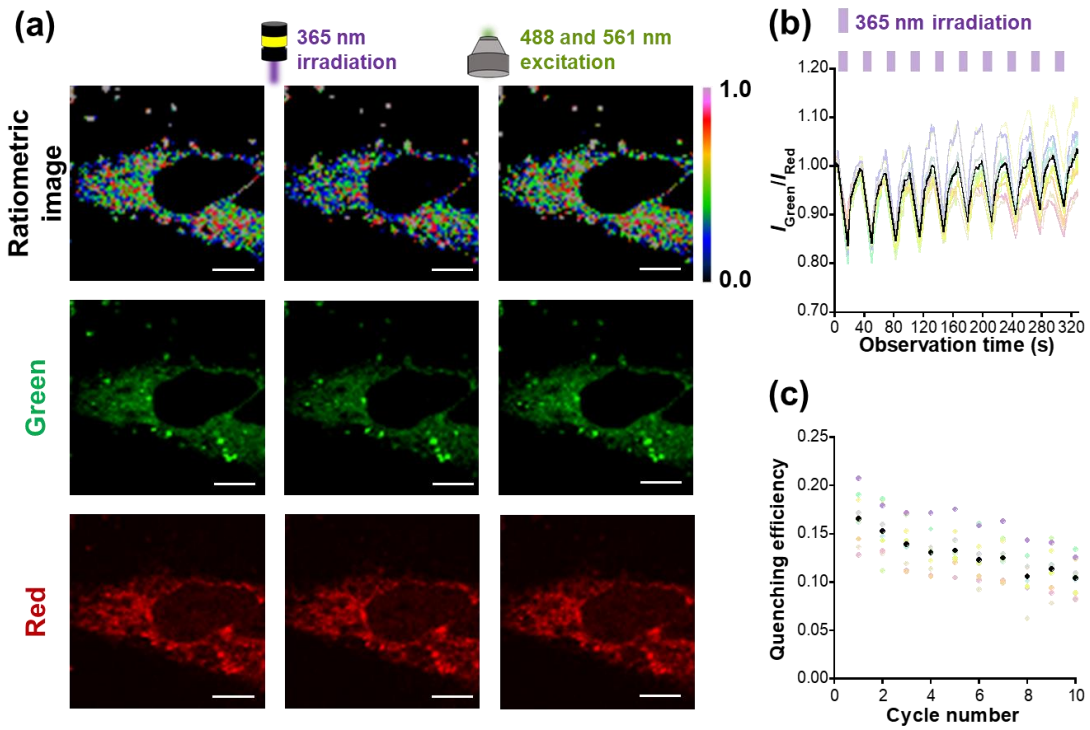

Figure S27. (a) Ratiometric imaging of living HeLa cells transfected with pcDNA3.1(+)-Tom20-Halo-mCherry, using confocal microscope (Ti2-E). After adding 1.0 μM, HTL-Trp-BODIPY-FF (0.1% DMSO), cells were incubated for 20 min. Samples were alternately irradiated at 365 nm (10 mW/cm^2 for 10 s) and 488 and 561 nm excitation light exposure (20 s). Scale bar: 10 μm. Green channel: λ_{ex} = 488 nm, λ_{em} = 499-551 nm. Red channel: λ_{ex} = 561 nm, λ_{em} = 571-625 nm. Ratiometric images were generated by dividing the intensity of green channel by that of red channel in each pixel. Maximum ratio: 0.8; minimum ratio: 0.1. **(b)** Time course of the ratio for fluorescence intensities of green channel to red channel with 365 nm irradiation (10 cycles). The fluorescence intensity ratio (I_{Green}/I_{Red}) was obtained from a random selection of 10 cells in three different cell plates (the number of replicates: N=3). **(c)** Quenching efficiency calculated from the data of **(b)**. The black **(b)** line and **(c)** dots represent the average ratio intensity and quenching efficiency from 10 different cells. Other pale-colored **(b)** lines and **(c)** dots describe each ratio intensity/quenching efficiency from each cell.

3. Supporting Tables

Table S1. Optical properties of FF

Solvent	PB, BSA(-)[*1]	Glycerol	Octanol	PB, BSA(+)
$\lambda_{max,c}$ [nm][*2]	529	529	500	514
$\varepsilon_{max,c}$ [$M^{-1}cm^{-1}$][*2]	6.1×10^{3}	5.1×10^{3}	6.4×10^{3}	6.4×10^{3}
k_{oc}/I_{irr} [s^{-1}/mW]	6.4×10^{-3}	5.2×10^{-3}	4.3×10^{-3}	8.9×10^{-3}
k_{co}/I_{irr} [s^{-1}/mW]	5.7×10^{-5}	2.8×10^{-4}	9.4×10^{-4}	8.4×10^{-4}
Φ_{OC}	0.72	0.24	0.42	0.91
Φ_{CO}	3.5×10^{-3}	1.6×10^{-2}	6.8×10^{-2}	5.2×10^{-2}

*[1]Quoted from ref. 7. *[2]maximam absorption wavelength ($\lambda_{max,c}$) and molar extinction coefficient ($\varepsilon_{max,c}$) of closed-ring form was recorded after light irradiation at 365 nm (10 mW/cm^2) for 10 min.

Table S2. Optical properties of Trp-BODIPY

Solvent	PB, BSA(-)	Glycerol	Octanol	PB, BSA(+)
$\lambda_{ex,max}$ [nm]	502	506	506	507
ε_{max} [$M^{-1}cm^{-1}$]	2.5×10^{4}	4.6×10^{4}	4.8×10^{4}	3.5×10^{4}
$\lambda_{em,max}$ [nm]	516	517	518	518
Φ_{FL}	4.5×10^{-3}	4.2×10^{-2}	2.6×10^{-2}	2.7×10^{-2}
Brightness [$M^{-1}cm^{-1}$]	1.1×10^{2}	1.9×10^{3}	1.2×10^{3}	9.5×10^{2}

Table S3. Optical properties of Trp-BODIPY-FF

Solvent		PB, BSA(-)	Glycerol	Octanol	PB, BSA(+)
$\lambda_{ex,max}$ [nm]	O*[1]	508	507	507	509
	C*[1]	507	507	507	509
ε_{max} [$M^{-1}cm^{-1}$]	O	2.3×10^{4}	5.3×10^{4}	5.2×10^{4}	4.7×10^{4}
	C	2.4×10^{4}	5.5×10^{4}	5.6×10^{4}	5.0×10^{4}
$\lambda_{em,max}$ [nm]	O	517	518	519	518
	C	517	518	519	518
Φ_{FL}	O	4.4×10^{-3}	4.9×10^{-2}	3.2×10^{-2}	2.9×10^{-2}
	C	2.2×10^{-3}	2.2×10^{-2}	1.1×10^{-2}	7.4×10^{-3}
Brightness [$M^{-1}cm^{-1}$]	O	1.0×10^{2}	2.6×10^{3}	1.7×10^{3}	1.4×10^{3}
	C	53	1.2×10^{3}	6.2×10^{2}	3.7×10^{2}
k_{oc}/I_{irr} [s^{-1}/mW]		7.0×10^{-3}	6.5×10^{-3}	9.2×10^{-3}	1.2×10^{-2}
k_{co}/I_{irr} [s^{-1}/mW]		2.3×10^{-3}	3.7×10^{-4}	4.0×10^{-3}	1.6×10^{-3}
Φ_{OC}		4.3×10^{-2}	3.1×10^{-2}	4.8×10^{-2}	5.0×10^{-2}
Φ_{CO}		5.1×10^{-3}	6.2×10^{-2}	0.11	0.16

*[1]O: open-ring form, C: closed-ring form obtained by irradiation at 365 nm (10 mW/cm^2) for 3 min.

Table S4. Optical properties of HTL-Trp-BODIPY-FF

Solvent		PB, Halo-tag(-)	Glycerol	Octanol	PB, Halo-tag(+)
$\lambda_{ex,max}$ [nm]	O*[1]	511	508	508	505
	C*[1]	510	508	508	505
ε_{max} [$M^{-1}cm^{-1}$]	O	2.6×10^{4}	4.5×10^{4}	5.0×10^{4}	3.4×10^{4}
	C	2.7×10^{4}	4.8×10^{4}	5.5×10^{4}	3.7×10^{4}
$\lambda_{em,max}$ [nm]	O	517	519	518	520
	C	517	519	518	520
Φ_{FL}	O	2.8×10^{-3}	6.5×10^{-2}	2.8×10^{-2}	3.0×10^{-2}
	C	1.5×10^{-3}	2.3×10^{-2}	1.1×10^{-2}	1.1×10^{-2}
Brightness [$M^{-1}cm^{-1}$]	O	73	2.9×10^{3}	1.4×10^{3}	1.0×10^{3}
	C	41	1.1×10^{3}	6.1×10^{2}	4.1×10^{2}
k_{oc}/I_{irr} [s^{-1}/mW]		6.2×10^{-3}	4.2×10^{-3}	9.5×10^{-3}	1.1×10^{-2}
k_{co}/I_{irr} [s^{-1}/mW]		3.5×10^{-3}	1.0×10^{-3}	4.4×10^{-3}	5.1×10^{-4}
Φ_{OC}		3.2×10^{-2}	1.5×10^{-2}	2.6×10^{-2}	7.1×10^{-2}
Φ_{CO}		9.9×10^{-3}	8.5×10^{-2}	0.12	0.14

*[1]O: open-ring form, C: closed-ring form obtained by irradiation at 365 nm (10 mW/cm^2) for 3 min.

Table S5. Comparison of photophysical properties of representative photoswitchable fluorescent proteins and HTL-Trp-BODIPY-FF

	rsEGFP2*[1]	Dronpa*[2]	Padron2*[3]	HTL-Trp-BODIPY-FF*[4]
$\lambda_{ex,max}$ [nm]*[5]	478	503	495	505
ε_{max} [$M^{-1}cm^{-1}$]*[5]	6.1×10^{4}	9.5×10^{4}	2.4×10^{4}	3.4×10^{4}
$\lambda_{em,max}$ [nm]*[5]	503	518	513	520
Φ_{FL}*[5]	0.30	0.85	0.49	3.0×10^{-2}
Brightness [$M^{-1}cm^{-1}$]	1.7×10^{4}	8.1×10^{4}	1.2×10^{4}	1.0×10^{3}
$\Phi_{ON\text{-}OFF}$*[6]	8.9×10^{-3}	3.2×10^{-4}	8.9×10^{-2}	7.1×10^{-2}
$\Phi_{OFF\text{-}ON}$*[6]	0.12	0.37	1.5×10^{-2}	0.14

*1: Cited from S13. *2: Cited from S14. *3: Cited from S15. *4: After labeling with Halo-tag. *5: ON state. *6: photoswitching quantum yield from ON to OFF state ($\Phi_{ON\text{-}OFF}$) and from OFF to ON state ($\Phi_{OFF\text{-}ON}$). $\Phi_{ON\text{-}OFF}$ and $\Phi_{OFF\text{-}ON}$ of HTL-Trp-BODIPY-FF are Φ_{OC} and Φ_{CO} respectively.

4. Synthetic Schemes

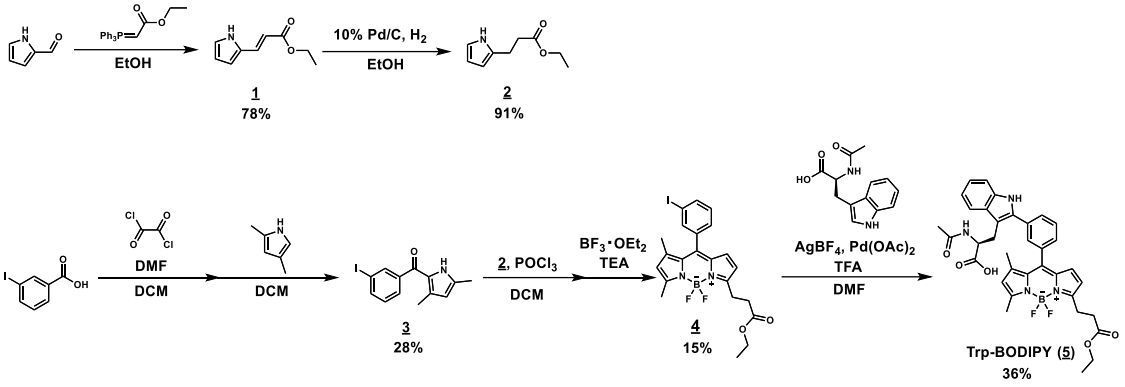

Scheme S1. Synthesis of Trp-BODIPY

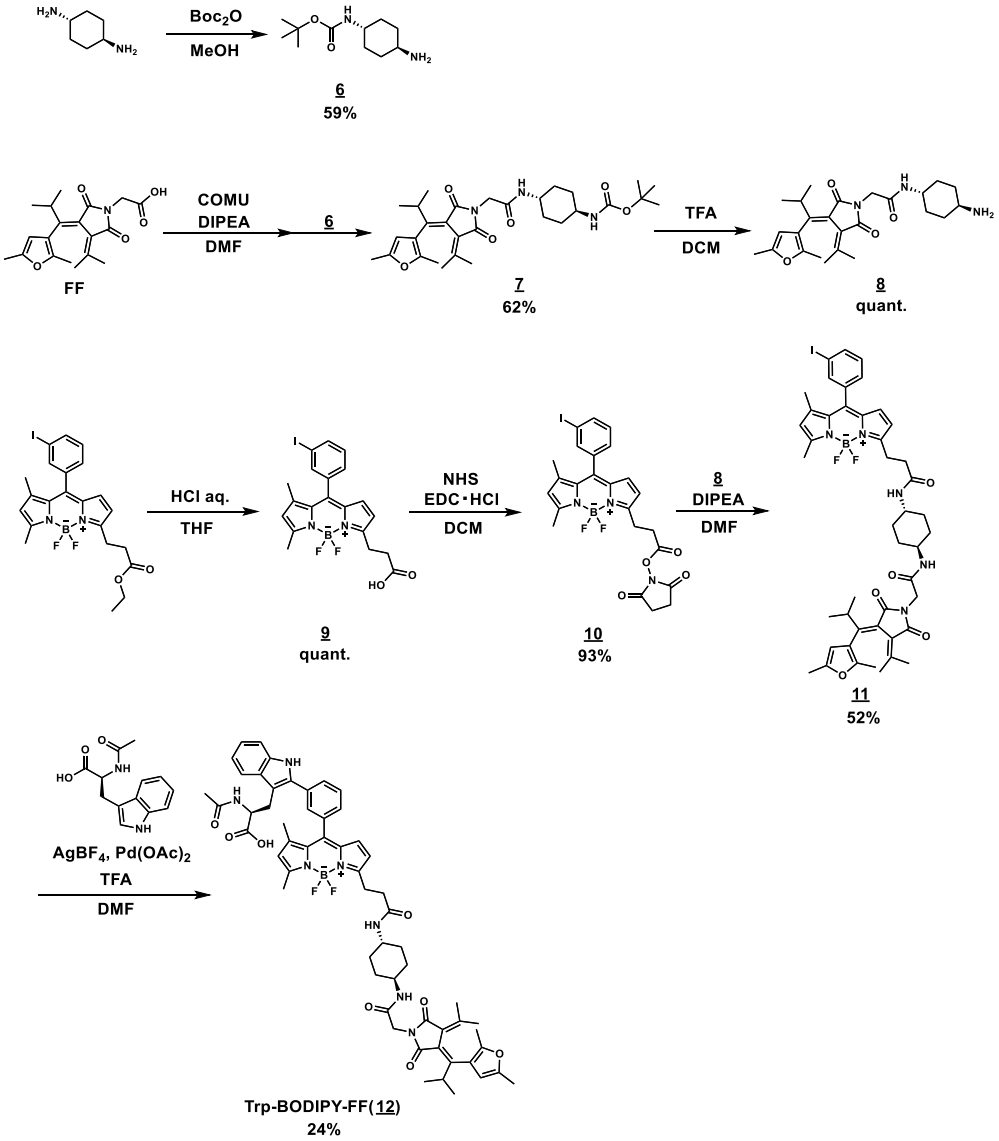

Scheme S2. Synthesis of Trp-BODIPY-FF

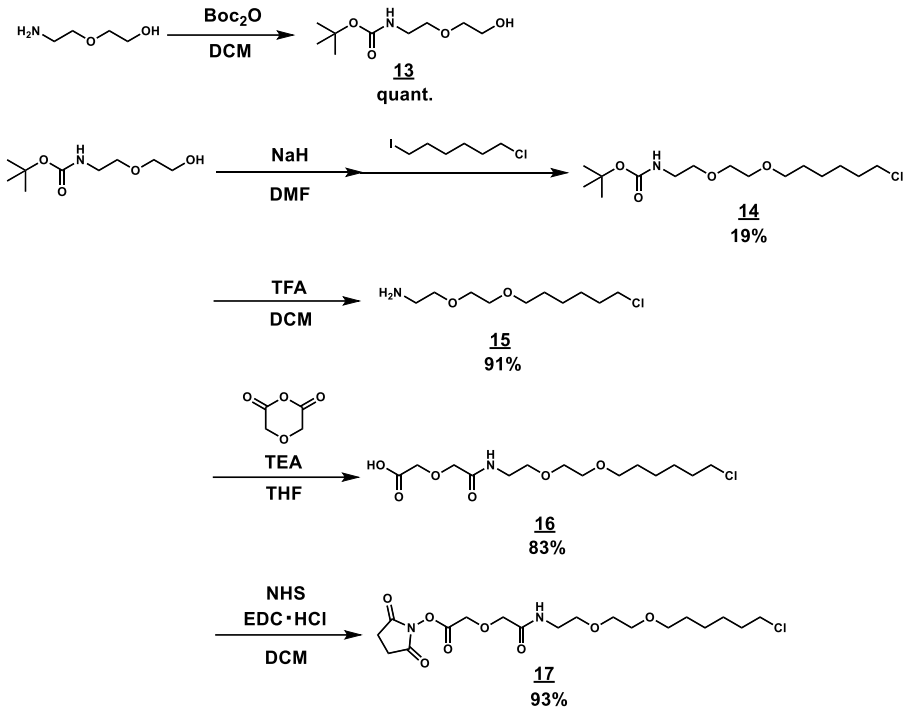

Scheme S3. Synthesis of Halo-tag ligand

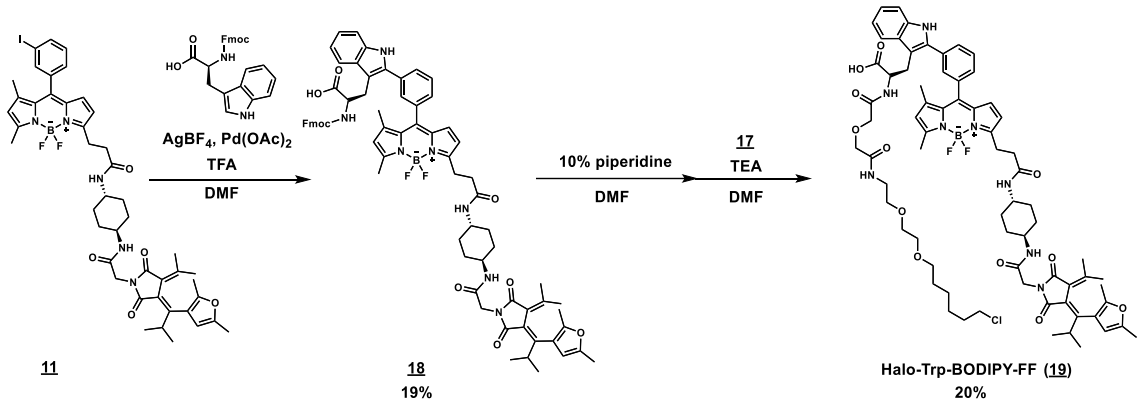

Scheme S4. Synthesis of HTL-Trp-BODIPY-FF

5. Synthetic Procedures

ethyl (*E*)-3-(1*H*-pyrrol-2-yl)acrylate, (1)

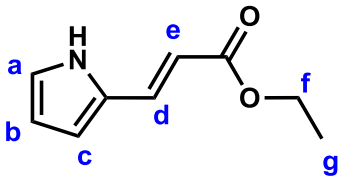

1*H*-pyrrole-2-carbaldehyde (800mg, 8.4 mmol, 1.0 eq) and ethyl (triphenylphosphoranylidene)acetate (3.70 g, 10.6 mmol, 1.3 eq.) were dissolved in ethanol (35 mL). The reaction mixture was heated to 80 °C and stirred for 36 h. After evaporating the solvent under vacuum, the crude product was purified using column chromatography (methanol/dichloromethane (DCM) = 1/200) to get compound 1 (1.08 g, 6.5 mmol, 78%) as a pale-yellow needle crystal. **^{1}H NMR, 500 MHz, $CDCl_3$** δ 8.84 (s(br), 1H, NH), 7.55 (d, J_{ed}= 15 Hz, 1H, e), 6.92 (m, 1H, b), 6.56 (m, 1H, a), 6.28 (m, 1H, c), 6.02 (d, J_{de}= 15 Hz, 1H, d), 4.24 (q, J_{fg}= 6.8 Hz, 2H, f), 1.32 (t, J_{gf}= 6.8 Hz, 3H, g). **^{13}C NMR, 125 MHz, $CDCl_3$** δ 167.78, 134.26, 128.47, 122.38, 114.29, 111.32, 110.96, 60.31, 14.37. **HRMS (ESI+)** [M＋Na^+] found: 188.0680, calculated: 188.0682.

ethyl 3-(1*H*-pyrrol-2-yl)propanoate, (2)

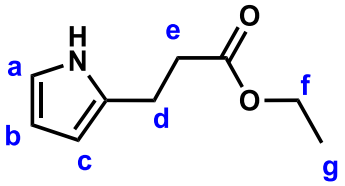

Palladium-activated carbon (Pd 10%) (100 mg) was added to a solution of compound 1 (1.08 g, 6.5 mmol, 1.0 eq.) in ethanol (15 mL). After performing three vacuum and nitrogen purging cycles, the reaction vessel was filled with hydrogen gas. The reaction mixture was stirred vigorously at room temperature for 5 h. Upon completion, celite filtration was conducted to remove palladium-activated carbon. The filtrate was evaporated to dryness by a rotary evaporator, and compound 2 (982 mg, 5.88 mmol, 91%) was obtained as a colorless oil without further purification.
^{1}H NMR, 500 MHz, $CDCl_3$ δ 8.54 (s(br), 1H, NH), 6.67 (m, 1H, b), 6.10 (m, 1H, a), 5.92 (m, 1H, c), 4.16 (q, J_{fg}=7.0 Hz, 2H, f), 2.91 (t, J_{ed}=7.0 Hz, 2H, e), 2.63 (t, J_{de}=6.8 Hz, 2H, d), 1.26 (t, J_{gf}=6.8 Hz, 3H, g).**^{13}C NMR, 125 MHz, $CDCl_3$** δ 174.17, 131.07, 116.78, 107.98, 105.50, 60.70, 34.61, 22.54, 14.19. **HRMS (EI+)** [M^+] found: 167.0942, calculated: 167.0946.

(3,5-dimethyl-1*H*-pyrrol-2-yl)(3-iodophenyl)methanone, (3)

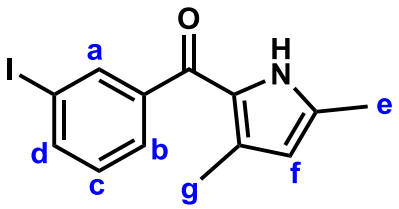

A solution of 3-iodobenzoic acid (3.0 g, 12.1 mmol, 1.0 eq.) in anhydrous DCM (80 mL) including 100 µL *N, N*-dimethylformamide (DMF) was added dropwise oxalyl chloride (1.5 mL, 17.5 mmol, 1.4 eq.) at 0 °C with stirring for 1 h. The solution was allowed to warm to room temperature with stirring for 4 h and then removed solvent using a rotary evaporator to afford crude 3-iodobenzoyl chloride which was used for the next reaction without further purification. The solution of 3-iodobenzoyl chloride in anhydrous DCM (40 mL) was added dropwise 2,4-dimethylpyrrole (1.2 mL, 12.1 mmol, 1.0 eq.) for 5 min. The mixture was stirred for 3 h and quenched with saturated $NaHCO_3$ aqueous solution. The organic layer was extracted with DCM three times. After washing the organic layer with brine and drying over Na_2SO_4, the residue was concentrated under reduced pressure. The crude product was purified using column chromatography (DCM/hexane = 2/5-4/5) to afford compound 3 (1.12 g, 3.44 mmol, 28%) as a pale-red powder.

^{1}H NMR, 500 MHz, $CDCl_3$ δ 8.95 (s(br), 1H, NH), 7.96 (m, 1H, a), 7.84 (m, 1H, d), 7.59 (m, 1H, b), 7.20 (m, 1H, c), 5.89 (m, 1H, f), 2.31(s, 3H, e), 1.93 (s, 3H, g). **^{13}C NMR, 125 MHz, $CDCl_3$** δ 183.64, 141.85, 139.67, 137.02, 136.09, 131.00, 130.04, 127.36, 127.21, 113.28, 93.93, 14.15, 13.23. **HRMS (MALDI)** [$M+H^+$] found: 326.0037, calculated: 326.0036.

ethyl 3-(5,5-difluoro-10-(3-iodophenyl)-7,9-dimethyl-5*H*-4λ^4,5λ^4-dipyrrolo[1,2-*c*:2',1'-*f*][1,3,2]diazaborinin-3-yl)propanoate, (4)

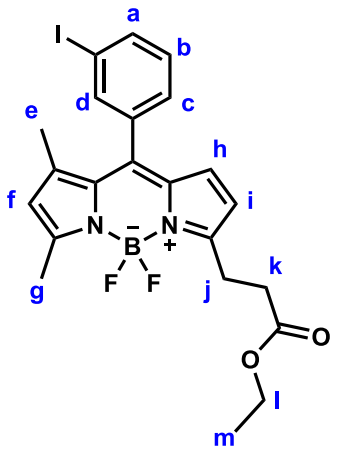

Compound 2 (860 mg, 5.15 mmol, 1.5 eq.) and compound 3 (1.12 g, 3.44 mmol, 1.0 eq.) were dissolved in anhydrous DCM (10 mL) and cooled to 0 °C under a nitrogen atmosphere. The reaction mixture was then added dropwise phosphoryl chloride (320 µL, 3.43 mmol, 1.0 eq.) and kept at 0 °C for 1 h. The solution was allowed to warm to room temperature with stirring for 18 h. After cooling the solution to 0 °C again, the mixture was then added to boron trifluoride - ethyl ether complex (5.2 mL, 41.2 mmol, 12 eq.) and triethylamine (4.8 mL, 34.3 mmol, 10 eq.) and gradually warmed to room temperature with stirring for 1 h. Upon completion, the reaction was quenched by adding a saturated $NaHCO_3$ aqueous solution, and the organic layer was extracted with DCM three times. After washing the organic layer with brine and drying it using Na_2SO_4, the solvent was removed under reduced pressure. The crude product was purified using column chromatography (DCM/hexane = 1/1) to get compound 4 (264 mg, 506 µmol, 15%) as a red-brown oil.

^{1}H NMR, 500 MHz, $CDCl_3$ δ 7.83 (ddd, J_{ab}=7.5 Hz, J_{ac}=1.5 Hz, J_{ad}=1.0 Hz, 1H, a), 7.71 (dd, J_{da}=1.5 Hz, J_{dc}=1.5 Hz, 1H, d), 7.31 (ddd, J_{cb}=7.5 Hz, J_{ca}=1.5 Hz, J_{cd}=1.5 Hz, 1H, c), 7.21 (dd, J_{ca}=1.5 Hz, J_{cd}=1.5 Hz, 1H, b), 6.36 (d, J_{hi}=4.0 Hz, 1H, h), 6.23 (d, J_{ih}=4.0 Hz, 1H, i), 6.09 (s, 1H, f), 4.15 (q, J_{lm}=7.5 Hz, 2H, l), 3.31 (t, J_{jk}=7.5 Hz, 2H, j), 2.77 (t, J_{kj}=7.5 Hz, 2H, k), 2.60 (s, 3H, e), 1.54 (s, 3H, g), 1.26 (t, J_{ml}=7.5 Hz, 3H, m). **^{13}C NMR, 125 MHz, $CDCl_3$** δ 172.53, 160.11, 157.14, 144.93, 139.81, 138.24, 137.51, 136.12, 134.60, 132.22, 130.00, 128.42, 128.11, 122.74, 116.68, 93.76, 60.58, 33.45, 23.92, 14.99, 14.22. **HRMS (MALDI)** [M+Na$^+$] found: 545.0682, calculated: 545.0679.

Trp-BODIPY, (5)

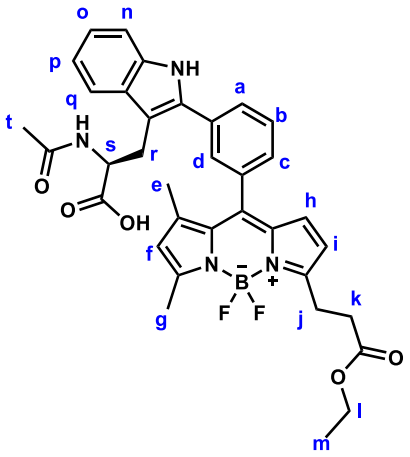

Acetyl-*L*-tryptophan (9.5 mg, 38.3 µmol, 1.0 eq.), palladium(II) acetate (1.8 mg, 7.7 µmol, 0.2 eq.), silver(I) tetrafluoroborate (7.6 mg, 38.3 µmol, 1.0 eq.), compound 4 (20.0 mg, 38.3 µmol, 1.0 eq.), and trifluoroacetic acid (2.9 µL, 38.3 µmol, 1.0 eq.) were dissolved in DMF (2 mL). The reaction mixture was placed under microwave irradiation at 80 °C for 30 min. After the reaction, celite filtration was conducted to remove metal complexes. The filtrate was evaporated to dryness using a rotary evaporator and purified using reverse-phase chromatography (0.1% formic acid acetonitrile/water= 50/50-95/5). After lyophilization, compound 5 (8.9 mg, 13.9 µmol, 36%) was obtained as an orange powder.

^{1}H NMR, 500 MHz, acetone-d6 δ 10.49 (s, 1H, COOH), 7.96 (m, 1H, a), 7.76 (m, 2H, d and p), 7.69 (m, 1H, n), 7.46 (m, 1H, b), 7.38 (m, 1H, o), 7.23 (m, 1H, NH(indole)), 7.13 (m, 1H, c), 7.05 (m, 1H, q), 6.58 (d, 1H, J_{hi}=5.0 Hz, h), 6.35 (d, J_{ih}=5.0 Hz, 1H, i), 6.27 (s, 1H, f), 4.82 (m, 2H, r), 4.13 (q, J_{lm}=7.5 Hz, 2H, l), 3.48 (m, 2H, s), 3.28 (t, J_{jk}=7.5 Hz, 2H, j), 2.78 (t, J_{kj}=7.5 Hz, 2H, k), 2.58 (s, 3H, e), 1.76 (d, 3H, g), 1.70 (d, 3H, t), 1.63 (s, 3H, g), 1.23 (dt, J_{ml}=7.5 Hz, 3H, m) **^{13}C NMR, 125 MHz, CD_3OD** δ 173.48, 172.71, 170.04, 160.52, 157.62, 146.34, 142.98, 137.36, 135.73, 135.61, 135.44, 134.63, 133.18, 130.29, 130.10, 129.97, 129.89, 129.63, 129.16, 128.83, 123.44, 122.94, 120.10, 117.40, 111.94, 109.36, 60.90, 53.88, 33.67, 28.30, 24.57, 22.72, 15.15, 14.94, 14.55. **HRMS (MALDI)** [M+Na^+] found: 663.2569, calculated: 663.2561.

***tert*-butyl ((1*r*,4*r*)-4-aminocyclohexyl)carbamate, (6)**

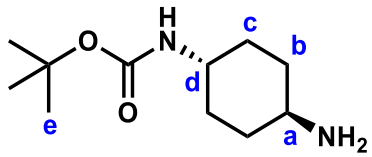

A solution of *trans*-1,4-cyclohexanediamine (500 mg, 4.39 mmol, 3.6 eq.) in methanol (15 mL) was added dropwise di-*tert*-butyl decarbonate (280 µL, 1.22 mmol, 1.0 eq.) at room temperature with stirring for 2 h. The solvent was removed under reduced pressure and dissolved in ethyl acetate and water. The organic layer was extracted with ethyl acetate three times, washed with brine, and dried over by Na_2SO_4. After removing the solvent, compound 6 (157 mg, 715 µmol, 59%) was afforded as a white powder.

^{1}H NMR, 500 MHz, $CDCl_3$ δ 4.35 (m, 1H, NH), 3.38 (s(br), 1H, a), 2.62 (s(br), 1H, d), 1.90 (m, 4H, b and c), 1.43 (s, 9H, e), 1.18 (s, 4H, b and c). **^{13}C NMR, 125 MHz, $CDCl_3$** δ 155.27, 79.15, 49.95, 49.25, 35.39, 32.22, 28.42. **HRMS (MALDI)** [M+Na^+] found: 237.1579, calculated: 237.1574.

(E)-2-(3-(1-(2,5-dimethylfuran-3-yl)-2-methylpropylidene)-2,5-dioxo-4-(propan-2-ylidene)pyrrolidin-1-yl)acetic acid (FF)

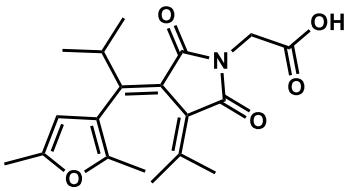

FF was synthesized following the previously reported method [S[3]].

***tert*-butyl ((1*r*,4*r*)-4-(2-((*E*)-3-(1-(2,5-dimethylfuran-3-yl)-2-methylpropylidene)-2,5-dioxo-4-(propan-2-ylidene)pyrrolidin-1-yl)acetamido)cyclohexyl)carbamate, (7)**

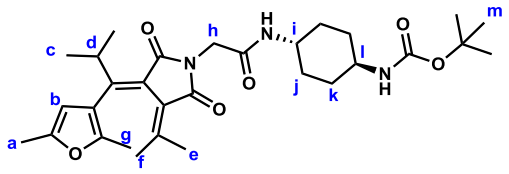

A solution of FF (543 mg, 1.57 mmol, 1.0 eq.) in anhydrous DMF (12 mL) was added a solution of 1-[(1-(Cyano-2-ethoxy-2-oxoethylideneaminooxy) dimethylaminomorpholino)] uronium hexafluorophosphate (1.01 g, 2.36 mmol, 1.5 eq.) and *N*, *N*-diisopropylethylamine (543 µL, 3.12 mmol, 2.0 eq.) in DMF (10 mL) and stirred at room temperature for 30 min. The mixture was then added to a solution of compound 6 (337 mg, 1.57 mmol, 1.0 eq.) at room temperature with stirring for 1 h under a nitrogen atmosphere. After confirming the reaction was completely proceeded by TLC plate monitoring, the solvent was removed by a rotary evaporator. The crude product was washed with water and then extracted with DCM three times, washed with brine, and dried over Na_2SO_4. After removing the solvent, the crude product was purified using column chromatography (ethyl acetate/hexane = 1/10-1/1) to get compound 7 (510 mg, 943 µmol, 62%) as a white powder.

^{1}H NMR, 500 MHz, $CDCl_3$ δ 5.93 (d, 1H, b), 5.64 (d, 1H, NH), 4.47 (sept, J_{dc}=7.0 Hz, 1H, d), 4.43 (m, 1H, NH), 4.21 (m, 2H, h), 3.73 (m, 1H, i), 3.40 (s(br), 1H, l), 2.25 (s, 3H, a), 2.25 (s, 3H, e), 2.00 (m, 4H, j and k), 1.87 (s, 3H, g), 1.43 (s, 9H, m), 1.35 (s, 3H, f), 1.29 (d, J_{cd}=7.5 Hz, 3H, c), 1.21 (m, 4H, j and k), 0.84 (d, J_{cd}=7.5 Hz, 3H, c). **^{13}C NMR, 125 MHz, $CDCl_3$** δ 167.82, 167.74, 165.68, 155.24, 153.33, 149.93, 149.93, 148.97, 147.01, 123.20, 123.07, 119.48, 106.29, 48.82, 48.05, 40.81, 31.90, 31.57, 29.93, 28.41, 27.08, 22.84, 21.96, 20.64, 13.34, 12.75. **HRMS (MALDI)** [M+Na^+] found: 564.3047, calculated: 564.3044.

***N*-((1*r*,4*r*)-4-aminocyclohexyl)-2-((*E*)-3-(1-(2,5-dimethylfuran-3-yl)-2-methylpropylidene)-2,5-dioxo-4-(propan-2-ylidene)pyrrolidin-1-yl)acetamide, (8)**

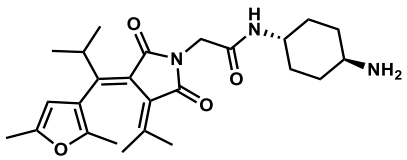

A solution of compound 7 (255 mg, 471 µmol) in DCM (10 mL) was added dropwise trifluoroacetic acid (2 mL) and stirred at room temperature for 1 h. After removing the solvent, compound 8 (208 mg, 471 µmol, quant.) was afforded as a red oil which was used for the next reaction without further purification.

HRMS (MALDI) [M+Na^+] found: 464.2520, calculated: 464.2520.

3-(5,5-difluoro-10-(3-iodophenyl)-7,9-dimethyl-5*H*-4λ^4,5λ^4-dipyrrolo[1,2-*c*:2',1'-*f*][1,3,2]diazaborinin-3-yl)propanoic acid, (9)

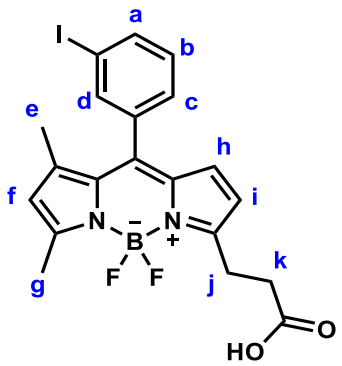

A solution of compound 4 (264 mg, 506 μmol) in tetrahydrofuran (30 mL) was added to 2M HCl aqueous solution (30 mL). The mixture was stirred at room temperature for 60 h. After confirming the hydrolysis was completely proceeded by TLC plate monitoring, the organic layer was extracted with DCM three times. After washing the organic layer with brine and drying it using Na_2SO_4, the solvent was removed under reduced pressure. The hydrolysis product, compound 5 (248 mg, 502 μmol, quant.) was obtained as a red oil without further purification.

^{1}H NMR, 500 MHz, $CDCl_3$ δ 7.84 (ddd, J_{ab}=7.5 Hz, J_{ac}=1.5 Hz, J_{ad}=1.0 Hz, 1H, a), 7.71 (dd, J_{da}=1.5 Hz, J_{dc}=1.5 Hz, 1H, d), 7.32 (ddd, J_{cb}=7.5 Hz, J_{ca}=1.5 Hz, J_{cd}=1.5 Hz, 1H, c), 7.21 (d, J_{ba}=7.5 Hz, J_{bc}=7.5 Hz, 1H, b), 6.36 (d, J_{hi}=4.0 Hz, 1H, h), 6.24 (d, J_{ih}=4.0 Hz, 1H, i), 6.10 (s, 1H, f), 3.32 (t, J_{jk}=7.5 Hz, 2H, j), 2.84 (t, J_{kj}=7.5 Hz, 2H, k), 2.60 (s, 3H, e), 1.55 (s, 3H, g). **^{13}C NMR, 125 MHz, $CDCl_3$** δ 176.05, 160.47, 156.37, 145.17, 139.92, 138.60, 138.29, 137.52, 136.09, 134.65, 132.38, 130.02, 128.35, 128.12, 122.88, 116.64, 93.78, 32.77, 23.66, 15.01. **HRMS (MALDI)** [M+Na$^+$] found: 517.0362, calculated: 517.0366.

2,5-dioxopyrrolidin-1-yl 3-(5,5-difluoro-10-(3-iodophenyl)-7,9-dimethyl-5*H*-4λ^4,5λ^4-dipyrrolo[1,2-*c*:2',1'-*f*][1,3,2]diazaborinin-3-yl)propanoate, (10)

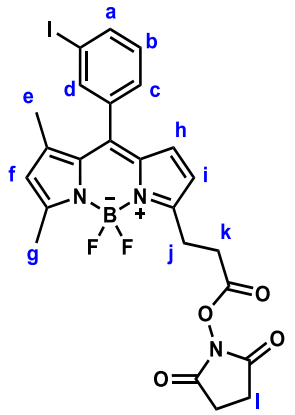

A solution of compound 9 (161 mg, 327 µmol, 1.0 eq.) in anhydrous DCM (10 mL) was added *N*-hydroxysuccinimide (56.4 mg, 490 µmol, 1.5 eq.) and 1-(3-dimethylaminopropyl)-3-ethylcarbodiimide hydrochloride (74.9 mg, 392 µmol, 1.2 eq.) at room temperature and stirred for 1 h under the nitrogen atmosphere. Upon completion of the reaction, the mixture was washed with water three times. The organic layer was then washed with brine and dried over Na_2SO_4. After removing the solvent under reduced pressure, compound 10 (179 mg, 304 µmol, 93%) was afforded as a red oil. **^{1}H NMR, 500 MHz, $CDCl_3$** δ 7.84 (ddd, J_{ab}=7.5 Hz, J_{ac}=1.5 Hz, J_{ad}=1.0 Hz, 1H, a), 7.72 (dd, J_{da}=1.5 Hz, J_{dc}=1.5 Hz, 1H, d), 7.32 (ddd, J_{cb}=7.5 Hz, J_{ca}=1.5 Hz, J_{cd}=1.5 Hz, 1H, c), 7.22 (dd, J_{ba}=7.5 Hz, J_{bc}=7.5 Hz, 1H, b), 6.37 (d, J_{hi}=4.0 Hz, 1H, h), 6.30 (d, J_{ih}=4.0 Hz, 1H, i), 6.11 (s, 1H, f), 3.40 (t, J_{jk}=7.5 Hz, 2H, j), 3.10 (t, J_{kj}=7.5 Hz, 2H, k), 2.84 (s, 4H, l), 2.60 (s, 3H, e), 1.55 (s, 3H, g). **^{13}C NMR, 125 MHz, $CDCl_3$** δ 169.49, 169.03, 168.99, 167.83, 160.94, 154.61, 145.52, 140.09, 138.32, 137.48, 135.99, 134.68, 132.54, 130.03, 128.29, 128.10, 123.06, 116.78, 93.79, 30.36, 25.59, 23.33, 15.06. **HRMS (MALDI)** [M+Na$^+$] found: 614.0535, calculated: 614.0530.

3-(5,5-difluoro-10-(3-iodophenyl)-7,9-dimethyl-5*H*-4λ^4,5λ^4-dipyrrolo[1,2-*c*:2',1'-*f*][1,3,2]diazaborinin-3-yl)-*N*-((1*r*,4*r*)-4-(2-((*E*)-3-(1-(2,5-dimethylfuran-3-yl)-2-methylpropylidene)-2,5-dioxo-4-(propan-2-ylidene)pyrrolidin-1-yl)acetamido)cyclohexyl)propenamide, (11)

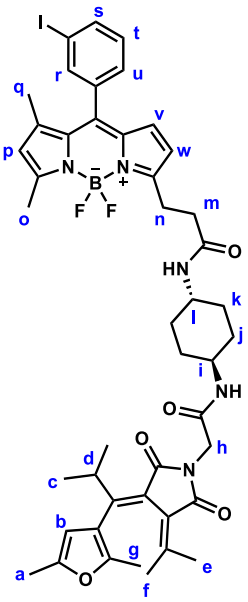

A solution of compound 10 (210 mg, 355 µmol, 1.0 eq.) in anhydrous DCM (10 mL) was added to a solution of compound 8 (208 mg, 471 µmol, 1.3 eq.), and *N*, *N*-diisopropylethylamine (500 µL, 2.87 mmol, 8.1 eq.) in anhydrous DCM (5 mL) at room temperature under nitrogen atmosphere. The reaction mixture was stirred at 40 °C for 1 h. Upon completion of the reaction, the residue was concentrated by using a rotary evaporator. The crude product was purified using column chromatography (ethyl acetate/hexane= 1/1-3/1) to obtain compound 11 (168 mg, 183 µmol, 52%) as a red solid.

^{1}H NMR, 500 MHz, $CDCl_3$ δ 7.83 (ddd, J_{st}=7.5 Hz, J_{su}=1.5 Hz, J_{sr}=1.0 Hz, 1H, s), 7.69 (dd, J_{rs}=1.0 Hz, J_{ru}=1.5 Hz, 1H, r), 7.30 (ddd, J_{ut}=7.5 Hz, J_{us}=1.5 Hz, J_{ur}=1.5 Hz, 1H, u), 7.23 (dd, J_{ts}=7.5 Hz, J_{tu}=7.5 Hz, 1H, t), 6.35 (d, J_{vw}=4.0 Hz, 1H, v), 6.23 (d, J_{wv}=4.0 Hz, 1H, w), 6.11 (s, 1H, p), 5.93 (s, 1H, b), 5.63 (s, 2H, NH), 4.47 (sept, J_{dc}=7.0 Hz, 1H, d), 4.20 (m, 2H, h), 3.70 (m, 2H, i and l), 3.26 (t, J_{nm}=7.5 Hz, 2H, n), 2.72 (s, 3H, q), 2.63 (t, J_{mn}=7.5 Hz, 2H, m), 2.59 (s, 3H, o), 2.25 (s, 3H, f), 2.24 (s, 3H, e), 2.00-1.80 (m, 4H, k and j), 1.87 (s, 3H, g), 1.35 (s, 3H, a), 1.28 (d, J_{cd}=7.0 Hz, 3H, c), 1.25-1.10 (m, 4H, k and j), 0.84 (d, J_{cd}=7.0 Hz, 3H, c). **^{13}C NMR, 125 MHz, $CDCl_3$** δ 171.68, 171.30, 167.84, 165.79, 160.27, 156.73, 153.39, 149.94, 149.03, 147.02, 145.30, 139.88, 138.33, 137.48, 135.96, 134.60, 132.24, 130.10, 128.51, 128.07, 123.17, 119.48, 117.46, 106.29, 93.83, 60.43, 47.94, 47.36, 40.81, 35.97, 31.43, 29.93, 27.09, 25.41, 24.79, 22.85, 21.97, 21.07, 20.65, 15.05, 14.20, 13.94, 12.76. **HRMS (FAB+)** [M+Na^+] found: 940.2898, calculated: 940.2888.

Trp-BODIPY-FF, (12)

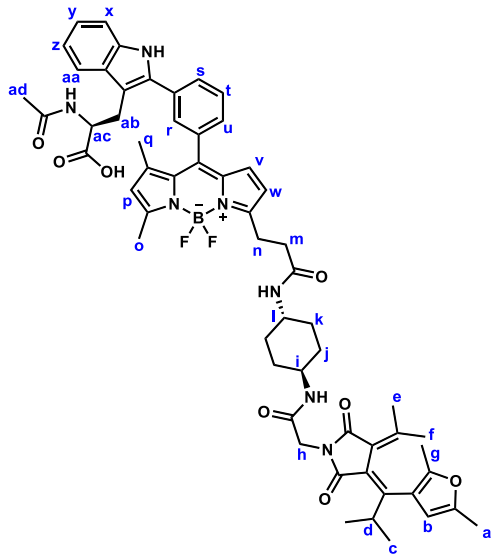

Acetyl-*L*-tryptophan (16 mg, 65.4 µmol, 1.0 eq.), palladium(II) acetate (3.0 mg, 13.1 µmol, 0.2 eq.), silver(I) tetrafluoroborate (13 mg, 65.4 µmol, 1.0 eq.), compound 11 (60 mg, 65.4 µmol, 1.0 eq.), and trifluoroacetic acid (5.0 µL, 65.4 µmol, 1.0 eq.) were dissolved in DMF (2 mL). The reaction mixture was placed under microwave irradiation at 80 °C for 30 min. After the reaction, celite filtration was conducted to remove metal complexes. The filtrate was evaporated to dryness using a rotary evaporator and purified using reverse-phase chromatography (0.1% formic acid acetonitrile/water= 60/40-95/5). After lyophilization, compound 12 (16.3 mg, 15.7 µmol, 24%) was obtained as an orange powder.

^{1}H NMR, 500 MHz, acetone-d6 δ 10.50 (d, 1H, COOH), 7.95 (m, 1H, s), 7.75 (m, 2H, r and aa), 7.68 (dd, J_{ts}=7.5 Hz, J_{tu}=7.5 Hz, 1H, t), 7.45 (m, 1H, x), 7.38 (d, J_{vw}=4.0 Hz, 1H, v), 7.27 (d, J_{wv}=4.0 Hz, 1H, w), 7.25 (m, 1H, NH(indole)), 7.12 (m, 2H, u and y), 7.05 (ddd, J_{zy}=7.5 Hz, J_{zaa}=7.5 Hz, J_{zx}=1.5 Hz, 1H, z), 6.56 (dd, 1H, NH), 6.32 (t, 1H, NH), 6.25 (s, 1H, p), 6.10 (s, 1H, b), 4.81 (m, 1H, ac), 4.54 (sept, J_{dc}=7.0 Hz, 1H, d), 4.18 (m, 2H, h), 3.70-3.60 (m, 2H, i and l), 3.55-3.35 (m, 2H, ab), 3.26 (m, 2H, n), 2.58 (t, J_{mn}=7.5 Hz, 2H, m), 2.56 (s, 3H, o), 2.25 (s, 3H, f), 2.22 (s, 3H, e), 2.00-1.80 (m, 4H, k and j), 1.88 (s, 3H, g), 1.75 (d, J=6.5 Hz, 3H, q), 1.62 (s, 3H, ad), 1.36 (s, 3H, a), 1.29 (m, J_{cd}=7.0 Hz, 3H, c), 1.35-1.20 (m, 4H, k and j), 0.82 (d, J_{cd}=7.0 Hz, 3H, c). **^{13}C NMR, 125 MHz, acetone-d6** δ 173.49, 171.19, 170.06, 168.29, 166.10, 159.87, 159.12, 152.10, 150.85, 147.80, 147.57, 145.87, 142.81, 137.38, 135.68, 135.52, 134.63, 132.95, 130.31, 129.97, 129.85, 129.27, 128.91, 125.04, 124.51, 123.20, 122.94, 120.24, 120.10, 117.82, 111.97, 109.46, 107.33, 53.93, 48.85, 48.44, 40.71, 35.50, 32.20, 32.17, 28.32, 28.29, 27.00, 25.19, 23.14, 22.74, 21.63, 20.91, 15.13, 15.10, 114.93, 13.28, 12.78. **MS (MALDI)** [M-F^{-}] found: 1016.4957, calculated: 1016.4893, [M+Na^{+}] found: 1058.4830, calculated: 1058.4775.

***tert*-butyl (2-(2-hydroxyethoxy)ethyl)carbamate, (13)**

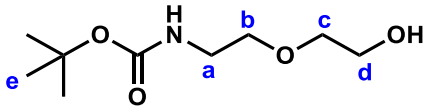

A solution of 2-(2-aminoethoxy)ethan-1-ol (10.0 g, 95.1 mmol, 1.0 eq.) in DCM (40 mL) was added dropwise di-*tert*-butyl decarbonate (22.8 g, 105 mmol, 1.1 eq.) at room temperature with stirring for 18 h. After concentrating the residue using a rotary evaporator, the crude product was washed with water and extracted with ethyl acetate three times. The organic layer was washed with brine and dried over Na_2SO_4. The solvent was removed under reduced pressure, and compound 13 (19.5 g, 94.9 mmol, quant.) was afforded as a colorless oil.

^{1}H NMR, 500 MHz, $CDCl_3$ δ 3.73 (m, 2H, a), 3.56 (m, 4H, b, c), 3.32 (t, J_{de}=5.5 Hz, 2H, d), 1.44 (s, 9H, e) **^{13}C NMR, 125 MHz, $CDCl_3$** δ 156.11, 79.43, 72.18, 70.32, 61.77, 40.37, 28.55, 28.40. **HRMS (FAB+)** [M+Na^+] found: 228.1208, calculated: 228.1212.

***tert*-butyl (2-(2-((6-chlorohexyl)oxy)ethoxy)ethyl)carbamate, (14)**

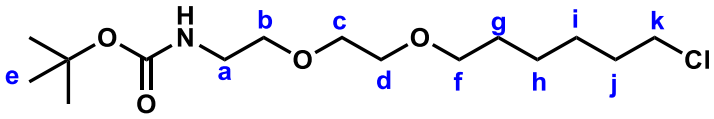

Compound 13 (2.20 g, 10.7 mmol, 1.0 eq.) was dissolved in anhydrous tetrahydrofuran (8 mL) and DMF (4 mL) and cooled to 0 °C. The mixture was added sodium hydride, 60% oil dispersion (470 mg, 11.8 mmol, 1.1 eq.), and stirred at 0 °C for 30 min under a nitrogen atmosphere. The mixture was added 1-chloro-6-iodohexane (2.63 g, 10.7 mmol, 1.0 eq.) and gradually warmed to room temperature with stirring for 18 h. The reaction was quenched by adding saturated NH_4Cl aqueous solution. The organic layer was extracted with ethyl acetate three times. After drying over Na_2SO_4, the solvent was removed under reduced pressure. The crude product was purified using column chromatography (ethyl acetate/hexane = 1/10-1/3) to afford compound 14 (660 mg, 2.04 mmol, 19%) as a colorless oil.

^{1}H NMR, 500 MHz, $CDCl_3$ δ 4.99 (s(br), 1H, NH), 3.65-3.50 (m, 8H, b-f), 3.49 (t, J_{kj}=7.0 Hz, 2H, k), 3.34 (t, 2H, a), 1.80 (m, 2H, g), 1.64 (m, 4H, h and H_2O), 1.44 (s, 9H, e), 1.50-1.35 (m, 4H, g and i). **^{13}C NMR, 125 MHz, $CDCl_3$** δ 156.01, 71.30, 70.29, 70.23, 70.04, 45.05, 40.38, 32.54, 29.44, 28.43, 26.69, 25.54. **HRMS (FAB+)** [M+Na^+] found: 346.1751, calculated: 346.1761.

2-(2-((6-chlorohexyl)oxy)ethoxy)ethan-1-amine, (15)

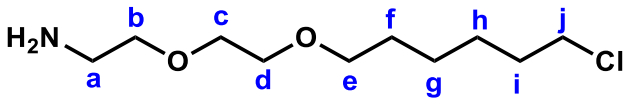

Compound 14 (200 mg, 619 µmol) was dissolved in DCM (10 mL) at 0 °C. The solution was added dropwise trifluoroacetic acid (2 mL) and allowed to warm to room temperature and stirred for 2 h. Upon completion, the reaction was quenched by adding 1M sodium hydroxide aqueous solution (1 mL). The crude product was washed with water and brine. After drying over Na_2SO_4, the solvent was removed under reduced pressure, and compound 15 (127 mg, 566 µmol, 91%) was obtained as a colorless oil.

^{1}H NMR, 500 MHz, $CDCl_3$ δ 3.60-3.55 (m, 4H, d and e), 3.55-3.50 (m, 4H, b and c), 3.47 (t, 2H, j), 2.87 (m, 2H, a), 1.78 (m, 2H, f), 1.61 (m, 2H, i), 1.52 (s(br), 2H, H_2O), 1.45-1.35 (m, 4H, g and h). **^{13}C NMR, 125 MHz, $CDCl_3$** δ 73.46, 71.27, 70.35, 70.09, 45.06, 41.80, 32.55, 29.47, 26.70, 25.44. **HRMS (FAB+)** [M+H$^+$] found: 224.1416 (^{35}Cl), calculated: 224.1412**.**

18-chloro-5-oxo-3,9,12-trioxa-6-azaoctadecanoic acid, (16)

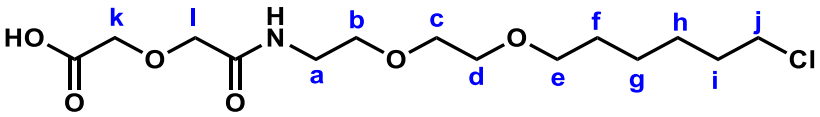

A solution of compound 15 (138 mg, 614 µmol, 1.0 eq.) and triethylamine (112µL, 805 µmol, 1.3 eq.) in anhydrous tetrahydrofuran (10 mL) was added 1,4-dioxane-2,6-dione (86 mg, 743 µmol, 1.2 eq.) at room temperature with stirring for 2 h. Upon completion, the residue was concentrated by using a rotary evaporator and washed with saturated $NaHCO_3$ aqueous solution three times. The water layer was added to 2 M HCl aqueous solution until the pH=1 and then extracted with ethyl acetate three times. After washing with brine and drying over Na_2SO_4, the solvent was removed under reduced pressure and compound 16 (174 mg, 513 µmol, 83%) was obtained as a colorless oil.

^{1}H NMR, 500 MHz, $CDCl_3$ δ 7.72 (s, 1H, NH), 4.18 (s, 2H, k), 4.15 (s, 2H, l), 3.65-3.50 (m, 12H, a, b, c, d, e, and j), 1.78 (m, 2H, f), 1.67 (m, 2H, i), 1.45-1.35 (m, 4H, g and h). **^{13}C NMR, 125 MHz, $CDCl_3$** δ 171.29, 169.93, 72.71, 71.50, 70.58, 70.25, 69.97, 69.80, 60.42, 45.00, 38.96, 32.45, 28.77, 26.58, 25.16, 21.06, 20.43, 14.20. **HRMS (FAB+)** [M+H$^+$] found: 340.1524 (^{35}Cl), calculated: 340.1528.

2,5-dioxopyrrolidin-1-yl 18-chloro-5-oxo-3,9,12-trioxa-6-azaoctadecanoate, (17)

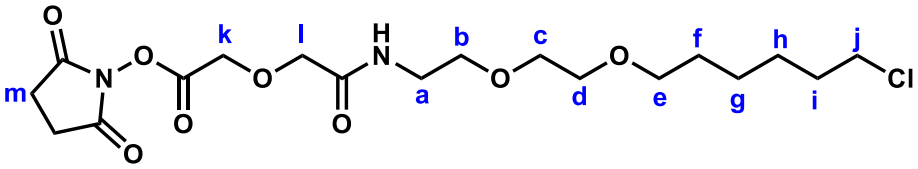

A solution of compound 16 (174 mg, 513 µmol, 1.0 eq.) in anhydrous DCM (5 mL) was added *N*-hydroxysuccinimide (89 mg, 769 µmol, 1.5 eq.) and 1-(3-dimethylaminopropyl)-3-ethylcarbodiimide hydrochloride (118 mg, 616 µmol, 1.2 eq.) at room temperature and stirred for 2 h under nitrogen atmosphere. Upon completion of the reaction, the mixture was washed with water three times. The organic layer was then washed with brine and dried over Na_2SO_4. After removing the solvent under reduced pressure, compound 17 (209 mg, 477 µmol, 93%) was afforded as a colorless oil. **^{1}H NMR, 500 MHz, $CDCl_3$** δ 6.92 (s, 1H, NH), 4.52 (s, 2H, k), 4.16 (s, 2H, l), 3.65-3.50 (m, 10H, a-e), 3.46 (t, 2H, j), 2.87 (s, 4H, m), 1.78 (m, 2H, f), 1.60 (m, 4H, i and H_2O), 1.45-1.35 (m, 4H, g and h). **^{13}C NMR, 125 MHz, $CDCl_3$** δ 168.51, 168.00, 165.14, 71.28, 71.16, 70.36, 70.04, 69.66, 66.26, 45.10, 38.72, 32.53, 29.45, 26.69, 25.58, 25.42. **HRMS (FAB+)** [$M+H^+$] found: 437.1705 (^{35}Cl), calculated: 437.1691.

(*S*)-2-((((9*H*-fluoren-9-yl)methoxy)carbonyl)amino)-3-(2-(3-(7-(3-(((1*r*,4*r*)-4-(2-((*E*)-3-(1-(2,5-dimethylfuran-3-yl)-2-methylpropylidene)-2,5-dioxo-4-(propan-2-ylidene)pyrrolidin-1-yl)acetamido)cyclohexyl)amino)-3-oxopropyl)-5,5-difluoro-1,3-dimethyl-5*H*-4λ^4,5λ^4-dipyrrolo[1,2-*c*:2',1'-*f*][1,3,2]diazaborinin-10-yl)phenyl)-1*H*-indol-3-yl)propanoic acid, (18)

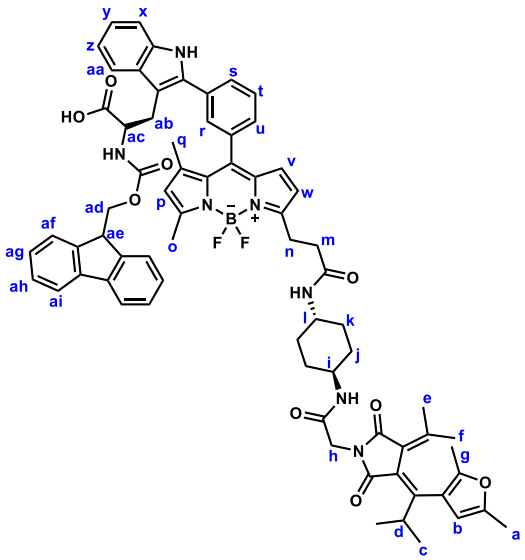

(((9*H*-fluoren-9-yl)methoxy)carbonyl)-*L*-tryptophan (49.5 mg, 116 µmol, 1.0 eq.), palladium(II) acetate (5.5 mg, 24.4 µmol, 0.2 eq.), silver(I) tetrafluoroborate (22.8 mg, 116 µmol, 1.0 eq.), compound 11 (107 mg, 116 µmol, 1.0 eq.), and trifluoroacetic acid (9.0 µL, 116 µmol, 1.0 eq.) were dissolved in DMF (4 mL). The reaction mixture was placed under microwave irradiation at 80 °C for 30 min. After the reaction, celite filtration was conducted to remove metal complexes. The filtrate was evaporated to dryness using a rotary evaporator and purified using reverse phase chromatography (0.1% formic acid acetonitrile/water= 75/25-95/5). After lyophilization, compound 18 (26.4 mg, 21.7 µmol, 19%) was obtained as an orange powder.

^{1}H NMR, 500 MHz, acetone-d6 δ 10.53 (d, 1H, COOH), 7.96 (m, 1H, s), 7.81 (m, 4H, t, aa, and af), 7.65 (dd, J_{rs}=3.0 Hz, J_{ru}=3.0 Hz, 1H, r), 7.58 (m, 2H, af), 7.40 (m, 4H, v, x, and ah), 7.26 (m, 3H, w and ag), 7.13 (dd, J_{yx}=7.5 Hz, J_{yz}=7.5 Hz, 1H, y), 7.05 (m, 2H, u and z), 6.56 (m, 2H, NH and NH(indole)), 6.29 (d, J_{yx}=4.0 Hz, 1H, NH), 6.20 (d, J=12 Hz, 1H, p), 6.10 (s, 1H, b), 4.63 (q, 1H, ac), 4.54 (sept, J_{dc}=7.0 Hz, 1H, d), 4.18 (m, 2H, h), 4.14 (m, 3H, ad and ae), 3.70-3.60 (m, 3H, i and l), 3.50 (dt, 1H, ab), 3.25 (m, 2H, n), 2.55 (m, 5H, m and o), 2.25 (s, 3H, f), 2.22 (s, 3H, e), 2.00-1.80 (m, 4H, k and j), 1.88 (s, 3H, g), 1.61 (d, J=5.0 Hz, 3H, q), 1.36 (s, 3H, a), 1.35-1.20 (m, 7H, c, k and j), 0.82 (d, J_{cd}=7.0 Hz, 3H, c). **^{13}C NMR, 125 MHz, acetone-d6** δ 173.55, 171.05, 168.28, 166.07, 159.77, 159.11, 156.69, 152.08, 150.83, 147.78, 147.54, 145.78, 144.99, 142.76, 141.99, 137.42, 135.70, 135.56, 134.55, 132.92, 130.30, 129.89, 129.19, 128.87, 128.47, 127.93, 126.23, 125.04, 124.50, 123.15, 122.98, 120.73, 120.39, 120.21, 120.09, 117.78, 112.01, 109.51, 107.32, 67.24, 55.77, 55.66, 48.85, 48.38, 47.89, 40.69, 35.51, 32.20, 32.16, 29.21, 28.22, 26.99, 25.16, 23.12, 21.62, 20.90, 15.11, 14.90, 13.27, 12.77. **HRMS (ESI+)** [M^+] found: 1238.5356, calculated: 1238.5345.

HTL-Trp-BODIPY-FF, (19)

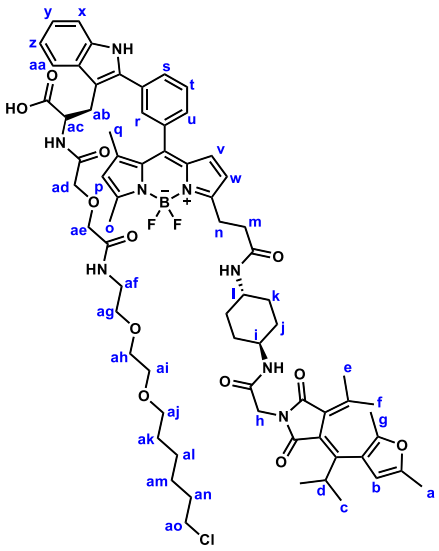

A solution of compound 18 (15.0 mg, 12.3 μmol, 1.0 eq.) in anhydrous DMF (100 μL) was added to a solution of piperidine (20 μL, 203 μmol, 16.5 eq.) in anhydrous DMF (100 μL) at room temperature with stirring for 5 min. Upon completion, the reaction was quenched by adding a saturated NH_4Cl aqueous solution. The organic layer was extracted with ethyl acetate three times, washed with brine, and dried over Na_2SO_4. The solvent was removed using a rotary evaporator and the crude deprotected product (H_2N-Trp-BODIPY-FF) was used for the next reaction without further purification. H_2N-Trp-BODIPY-FF was dissolved in anhydrous DMF (3 mL) and then added a solution of compound 17 (9.0 mg, 20.6 μmol, 1.7 eq.) and *N*, *N*-diisopropylethylamine (100 μL, 574 μmol, 47 eq.) under nitrogen atmosphere. The mixture was stirred at 40 °C for 2 h. Upon completion, the residue was concentrated under reduced pressure, and purified using reversed-phase chromatography (0.1% formic acid acetonitrile/water=65/35-95/5). After lyophilization, compound 19 (3.3 mg, 2.47 μmol, 20%) was obtained as an orange powder.

^{1}H NMR, 500 MHz, acetone-d6 δ 10.53 (s, 1H, COOH), 7.95 (m, 1H, s), 7.75 (dd, J_{rs}=4.0 Hz, J_{ru}=4.0 Hz, 1H, r), (ddd, J_{ut}=7.5 Hz, J_{ur}=1.5 Hz, J_{us}=1.5 Hz, 1H, u), 7.70 (ddd, J_{ts}=7.5 Hz, J_{tu}=7.5 Hz, J_{tr}=1.0 Hz, 1H, t), 7.53 (dd, 1H, NH(indole)), 7.45 (m, 1H, v), 7.39 (m, 1H, w), 7.29 (m, 2H, NH), 7.16 (ddd, J_{yx}=7.5 Hz, J_{yz}=7.5 Hz, J_{yaa}=1.5 Hz, 1H, y), 7.09 (m, 2H, z and aa), 6.58 (m, 1H, NH), 6.34 (m, 1H, NH), 6.25 (s, 1H, p), 6.11 (s, 1H, b), 4.81 (m, 1H, ac), 4.54 (sept, J_{dc}=7.0 Hz, 1H, d), 4.18 (m, 2H, h), 3.90-3.75 (m, 4H, i, l, and ac), 3.70-3.45 (m, 12H, ab, ae, and ag-aj), 3.40 (m, 1H, m), 3.26 (m, 2H, n), 2.58 (t, J_{mn}=7.5 Hz, 2H, m), 2.56 (s, 3H, q), 2.25 (s, 3H, f), 2.22 (s, 3H, e), 2.00-1.80 (m, 4H, k and j), 1.88 (s, 3H, g), 1.72 (m, 2H, ak), 1.63 (d, J=2.5 Hz, 3H, q), 1.52 (m, 2H, an), 1.43-1.37 (m, 2H, al), 1.36 (s, 3H, a), 1.35-1.25 (m, 9H, c, k, j, and am), 0.82 (d, J_{cd}=7.0 Hz, 3H, c). **^{13}C NMR, 125 MHz, acetone-d6** δ 173.09, 171.11, 171.07, 169.36, 168.28, 166.03, 159.80, 159.16, 152.08, 150.84, 147.78, 147.53, 145.77, 142.73, 137.37, 135.69, 135.54, 134.51, 132.97, 130.25, 129.99, 129.22, 128.89, 125.03, 124.50, 122.99, 120.39, 120.17, 120.03, 117.94, 122.04, 109.24, 107.32, 71.59, 71.53, 71.35, 70.92, 70.82, 70.26, 53.63, 53.50, 48.85, 48.39, 45.76, 40.68, 39.38, 35.51, 33.35, 32.20, 32.16, 29.20, 28.00, 27.36, 26.99, 26.16, 25.19, 23.14, 21.61, 20.90, 15.09, 14.93, 13.27, 12.77. **HRMS (ESI+)** [M+Na^+] found: 1337.6008, calculated: 1337.6007.

6. NMR spectra

Solvent peaks and trace impurities (if observed) are characterized using ref. S16.

ethyl (E)-3-(1H-pyrrol-2-yl)acrylate, (1)

^{1}H-NMR, $CDCl_3$ (7.26 ppm), residual water (1.69 ppm)

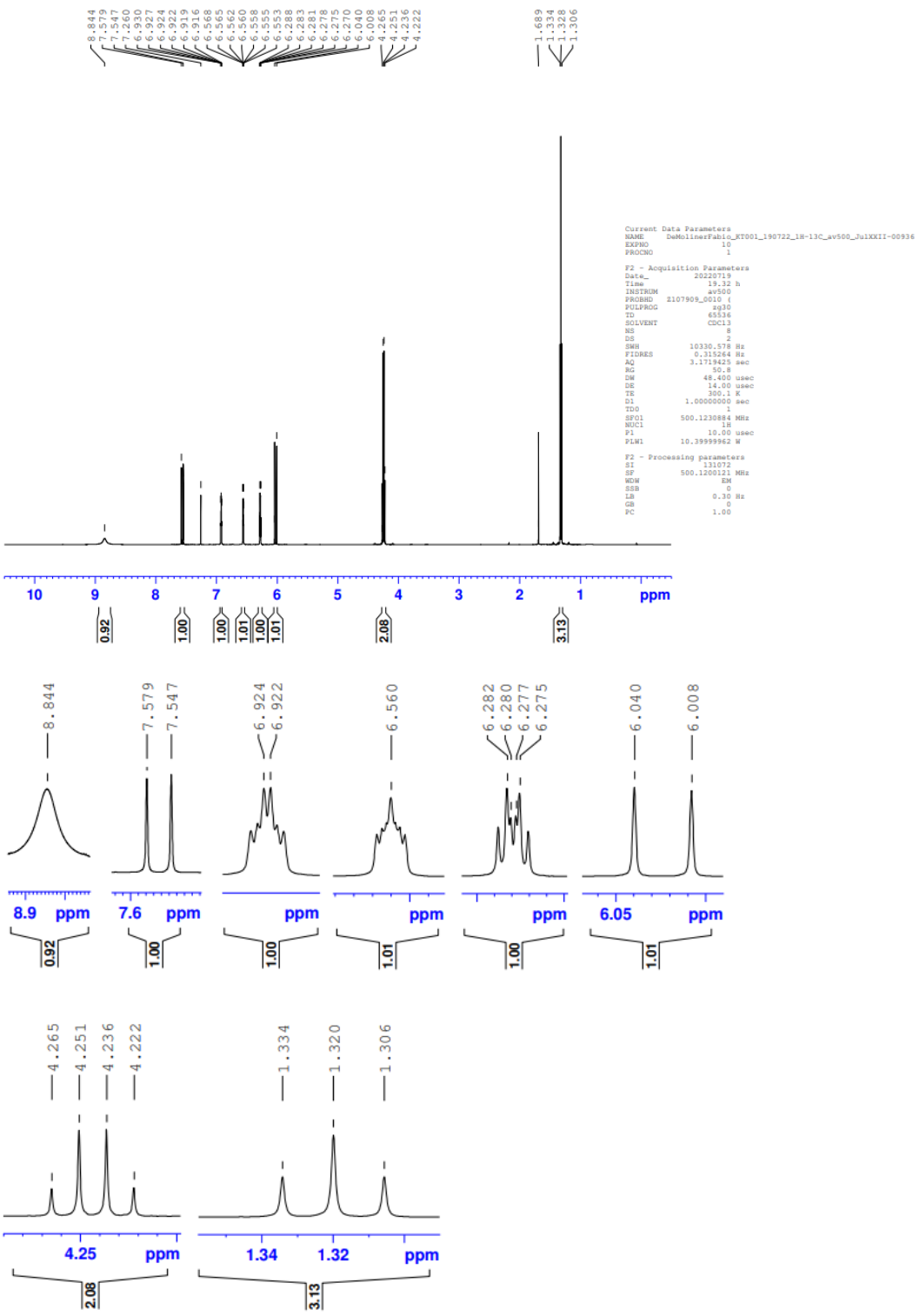

^{13}C-NMR, $CDCl_3$ (77.03 ppm)

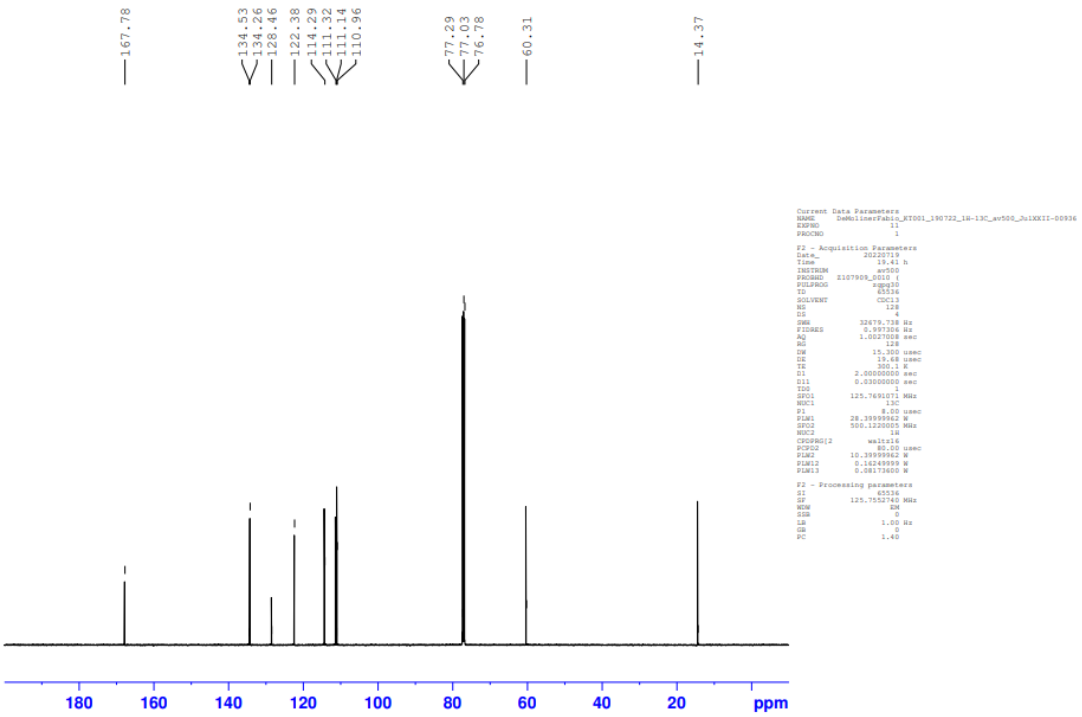

ethyl 3-(1*H*-pyrrol-2-yl)propanoate, (2)

^{1}H-NMR, $CDCl_3$ (7.26 ppm), residual water (1.57 ppm)

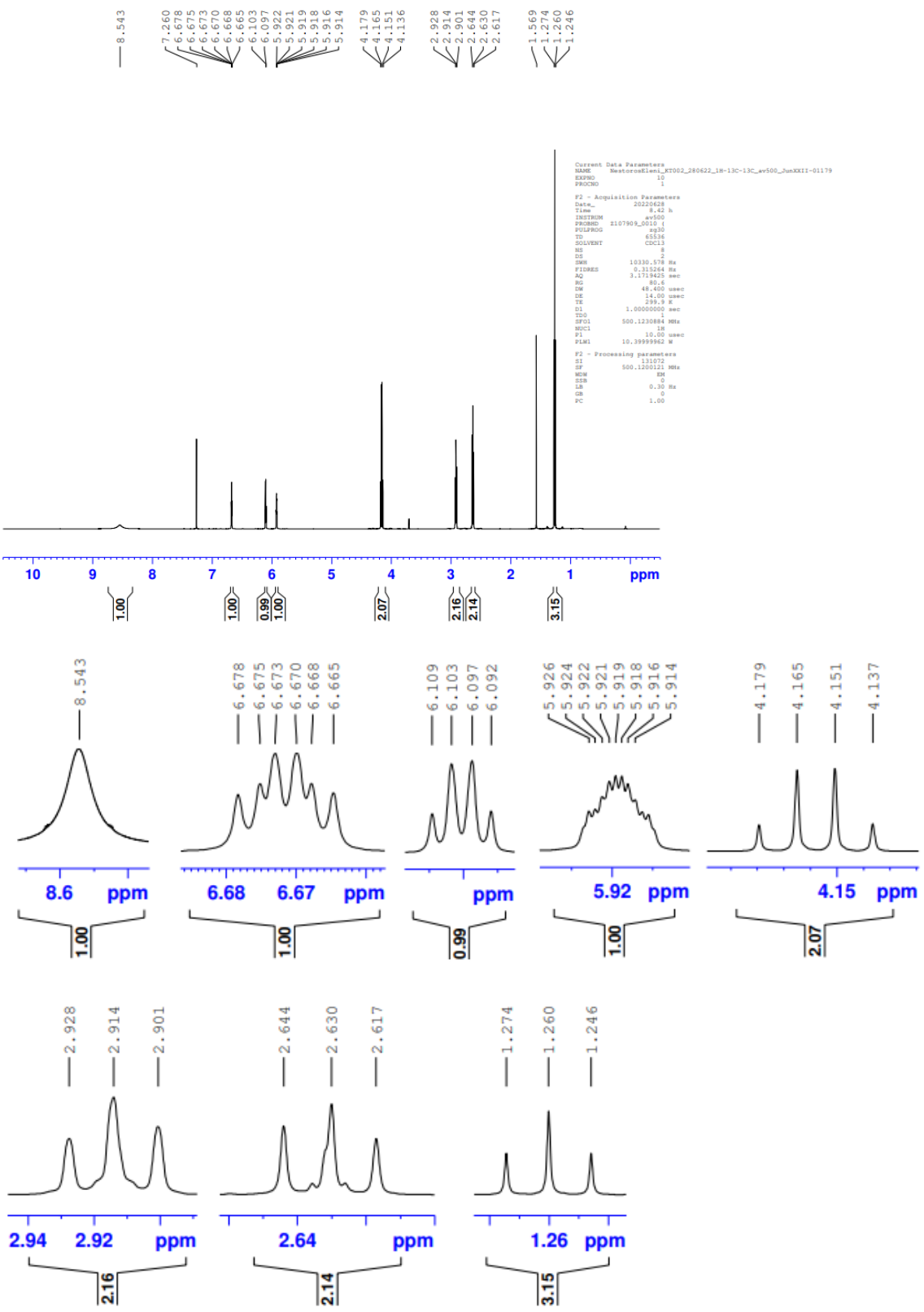

^{13}C-NMR, $CDCl_3$ (77.02 ppm)

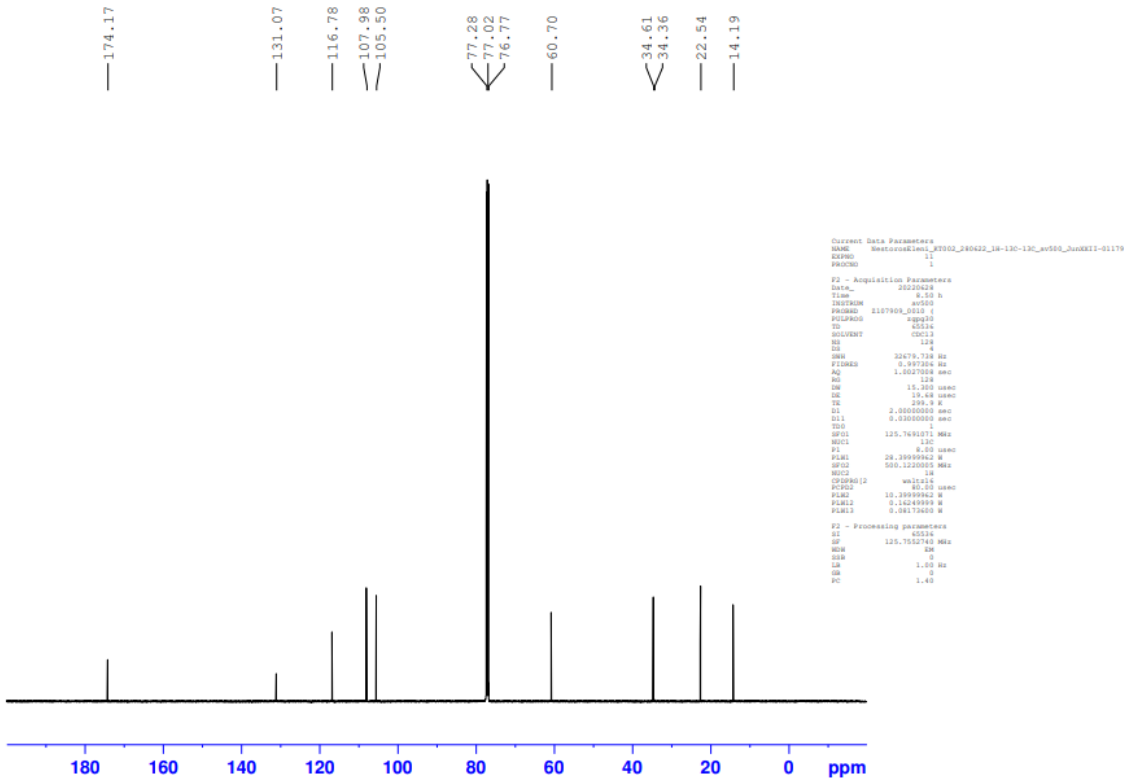

(3,5-dimethyl-1*H*-pyrrol-2-yl)(3-iodophenyl)methanone, (3)

^{1}H-NMR, $CDCl_3$ (7.26 ppm), residual water (1.59 ppm)

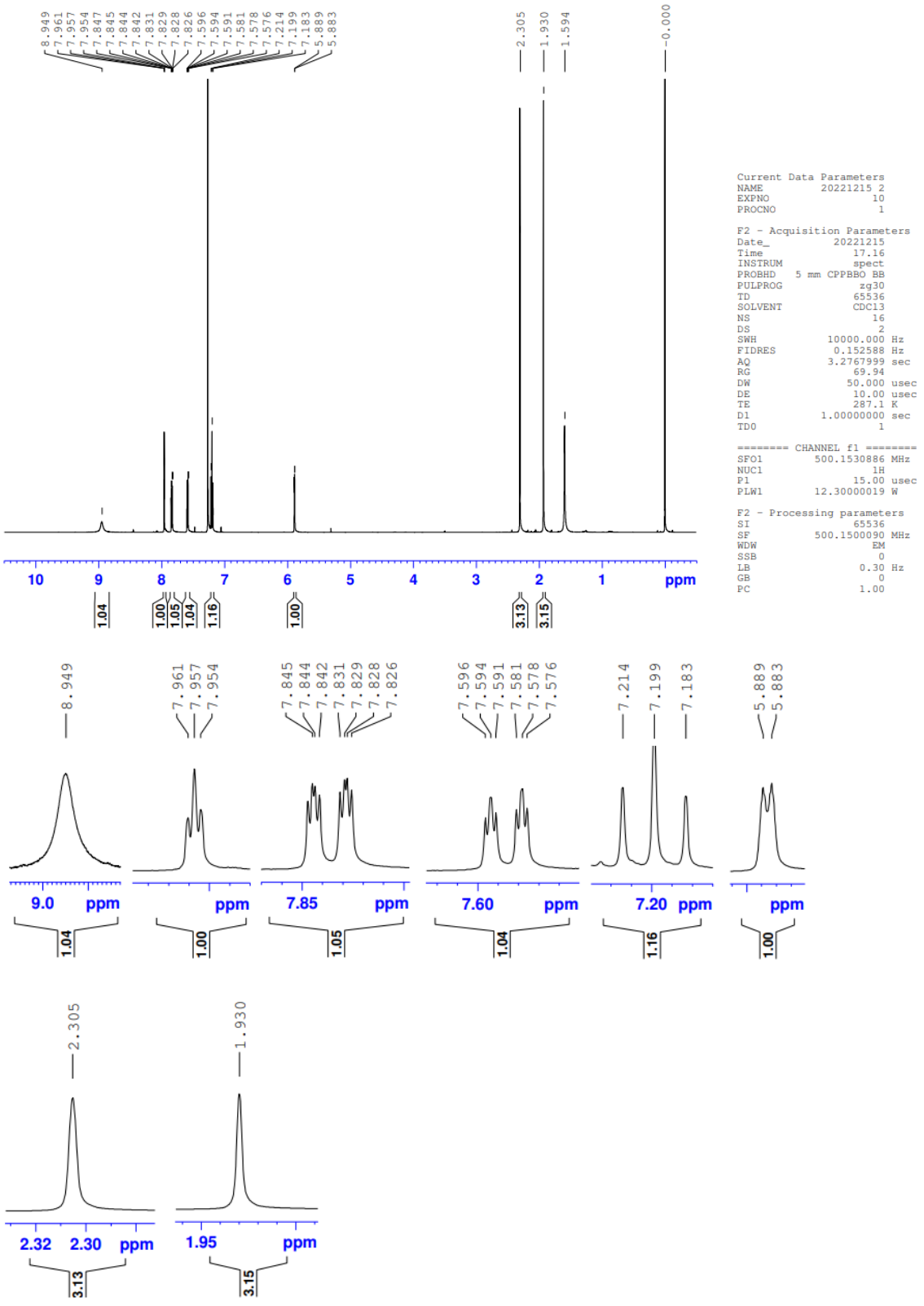

^{13}C-NMR, $CDCl_3$ (77.01 ppm)

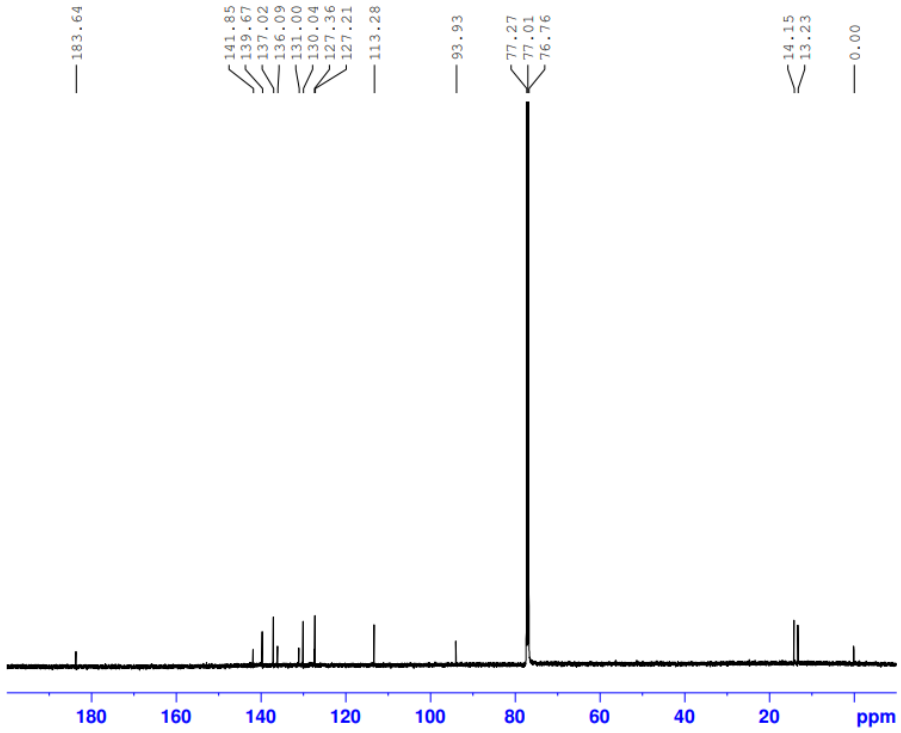


```
Current Data Parameters
NAME      20221215 compl3c
EXPNO               10
PROCNO               1

F2 - Acquisition Parameters
Date_          20221215
Time              18.30
INSTRUM           spect
PROBHD   5 mm CPPBBO BB
PULPROG         zgpg30
TD               65536
SOLVENT          CDCl3
NS                1024
DS                   4
SWH           29761.904 Hz
FIDRES        0.454131 Hz
AQ            1.1010048 sec
RG               197.07
DW               16.800 usec
DE               18.00 usec
TE               287.1 K
D1            2.00000000 sec
D11           0.03000000 sec
TD0                  1

======== CHANNEL f1 ========
SFO1        125.7753932 MHz
NUC1                13C
P1                10.00 usec
PLW1        77.00000000 W

======== CHANNEL f2 ========
SFO2        500.1520006 MHz
NUC2                1H
CPDPRG[2         waltz16
PCPD2             80.00 usec
PLW2        12.30000019 W
PLW12        0.43241999 W
PLW13        0.27675000 W

F2 - Processing parameters
SI                32768
SF          125.7628228 MHz
WDW                 EM
SSB                  0
LB                1.00 Hz
GB                   0
PC                1.40
```

ethyl 3-(5,5-difluoro-10-(3-iodophenyl)-7,9-dimethyl-5*H*-4λ^4,5λ^4-dipyrrolo[1,2-*c*:2',1'-*f*][1,3,2]diazaborinin-3-yl)propanoate, (4)

^{1}H-NMR, $CDCl_3$ (7.26 ppm)

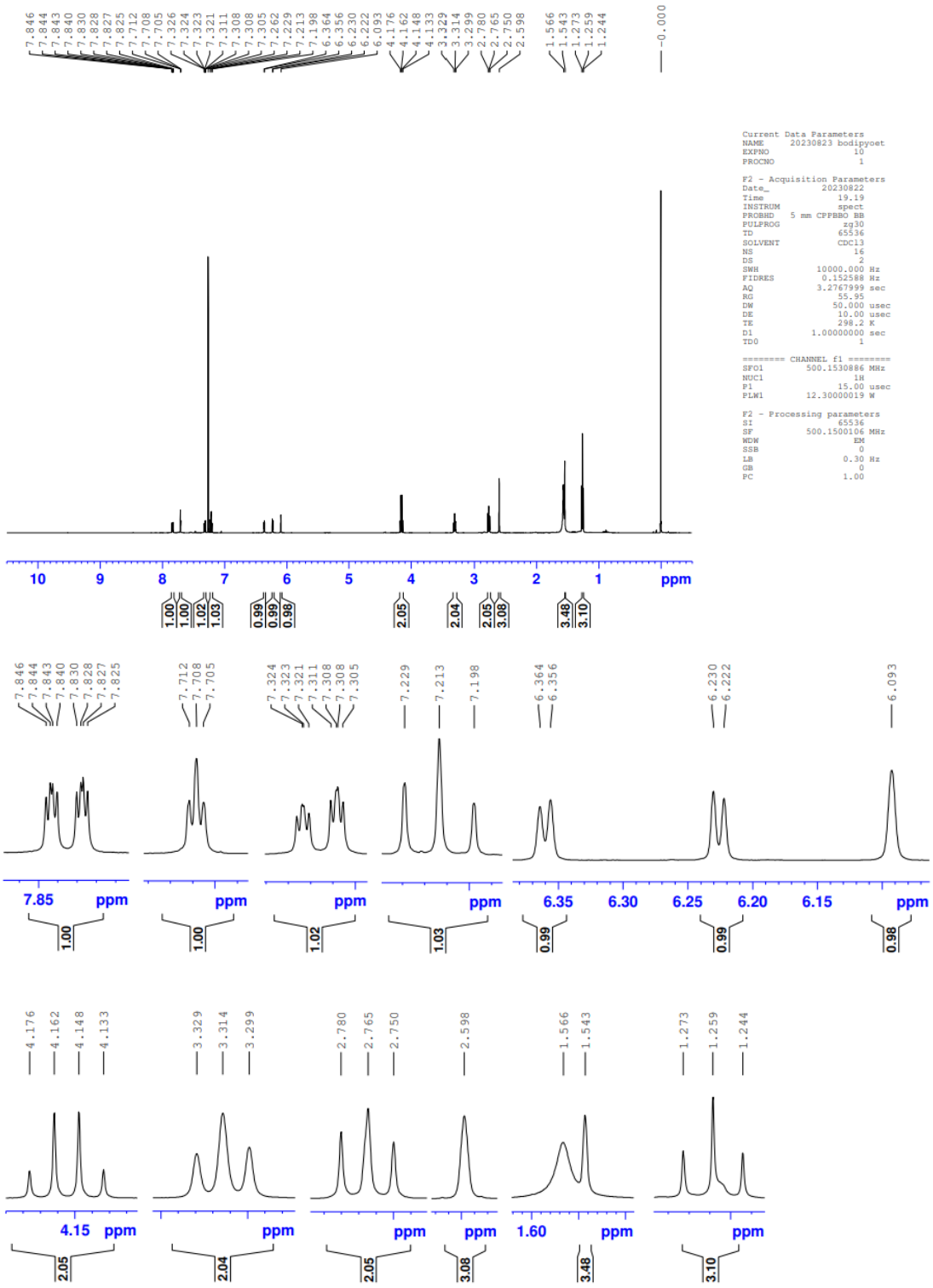

^{13}C-NMR, $CDCl_3$ (77.01 ppm)

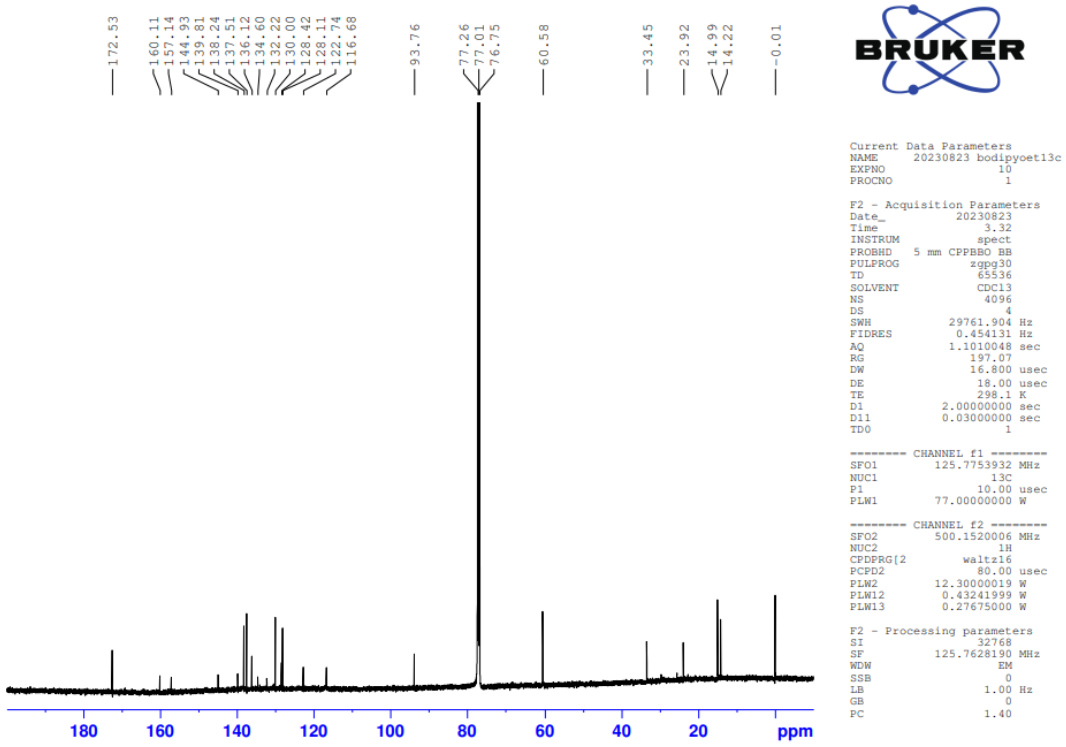

Trp-BODIPY, (5)

^{1}H-NMR, acetone-d6 (2.06 ppm)

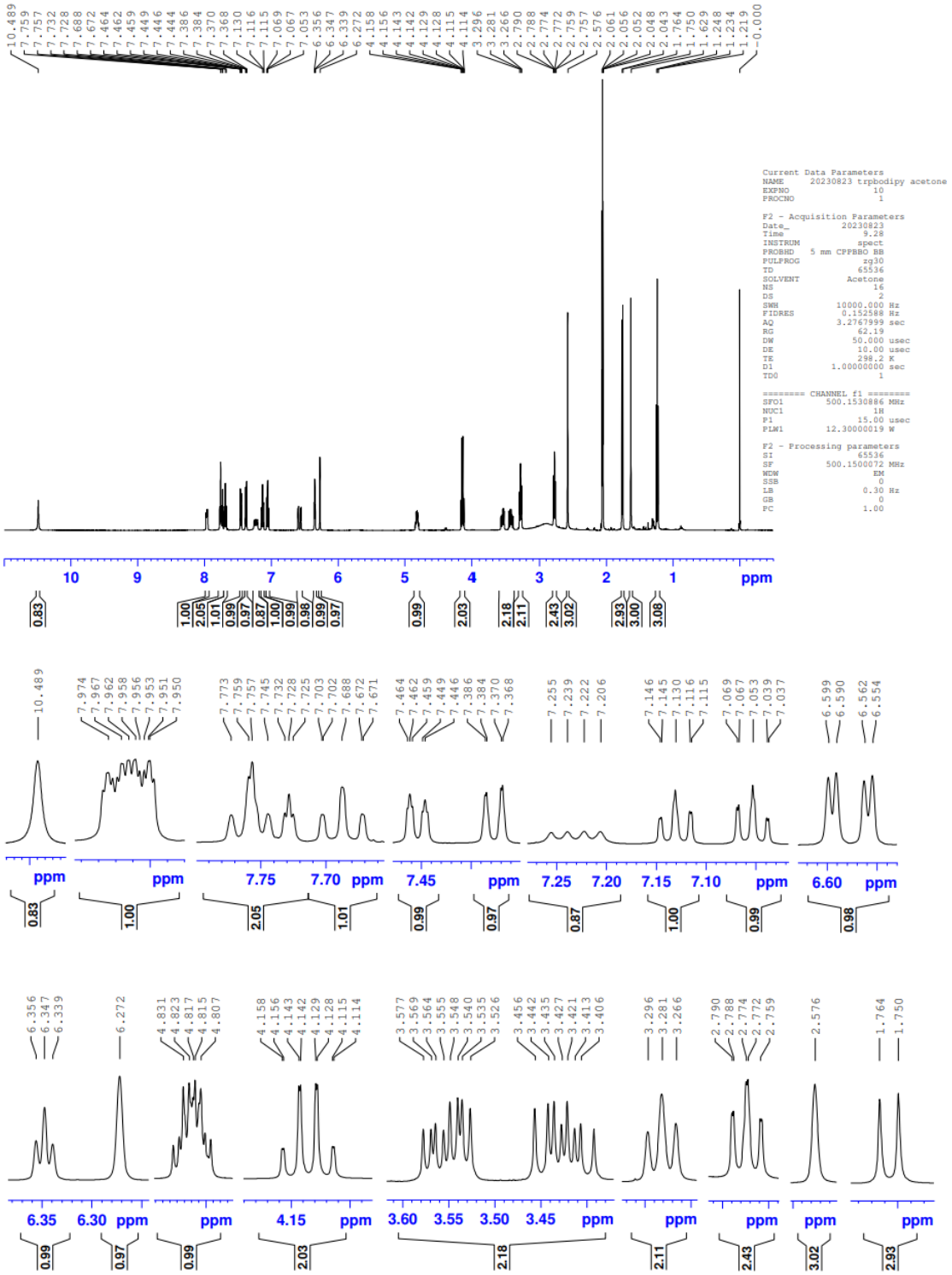

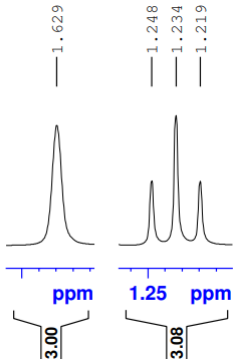

^{13}C-NMR, acetone-d6 (206.17, 29.84 ppm)

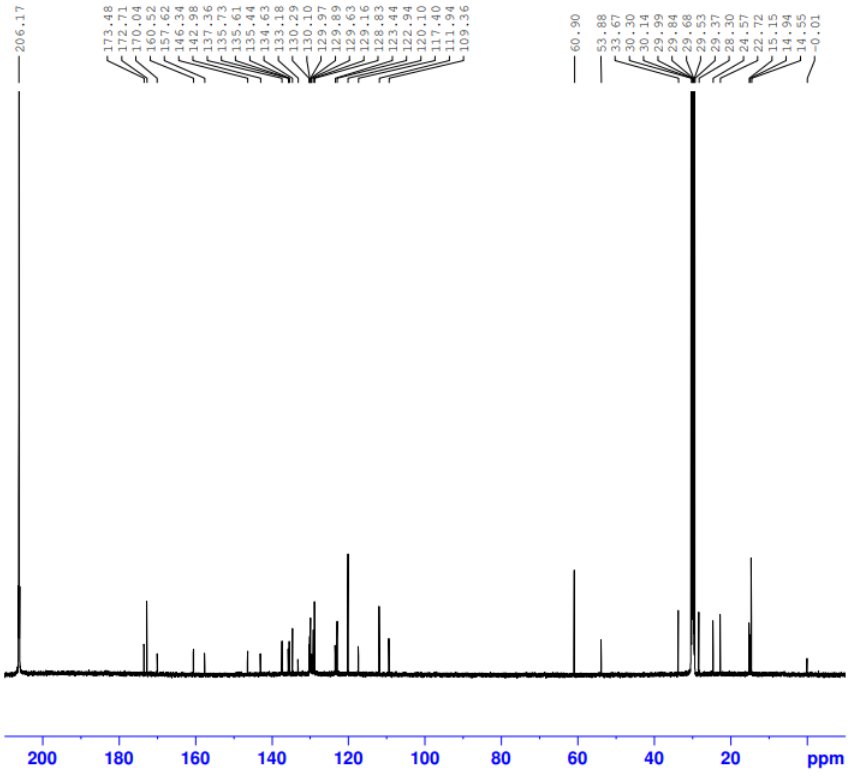


```
Current Data Parameters
NAME      20230823 trpbodipy13c acetone
EXPNO                 10
PROCNO                 1

F2 - Acquisition Parameters
Date_              20230823
Time                 10.30
INSTRUM              spect
PROBHD   5 mm CPPBBO BB
PULPROG            zgpg30
TD                  65536
SOLVENT           Acetone
NS                   1024
DS                      4
SWH              29761.904 Hz
FIDRES           0.454131 Hz
AQ               1.1010048 sec
RG                  197.07
DW                 16.800 usec
DE                 18.00 usec
TE                 298.2 K
D1              2.00000000 sec
D11             0.03000000 sec
TD0                     1

======== CHANNEL f1 ========
SFO1         125.7753932 MHz
NUC1               13C
P1                 10.00 usec
PLW1         77.00000000 W

======== CHANNEL f2 ========
SFO2         500.1520006 MHz
NUC2               1H
CPDPRG[2         waltz16
PCPD2              80.00 usec
PLW2         12.30000019 W
PLW12         0.43241999 W
PLW13         0.27675000 W

F2 - Processing parameters
SI                 32768
SF           125.7627058 MHz
WDW                  EM
SSB                   0
LB                 1.00 Hz
GB                    0
PC                 1.40
```

tert-butyl ((1r,4r)-4-aminocyclohexyl)carbamate, (6)

^{1}H-NMR, $CDCl_3$ (7.26 ppm)

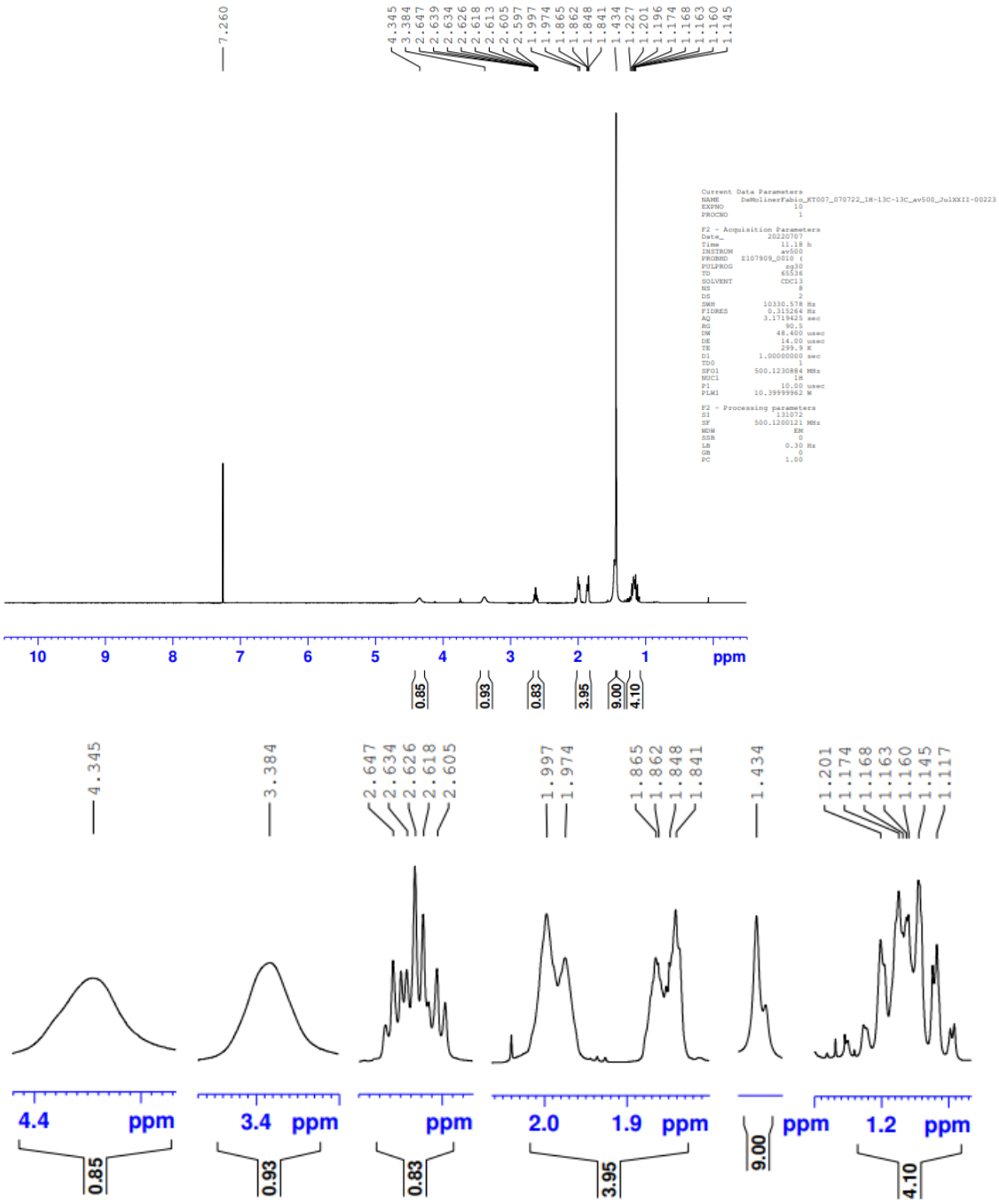

^{13}C-NMR, $CDCl_3$ (77.02 ppm)

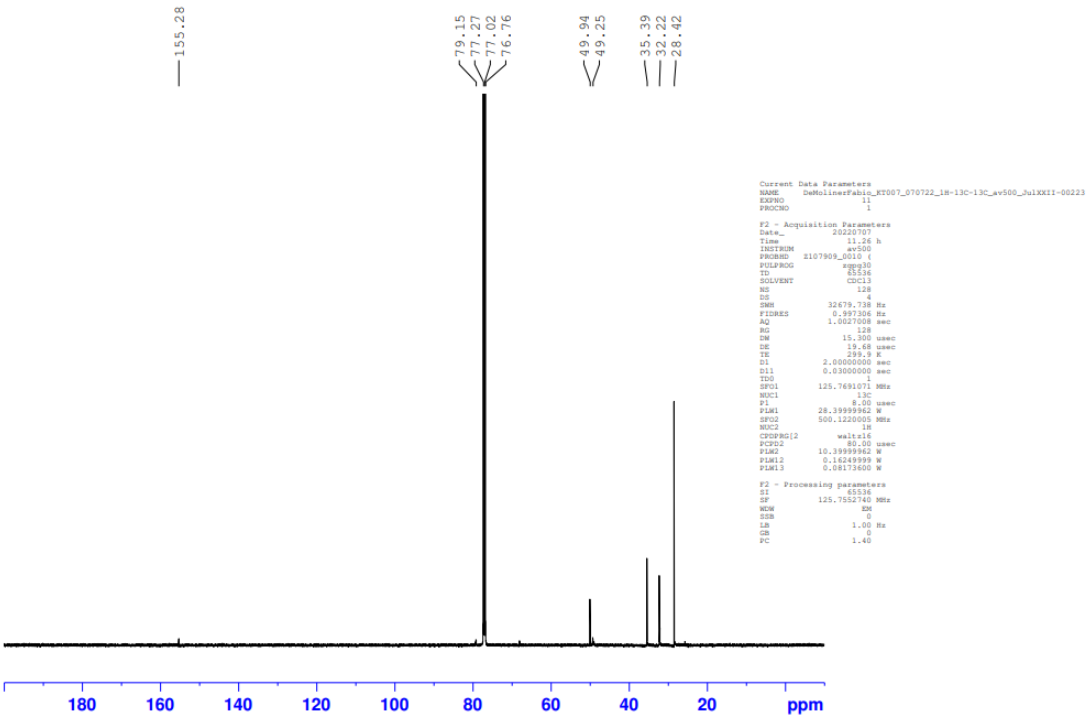

***tert*-butyl ((1*r*,4*r*)-4-(2-((*E*)-3-(1-(2,5-dimethylfuran-3-yl)-2-methylpropylidene)-2,5-dioxo-4-(propan-2-ylidene)pyrrolidin-1-yl)acetamido)cyclohexyl)carbamate, (7)**

^{1}H-NMR, $CDCl_3$ (7.27 ppm)

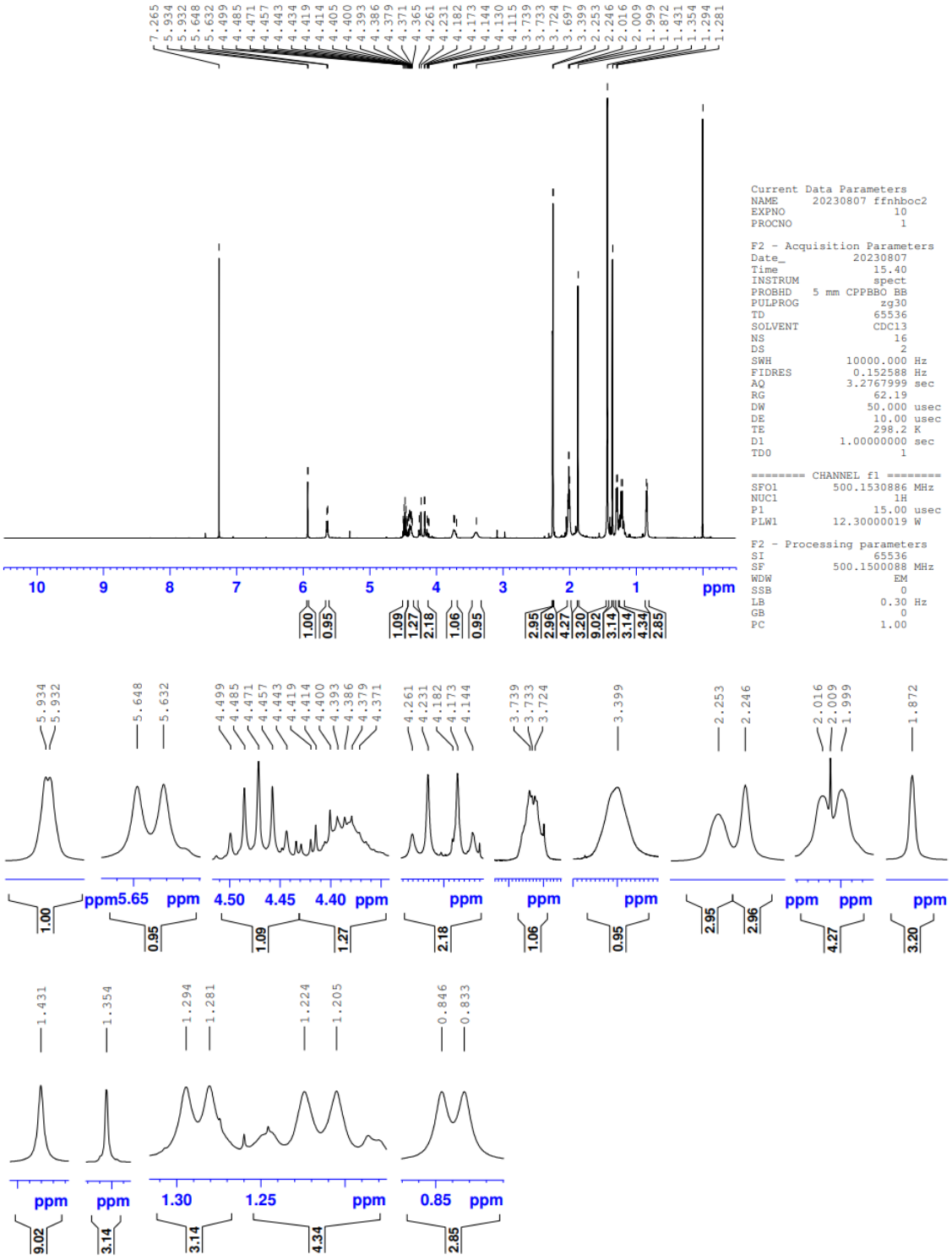

^{13}C-NMR, $CDCl_3$ (77.03 ppm)

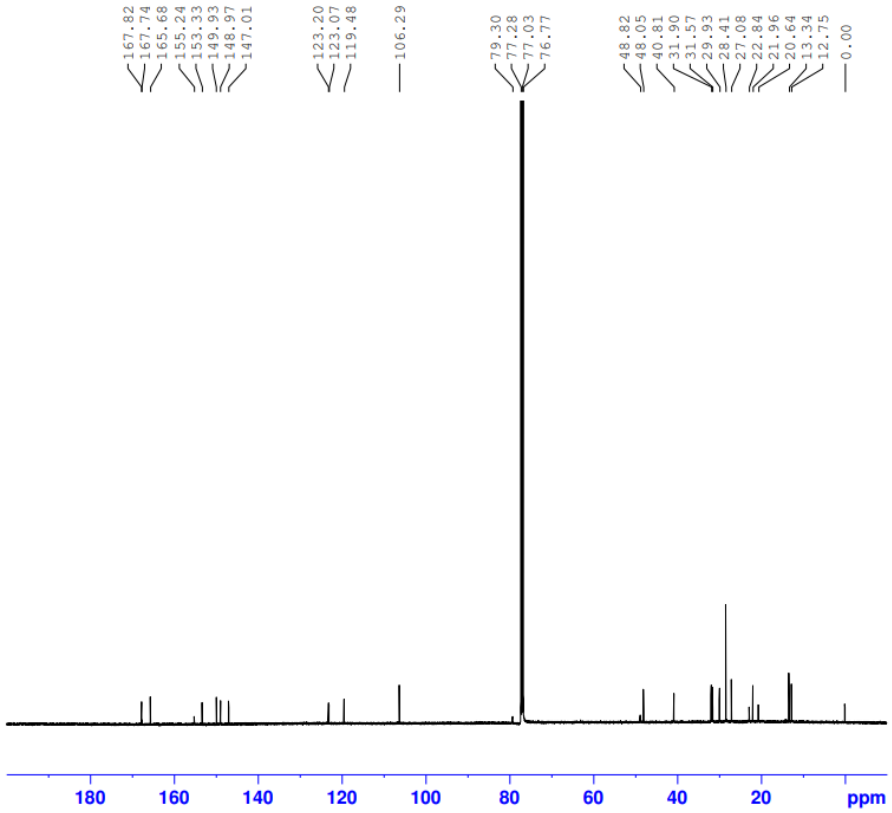


```
Current Data Parameters
NAME      20230807 ffnhboc 13c
EXPNO                      10
PROCNO                      1

F2 - Acquisition Parameters
Date_              20230807
Time                  17.43
INSTRUM               spect
PROBHD   5 mm CPPBBO BB
PULPROG             zgpg30
TD                   65536
SOLVENT              CDCl3
NS                    1024
DS                       4
SWH              29761.904 Hz
FIDRES           0.454131 Hz
AQ               1.1010048 sec
RG                  197.07
DW                 16.800 usec
DE                 18.00 usec
TE                 298.1 K
D1             2.00000000 sec
D11            0.03000000 sec
TD0                      1

======== CHANNEL f1 ========
SFO1          125.7753932 MHz
NUC1                   13C
P1                   10.00 usec
PLW1          77.00000000 W

======== CHANNEL f2 ========
SFO2          500.1520006 MHz
NUC2                   1H
CPDPRG[2            waltz16
PCPD2                80.00 usec
PLW2          12.30000019 W
PLW12          0.43241999 W
PLW13          0.27675000 W

F2 - Processing parameters
SI                    32768
SF           125.7628173 MHz
WDW                     EM
SSB                      0
LB                    1.00 Hz
GB                       0
PC                    1.40
```

3-(5,5-difluoro-10-(3-iodophenyl)-7,9-dimethyl-5H-4λ4,5λ4-dipyrrolo[1,2-c:2',1'-f][1,3,2]diazaborinin-3-yl)propanoic acid, (9)

^{1}H-NMR, $CDCl_3$ (7.26 ppm), residual DCM (5.30 ppm), and silicone grease (0.07 ppm)

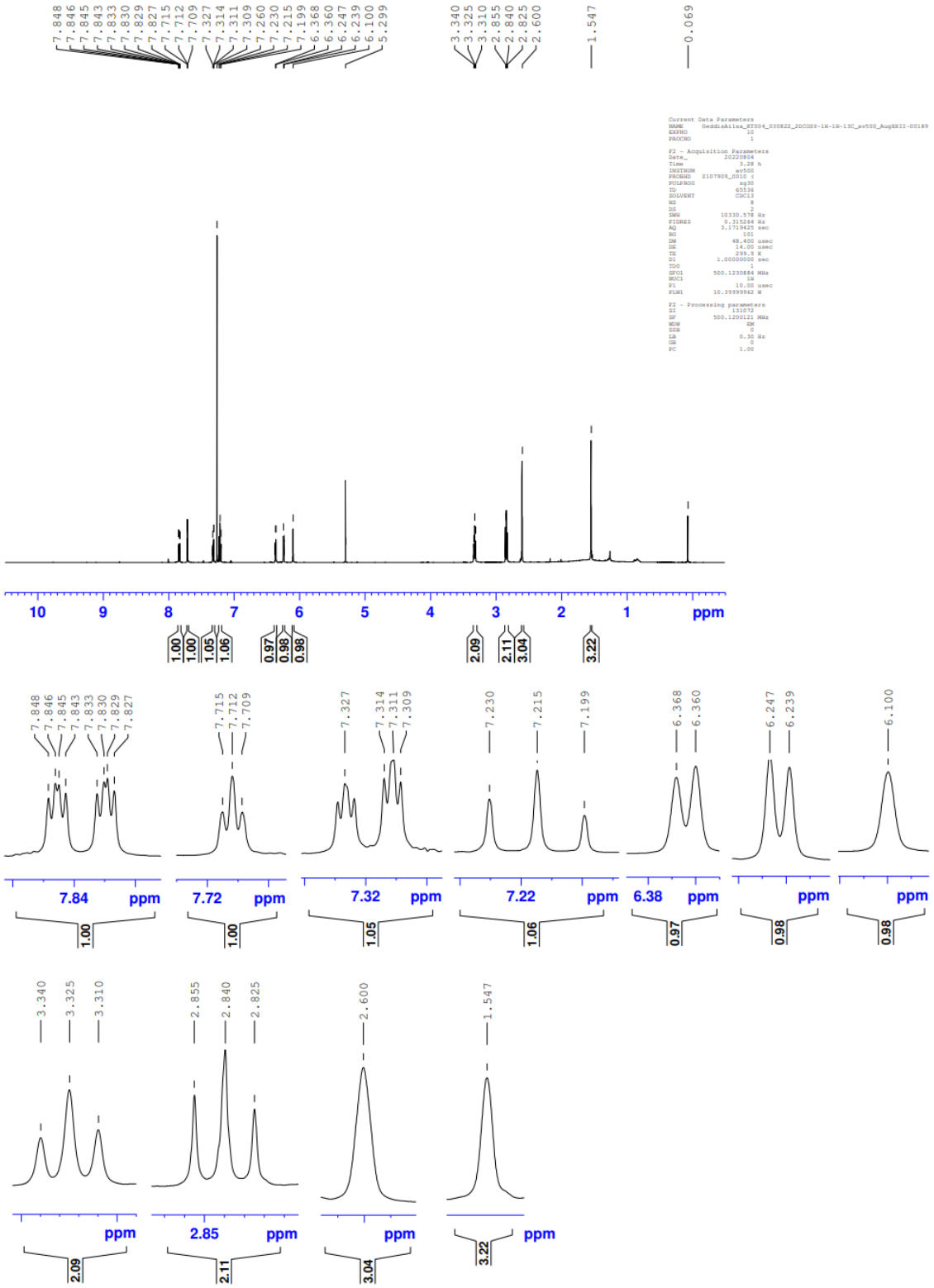

^{13}C-NMR, $CDCl_3$ (77.01 ppm), traces of residual DCM (53.42 ppm), and silicone grease (1.02 ppm)

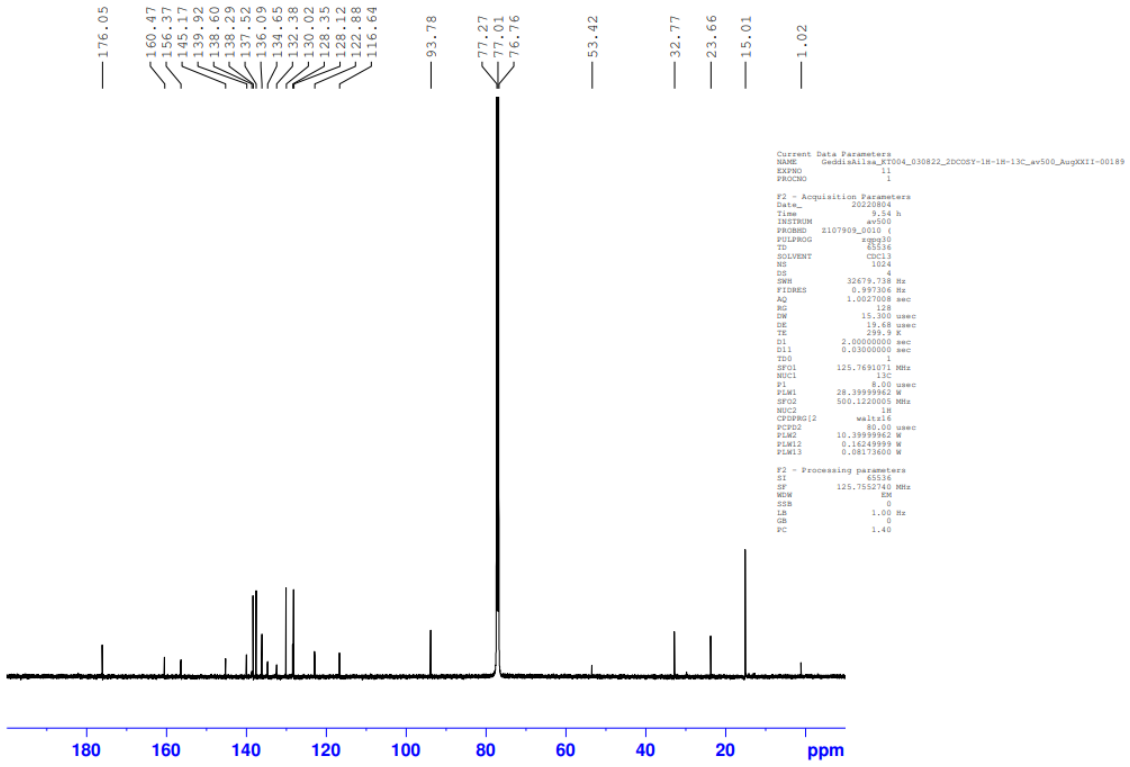

2,5-dioxopyrrolidin-1-yl 3-(5,5-difluoro-10-(3-iodophenyl)-7,9-dimethyl-5H-4λ4,5λ4-dipyrrolo[1,2-c:2',1'-f][1,3,2]diazaborinin-3-yl)propanoate, (10)

^{1}H-NMR, $CDCl_3$ (7.26 ppm), residual DCM (5.30 ppm)

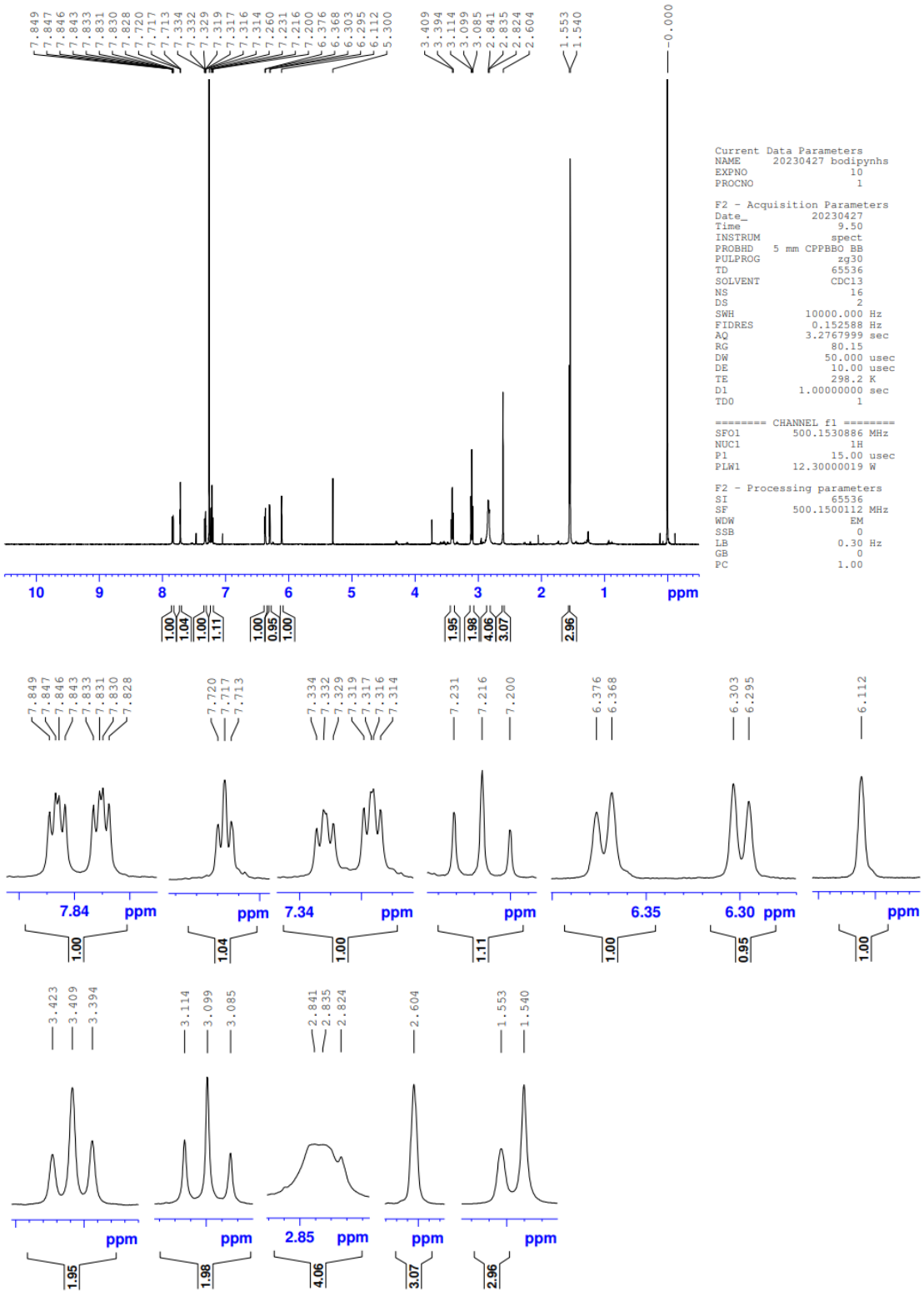

^{13}C-NMR, $CDCl_3$ (77.02 ppm)

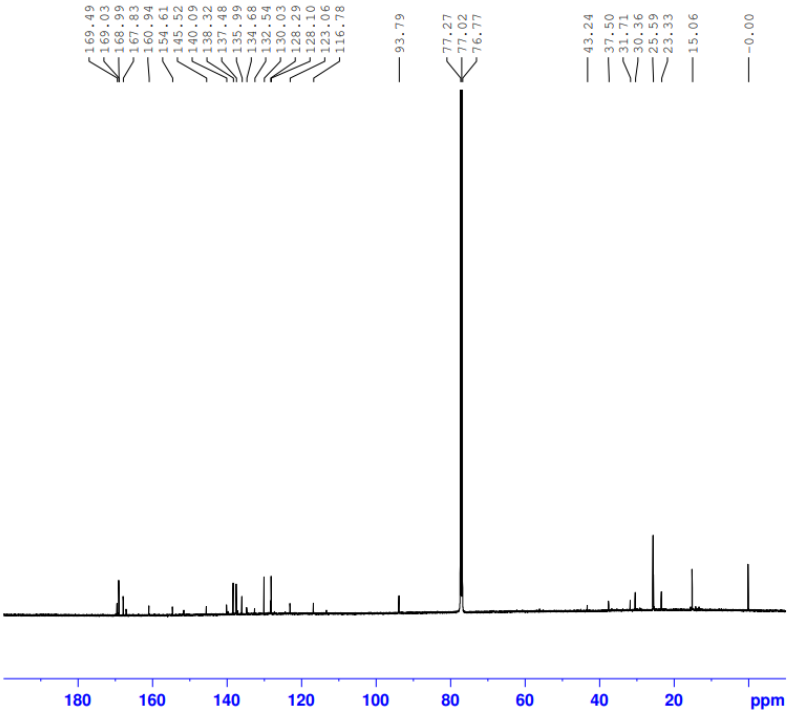


```
Current Data Parameters
NAME      20230803 bodipynhs13c
EXPNO                        10
PROCNO                        1

F2 - Acquisition Parameters
Date_              20230804
Time                   1.44
INSTRUM               spect
PROBHD    5 mm CPPBBO BB
PULPROG            zgpg30
TD                  65536
SOLVENT             CDCl3
NS                   4096
DS                      4
SWH             29761.904 Hz
FIDRES          0.454131 Hz
AQ              1.1010048 sec
RG                 197.07
DW                 16.800 usec
DE                 18.00 usec
TE                 298.1 K
D1              2.00000000 sec
D11             0.03000000 sec
TD0                     1

======== CHANNEL f1 ========
SFO1          125.7753932 MHz
NUC1                    13C
P1                  10.00 usec
PLW1          77.00000000 W

======== CHANNEL f2 ========
SFO2          500.1520006 MHz
NUC2                    1H
CPDPRG[2          waltz16
PCPD2               80.00 usec
PLW2          12.30000019 W
PLW12          0.43241999 W
PLW13          0.27675000 W

F2 - Processing parameters
SI                   32768
SF            125.7628179 MHz
WDW                     EM
SSB                      0
LB                    1.00 Hz
GB                       0
PC                    1.40
```

3-(5,5-difluoro-10-(3-iodophenyl)-7,9-dimethyl-5*H*-4λ^4,5λ^4-dipyrrolo[1,2-*c*:2',1'-*f*][1,3,2]diazaborinin-3-yl)-*N*-((1*r*,4*r*)-4-(2-((*E*)-3-(1-(2,5-dimethylfuran-3-yl)-2-methylpropylidene)-2,5-dioxo-4-(propan-2-ylidene)pyrrolidin-1-yl)acetamido)cyclohexyl)propenamide, (11)

^{1}H-NMR, $CDCl_3$ (7.26 ppm)

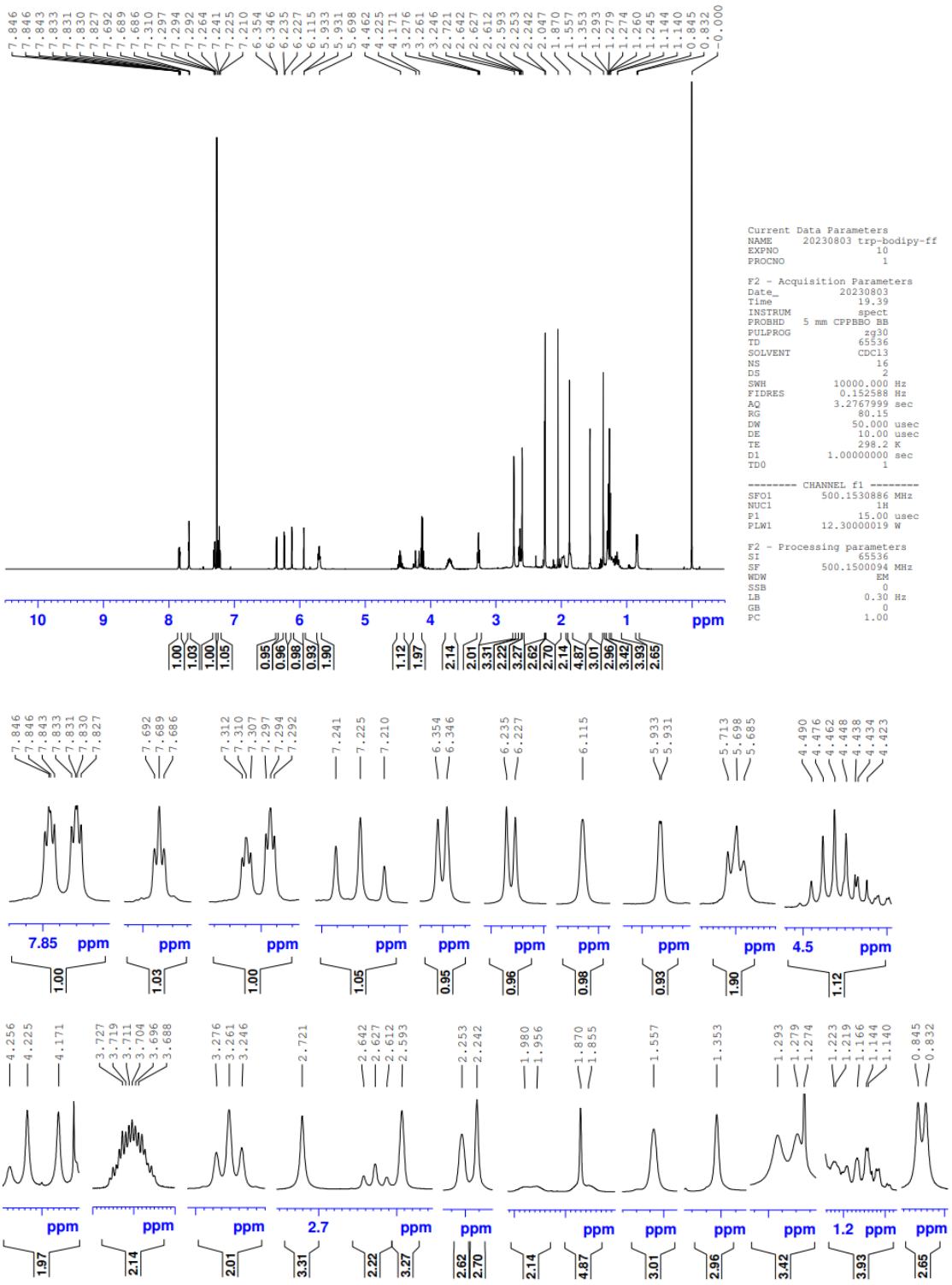

^{13}C-NMR, $CDCl_3$ (77.03 ppm)

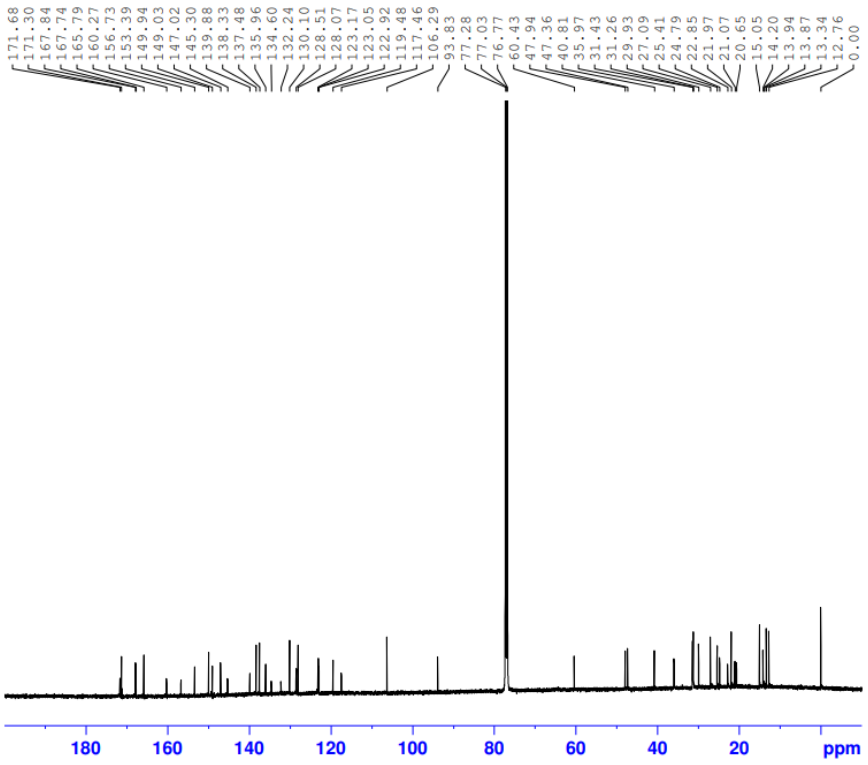


```
Current Data Parameters
NAME      20230803 trpbodipyff13c
EXPNO                          10
PROCNO                          1

F2 - Acquisition Parameters
Date_                    20230804
Time                         7.13
INSTRUM                     spect
PROBHD    5 mm CPPBBO BB
PULPROG                    zgpg30
TD                          65536
SOLVENT                     CDCl3
NS                           4096
DS                              4
SWH                      29761.904 Hz
FIDRES                    0.454131 Hz
AQ                       1.1010048 sec
RG                          197.07
DW                          16.800 usec
DE                          18.00 usec
TE                          298.1 K
D1                     2.00000000 sec
D11                    0.03000000 sec
TD0                             1

======== CHANNEL f1 ========
SFO1                 125.7753932 MHz
NUC1                         13C
P1                          10.00 usec
PLW1                77.00000000 W

======== CHANNEL f2 ========
SFO2                 500.1520006 MHz
NUC2                         1H
CPDPRG[2                 waltz16
PCPD2                       80.00 usec
PLW2                12.30000019 W
PLW12                0.43241999 W
PLW13                0.27675000 W

F2 - Processing parameters
SI                           32768
SF                   125.7628174 MHz
WDW                             EM
SSB                              0
LB                            1.00 Hz
GB                               0
PC                            1.40
```

Trp-BODIPY-FF, (12)

^{1}H-NMR, acetone-d6 (2.05 ppm), trace of residual water (2.92 ppm)

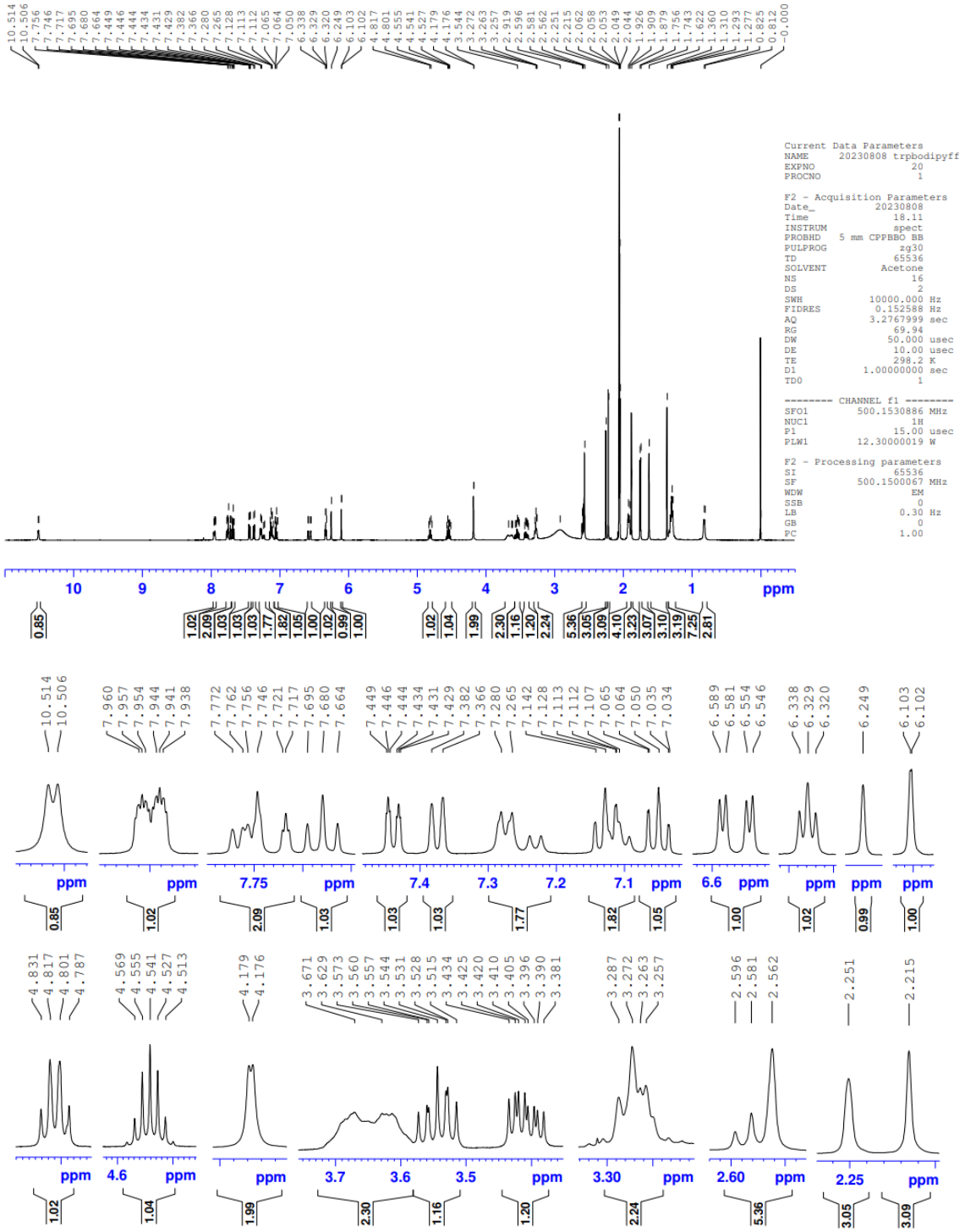

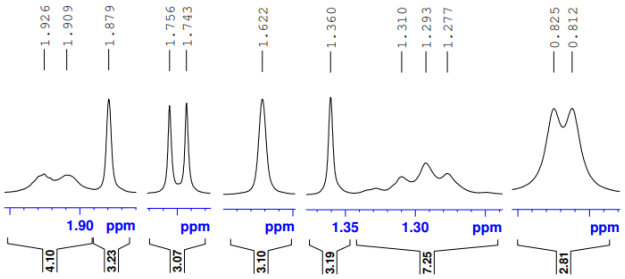

^{13}C-NMR, acetone-d6 (206.19, 29.85 ppm)

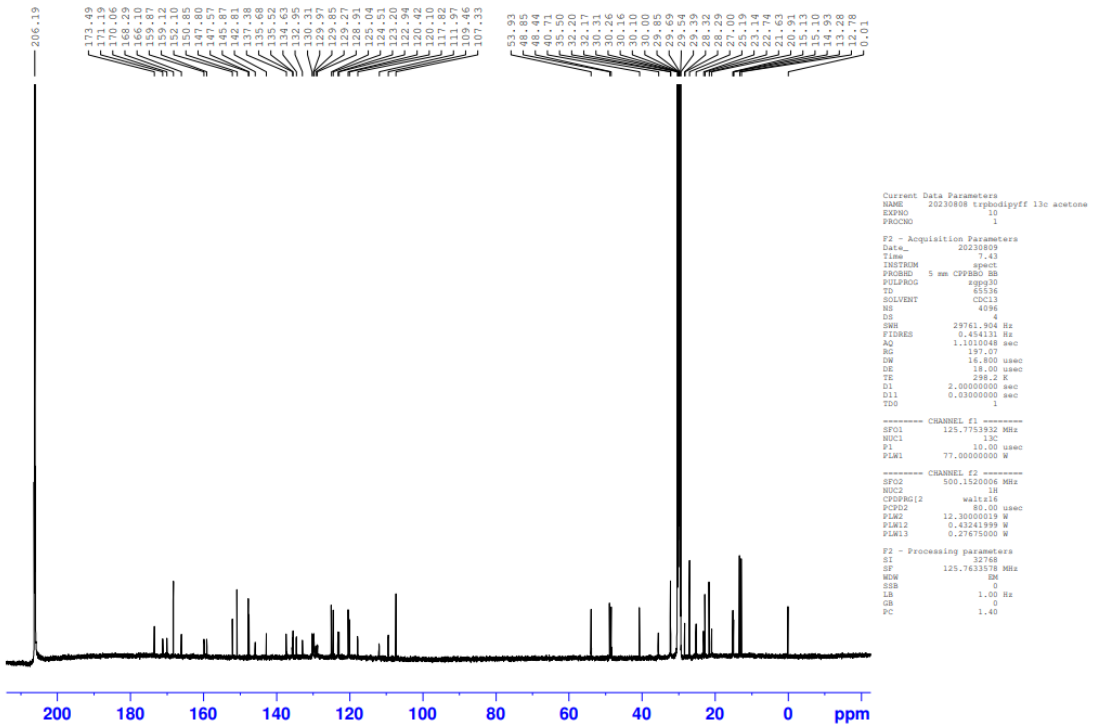

Current Data Parameters
NAME 20230808 trpbodipyff 13c acetone
EXPNO 10
PROCNO 1

F2 - Acquisition Parameters
Date_ 20230809
Time 7.43
INSTRUM spect
PROBHD 5 mm CPPBBO BB
PULPROG zgpg30
TD 65536
SOLVENT CDCl3
NS 4096
DS 4
SWH 29761.904 Hz
FIDRES 0.454131 Hz
AQ 1.1010048 sec
RG 197.07
DW 16.800 usec
DE 18.00 usec
TE 298.2 K
D1 2.00000000 sec
D11 0.03000000 sec
TD0 1

======== CHANNEL f1 ========
SFO1 125.7753932 MHz
NUC1 13C
P1 10.00 usec
PLW1 77.00000000 W

======== CHANNEL f2 ========
SFO2 500.1520006 MHz
NUC2 1H
CPDPRG[2 waltz16
PCPD2 80.00 usec
PLW2 12.30000019 W
PLW12 0.43241999 W
PLW13 0.27675000 W

F2 - Processing parameters
SI 32768
SF 125.7633578 MHz
WDW EM
SSB 0
LB 1.00 Hz
GB 0
PC 1.40

***tert*-butyl (2-(2-hydroxyethoxy)ethyl)carbamate, (13),**

^{1}H-NMR, $CDCl_3$ (7.26 ppm), residual ethyl acetate (4.11, 2.04, 1.24 ppm)

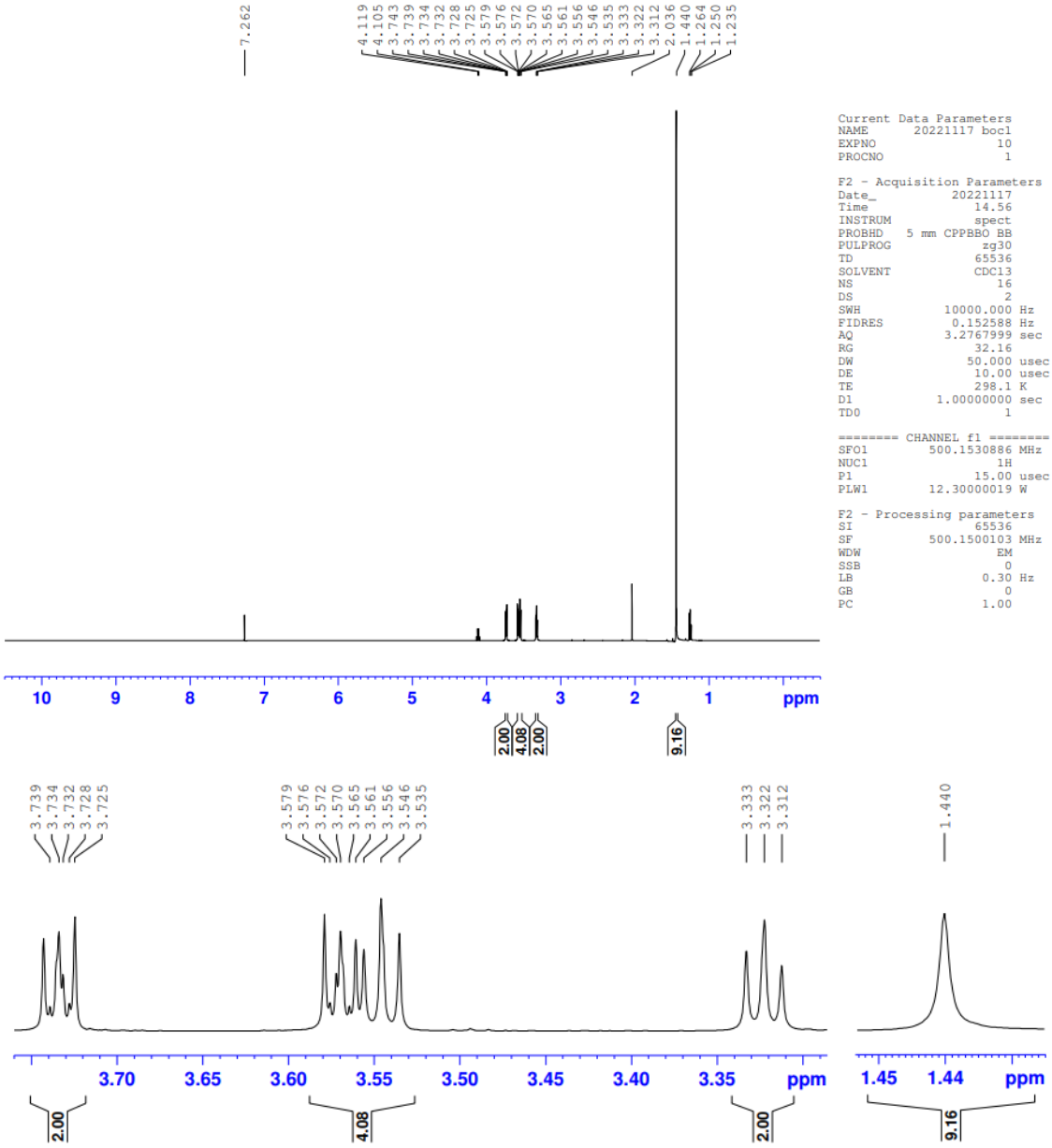

^{13}C-NMR, $CDCl_3$ (77.03 ppm)

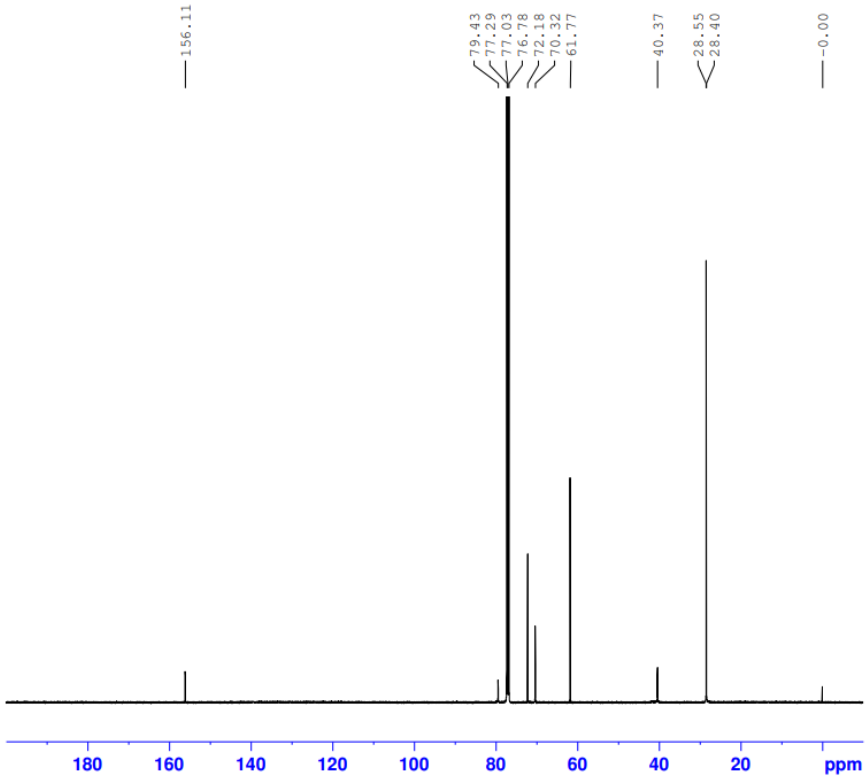


```
Current Data Parameters
NAME      20230809 compl3 13c
EXPNO                  10
PROCNO                  1

F2 - Acquisition Parameters
Date_           20230810
Time              15.27
INSTRUM           spect
PROBHD   5 mm CPPBBO BB
PULPROG          zgpg30
TD                65536
SOLVENT           CDCl3
NS                 1024
DS                    4
SWH           29761.904 Hz
FIDRES         0.454131 Hz
AQ            1.1010048 sec
RG               197.07
DW               16.800 usec
DE               18.00 usec
TE               298.2 K
D1           2.00000000 sec
D11          0.03000000 sec
TD0                   1

======== CHANNEL f1 ========
SFO1         125.7753932 MHz
NUC1                13C
P1                10.00 usec
PLW1        77.00000000 W

======== CHANNEL f2 ========
SFO2         500.1520006 MHz
NUC2                1H
CPDPRG[2         waltz16
PCPD2             80.00 usec
PLW2        12.30000019 W
PLW12        0.43241999 W
PLW13        0.27675000 W

F2 - Processing parameters
SI                32768
SF           125.7628173 MHz
WDW                  EM
SSB                   0
LB                 1.00 Hz
GB                    0
PC                 1.40
```

***tert*-butyl (2-(2-((6-chlorohexyl)oxy)ethoxy)ethyl)carbamate, (<u>14</u>)**

^{1}H-NMR, $CDCl_3$ (7.26 ppm)

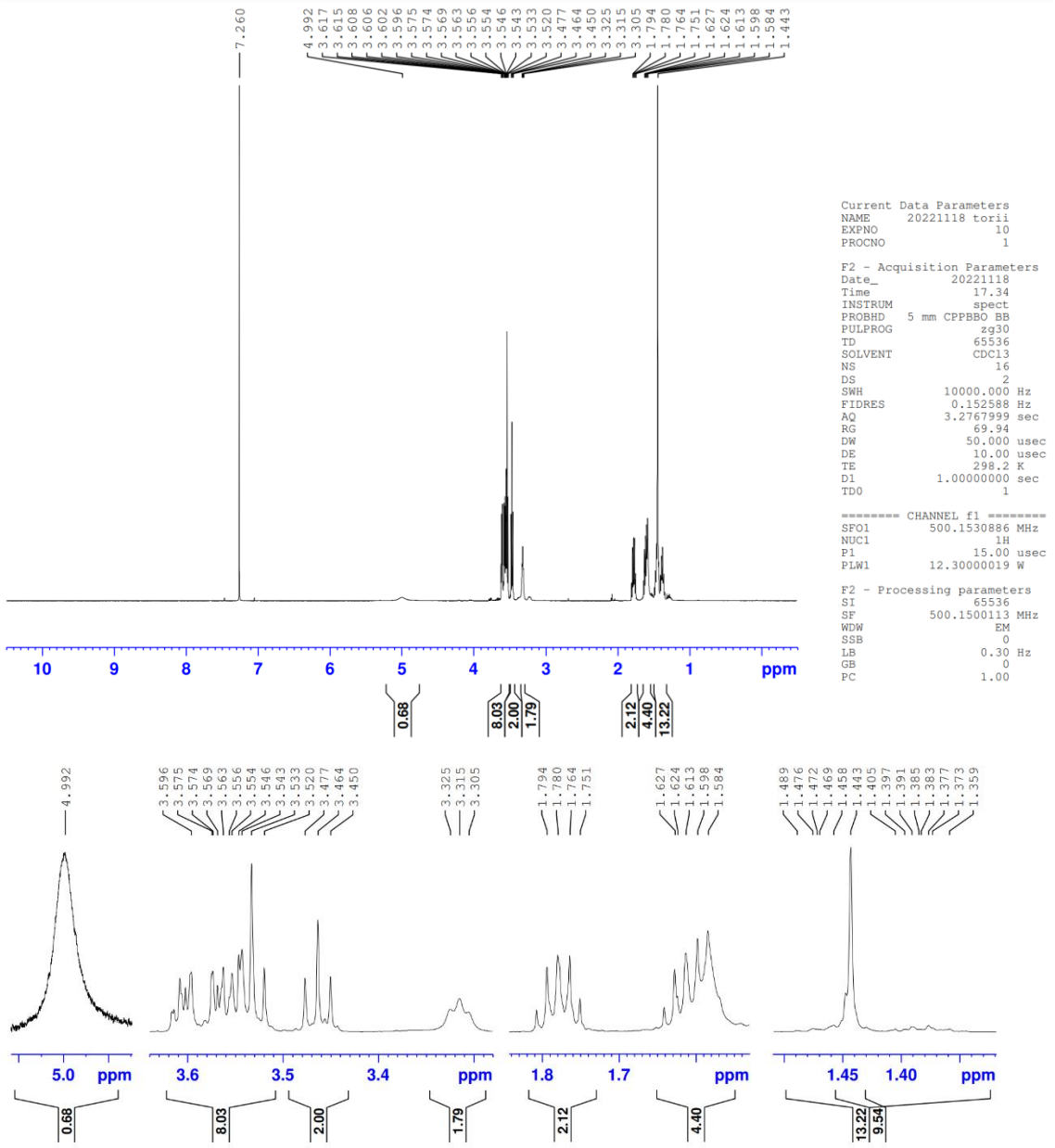


```
Current Data Parameters
NAME      20221118 torii
EXPNO               10
PROCNO               1

F2 - Acquisition Parameters
Date_          20221118
Time              17.34
INSTRUM           spect
PROBHD   5 mm CPPBBO BB
PULPROG            zg30
TD                65536
SOLVENT           CDCl3
NS                   16
DS                    2
SWH           10000.000 Hz
FIDRES        0.152588 Hz
AQ            3.2767999 sec
RG                69.94
DW               50.000 usec
DE               10.00 usec
TE               298.2 K
D1            1.00000000 sec
TD0                  1

======== CHANNEL f1 ========
SFO1        500.1530886 MHz
NUC1               1H
P1               15.00 usec
PLW1        12.30000019 W

F2 - Processing parameters
SI                65536
SF          500.1500113 MHz
WDW                  EM
SSB                   0
LB                 0.30 Hz
GB                    0
PC                 1.00
```

^{13}C-NMR, $CDCl_3$ (77.02 ppm)

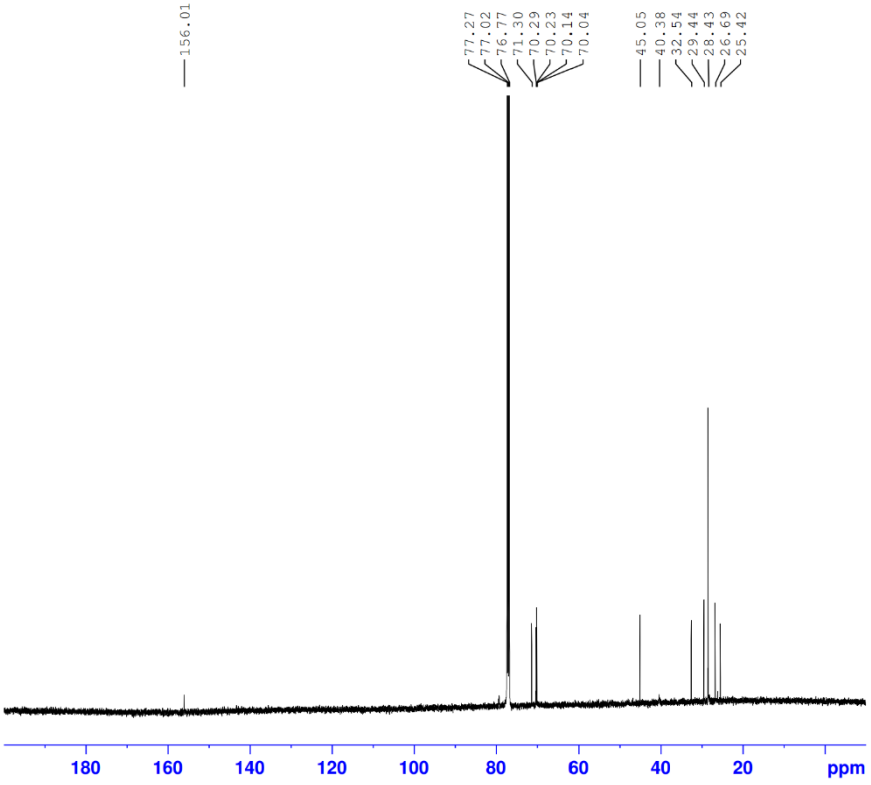


```
Current Data Parameters
NAME      20221118 halo ligand 13c
EXPNO                 10
PROCNO                 1

F2 - Acquisition Parameters
Date_           20221118
Time              19.10
INSTRUM           spect
PROBHD   5 mm CPPBBO BB
PULPROG          zgpg30
TD                65536
SOLVENT           CDCl3
NS                 1024
DS                    4
SWH           29761.904 Hz
FIDRES        0.454131 Hz
AQ            1.1010048 sec
RG               197.07
DW               16.800 usec
DE               18.00 usec
TE               298.1 K
D1            2.00000000 sec
D11           0.03000000 sec
TD0                   1

======== CHANNEL f1 ========
SFO1         125.7753932 MHz
NUC1                13C
P1                10.00 usec
PLW1         77.00000000 W

======== CHANNEL f2 ========
SFO2         500.1520006 MHz
NUC2                1H
CPDPRG[2          waltz16
PCPD2             80.00 usec
PLW2         12.30000019 W
PLW12         0.43241999 W
PLW13         0.27675000 W

F2 - Processing parameters
SI                32768
SF           125.7628175 MHz
WDW                  EM
SSB                   0
LB                 1.00 Hz
GB                    0
PC                 1.40
```

2-(2-((6-chlorohexyl)oxy)ethoxy)ethan-1-amine, (15)

^{1}H-NMR, $CDCl_3$ (7.27 ppm), residual DCM (5.30 ppm)

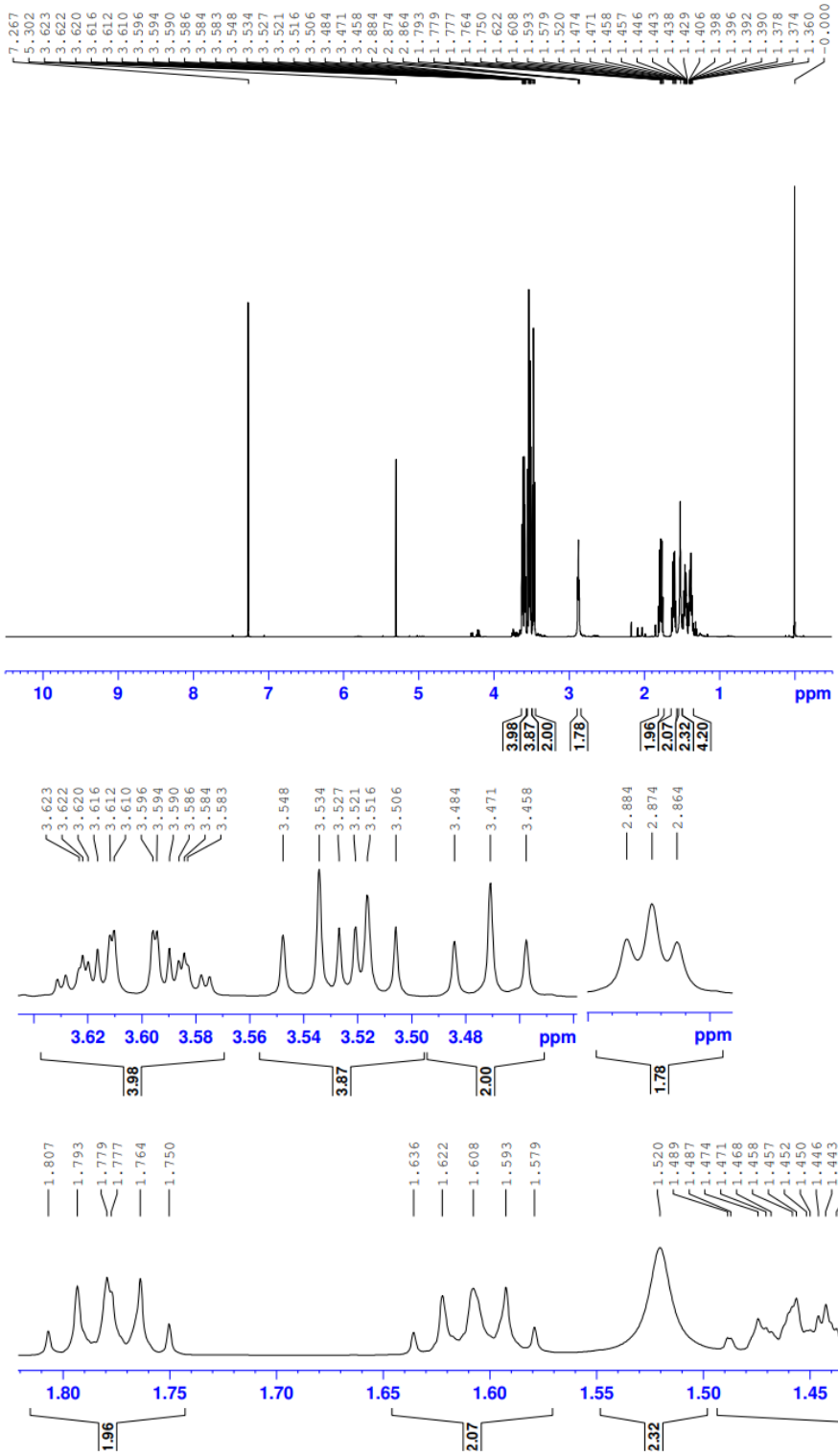

^{13}C-NMR, $CDCl_3$ (77.03 ppm)

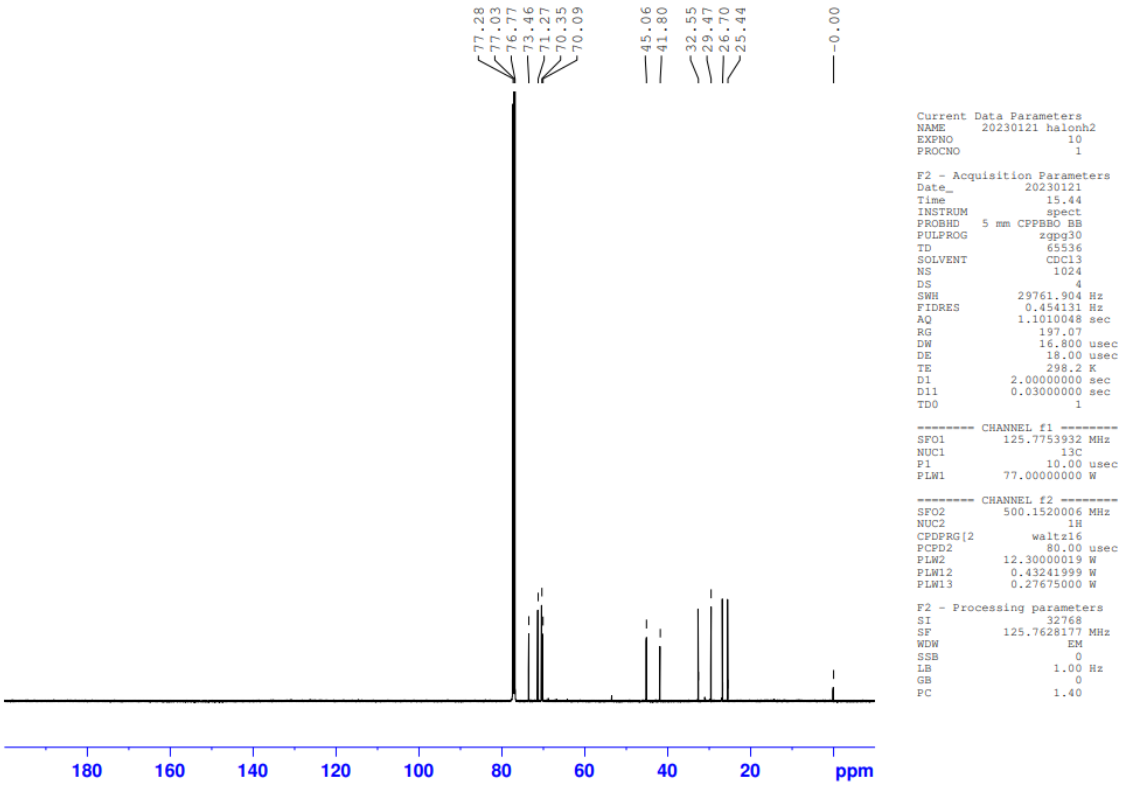

18-chloro-5-oxo-3,9,12-trioxa-6-azaoctadecanoic acid, (16)

^{1}H-NMR, $CDCl_3$ (7.26 ppm) residual ethyl acetate (4.14, 2.05, 1.27 ppm) and acetic acid (2.10 ppm)

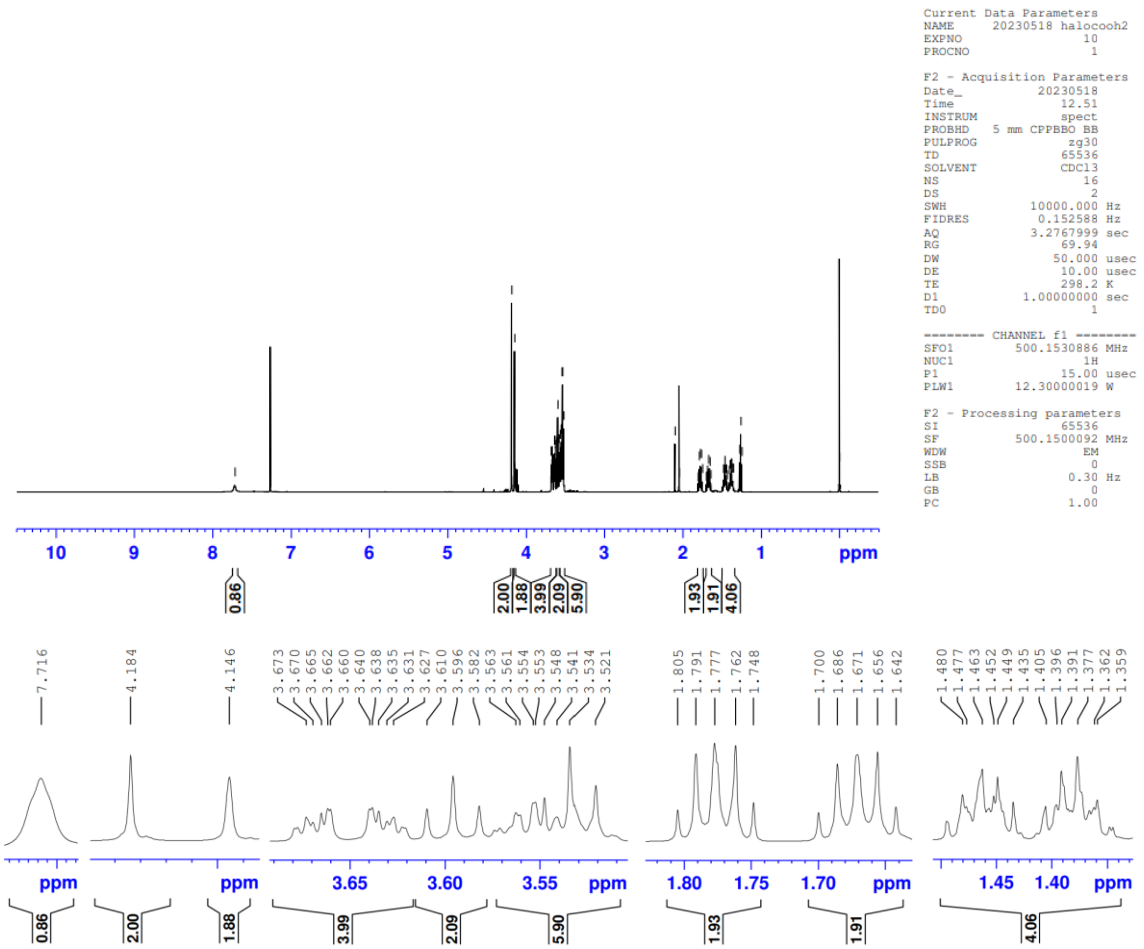

^{13}C-NMR, $CDCl_3$ (77.02 ppm)

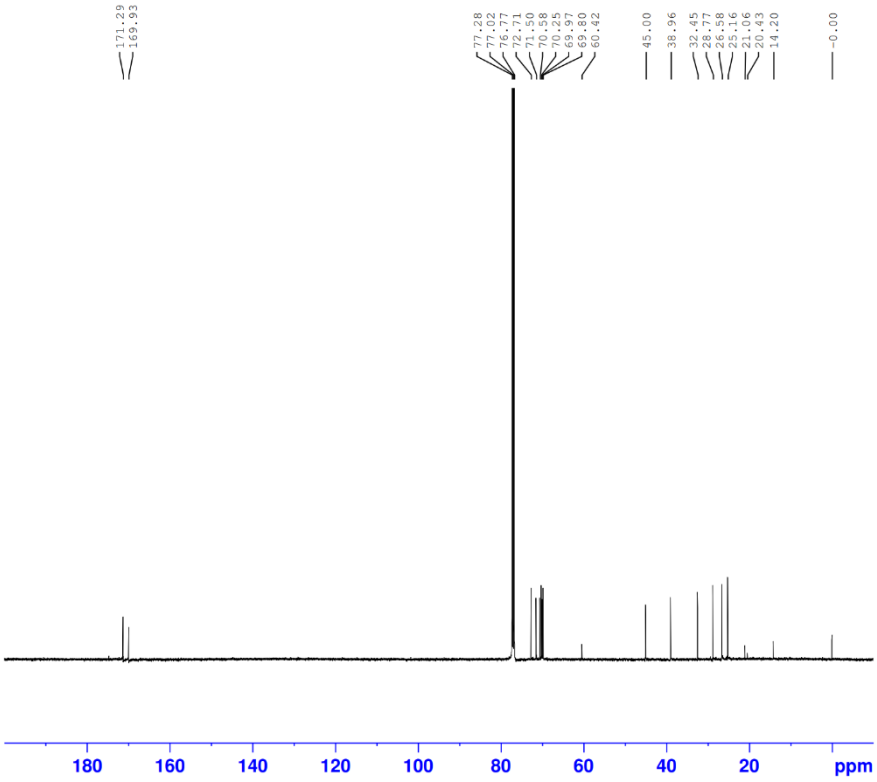


```
Current Data Parameters
NAME      20230518 halocooh2cl3
EXPNO                 10
PROCNO                 1

F2 - Acquisition Parameters
Date_           20230518
Time              13.49
INSTRUM           spect
PROBHD   5 mm CPPBBO BB
PULPROG           zgpg30
TD                65536
SOLVENT           CDCl3
NS                 1024
DS                    4
SWH           29761.904 Hz
FIDRES         0.454131 Hz
AQ             1.1010048 sec
RG               197.07
DW              16.800 usec
DE              18.00 usec
TE              298.2 K
D1            2.00000000 sec
D11           0.03000000 sec
TD0                   1

======== CHANNEL f1 ========
SFO1        125.7753932 MHz
NUC1               13C
P1              10.00 usec
PLW1        77.00000000 W

======== CHANNEL f2 ========
SFO2        500.1520006 MHz
NUC2               1H
CPDPRG[2        waltz16
PCPD2             80.00 usec
PLW2        12.30000019 W
PLW12        0.43241999 W
PLW13        0.27675000 W

F2 - Processing parameters
SI                32768
SF          125.7628176 MHz
WDW                EM
SSB                0
LB              1.00 Hz
GB                 0
PC              1.40
```

2,5-dioxopyrrolidin-1-yl 18-chloro-5-oxo-3,9,12-trioxa-6-azaoctadecanoate, (17)

^{1}H-NMR, $CDCl_3$ (7.26 ppm), residual DCM (5.30 ppm)

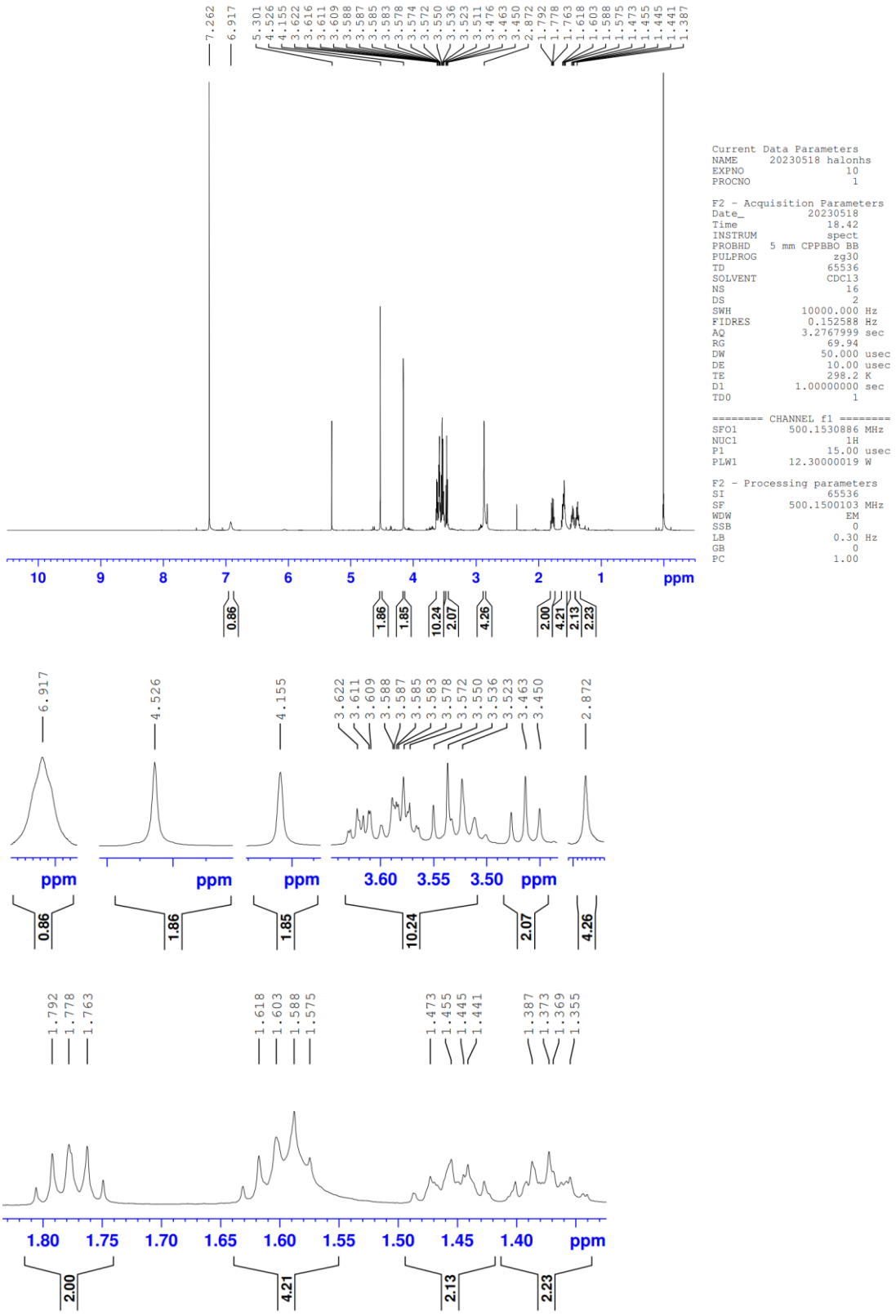

^{13}C-NMR, CDCl3 (77.02 ppm)

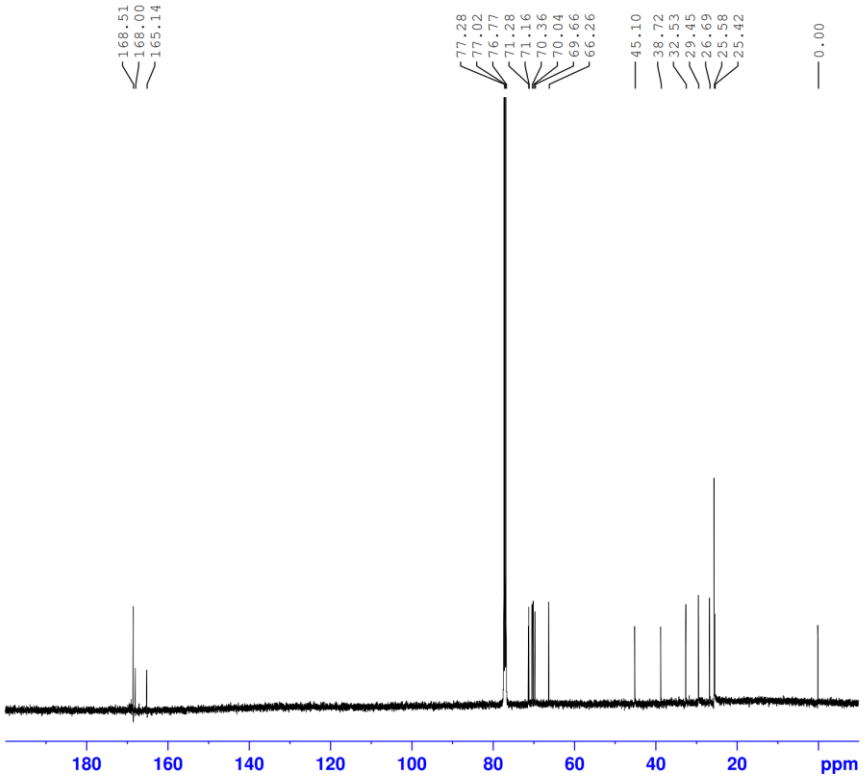


```
Current Data Parameters
NAME      20230519 halonhsc13
EXPNO                   10
PROCNO                   1

F2 - Acquisition Parameters
Date_           20230519
Time              20.21
INSTRUM           spect
PROBHD    5 mm CPPBBO BB
PULPROG          zgpg30
TD                65536
SOLVENT           CDCl3
NS                 1024
DS                    4
SWH           29761.904 Hz
FIDRES         0.454131 Hz
AQ            1.1010048 sec
RG               197.07
DW               16.800 usec
DE               18.00 usec
TE               298.2 K
D1            2.00000000 sec
D11           0.03000000 sec
TD0                   1

======== CHANNEL f1 ========
SFO1         125.7753932 MHz
NUC1              13C
P1               10.00 usec
PLW1          77.00000000 W

======== CHANNEL f2 ========
SFO2         500.1520006 MHz
NUC2              1H
CPDPRG[2        waltz16
PCPD2            80.00 usec
PLW2          12.30000019 W
PLW12          0.43241999 W
PLW13          0.27675000 W

F2 - Processing parameters
SI                32768
SF           125.7628173 MHz
WDW                EM
SSB                 0
LB               1.00 Hz
GB                  0
PC                1.40
```

(*S*)-2-((((9*H*-fluoren-9-yl)methoxy)carbonyl)amino)-3-(2-(3-(7-(3-(((1*r*,4*r*)-4-(2-((*E*)-3-(1-(2,5-dimethylfuran-3-yl)-2-methylpropylidene)-2,5-dioxo-4-(propan-2-ylidene)pyrrolidin-1-yl)acetamido)cyclohexyl)amino)-3-oxopropyl)-5,5-difluoro-1,3-dimethyl-5*H*-4λ^4,5λ^4-dipyrrolo[1,2-*c*:2',1'-*f*][1,3,2]diazaborinin-10-yl)phenyl)-1*H*-indol-3-yl)propanoic acid, (<u>18</u>)

^{1}H-NMR, acetone-d6 (2.05 ppm), residual water (2.85 ppm)

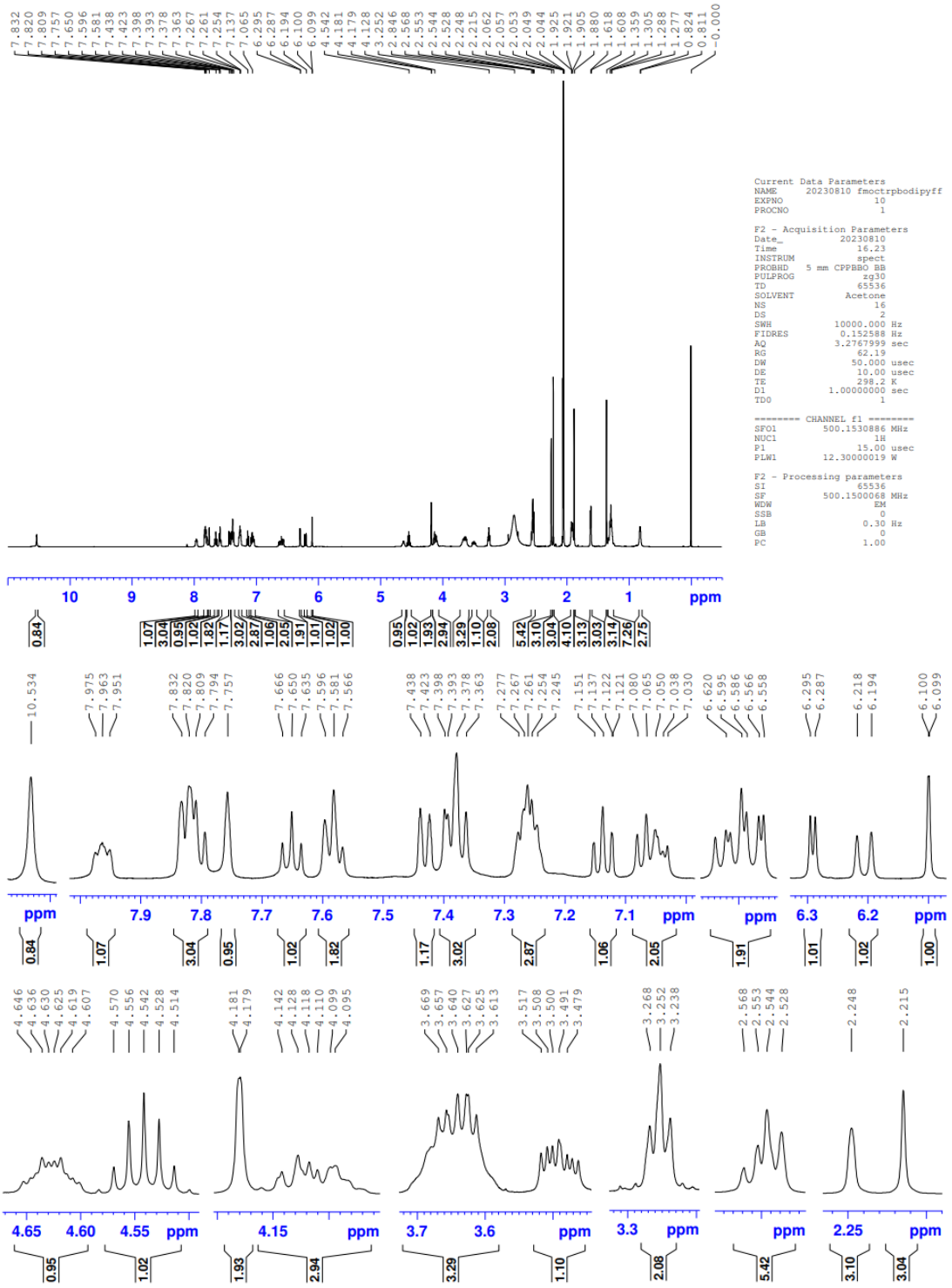

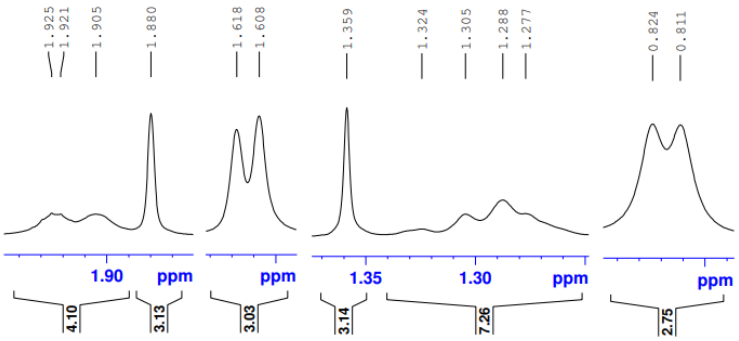

^{13}C-NMR, acetone-d6 (206.18, 29.84 ppm)

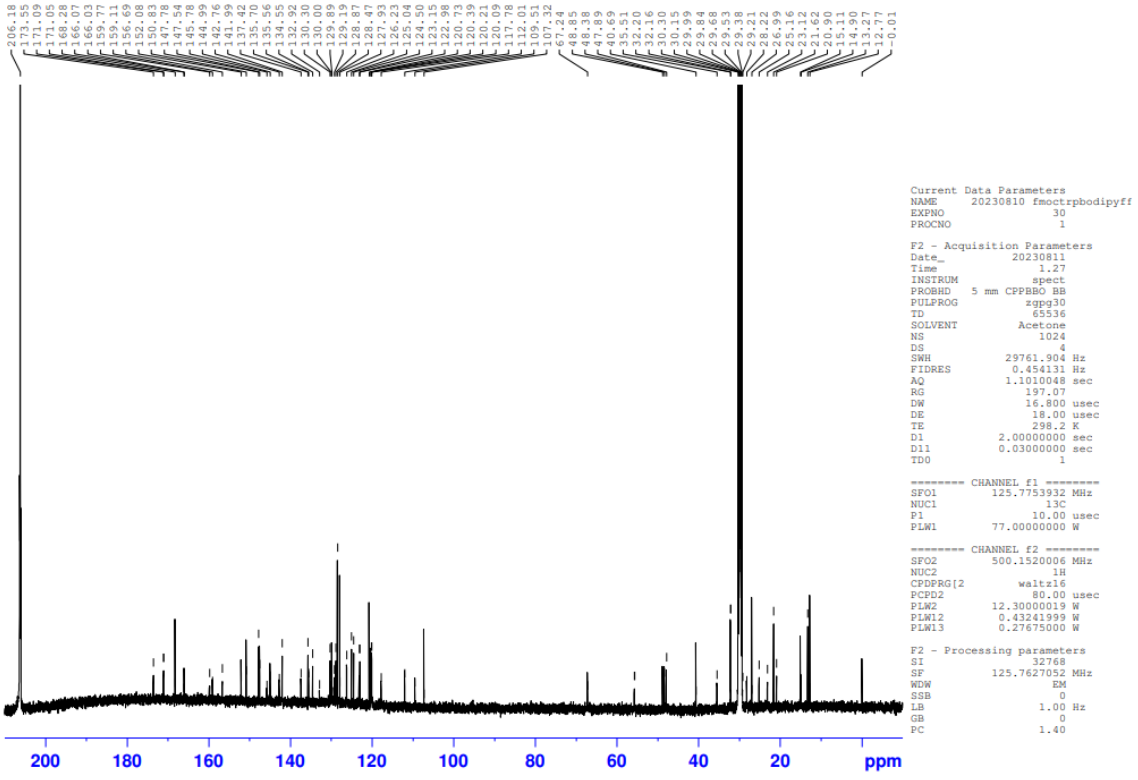

HTL-Trp-BODIPY-FF, (19)

^{1}H-NMR, acetone-d6 (2.05 ppm), residual water (2.83 ppm)

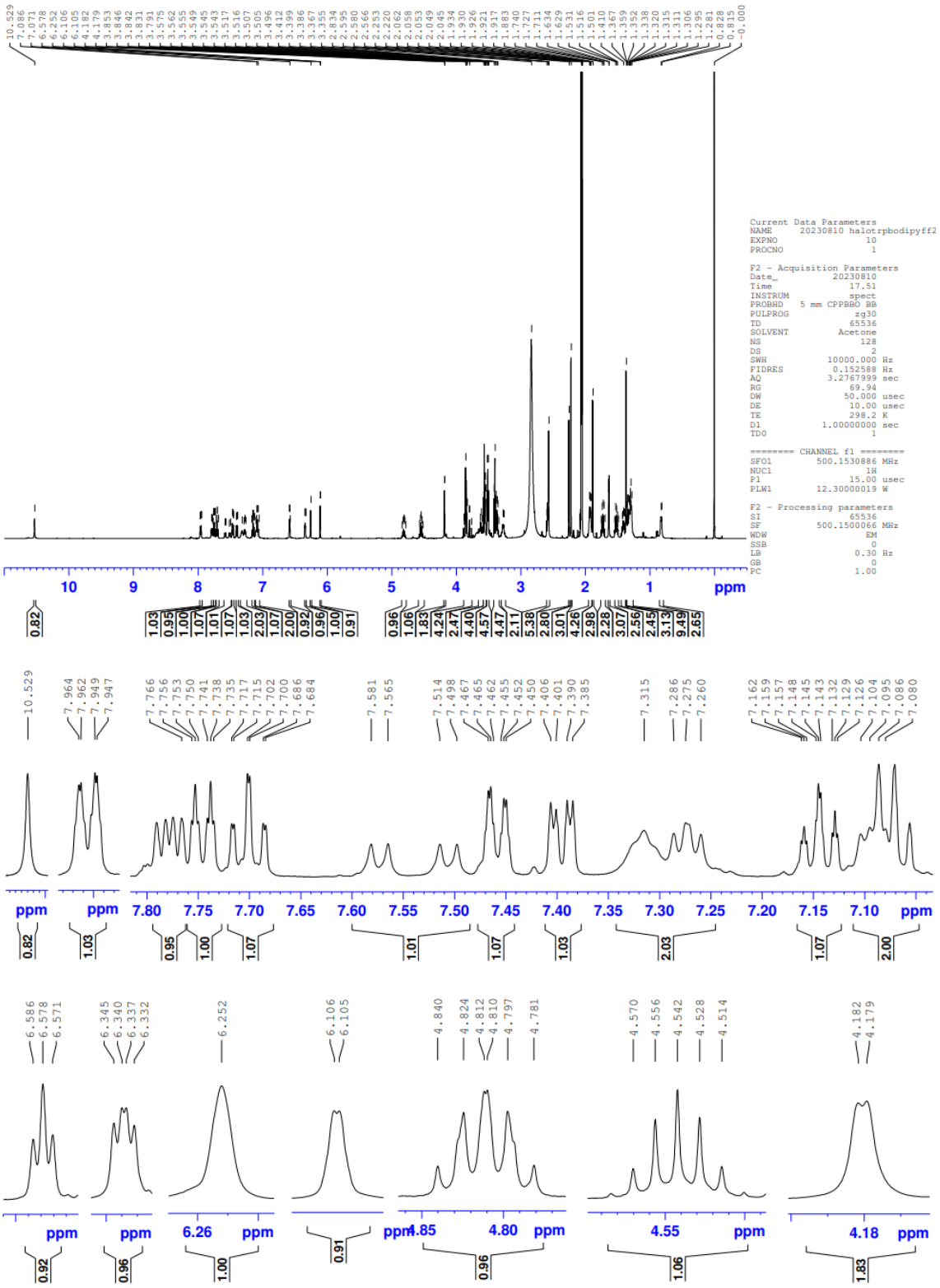

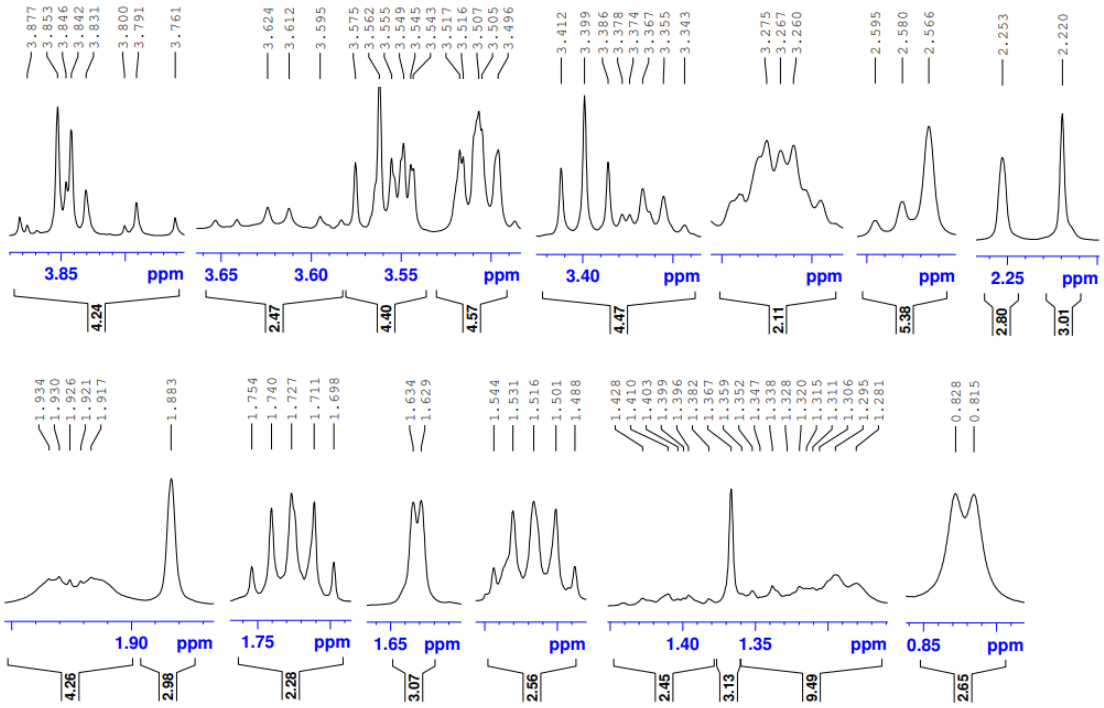

^{13}C-NMR, acetone-d6 (206.18, 29.83 ppm)

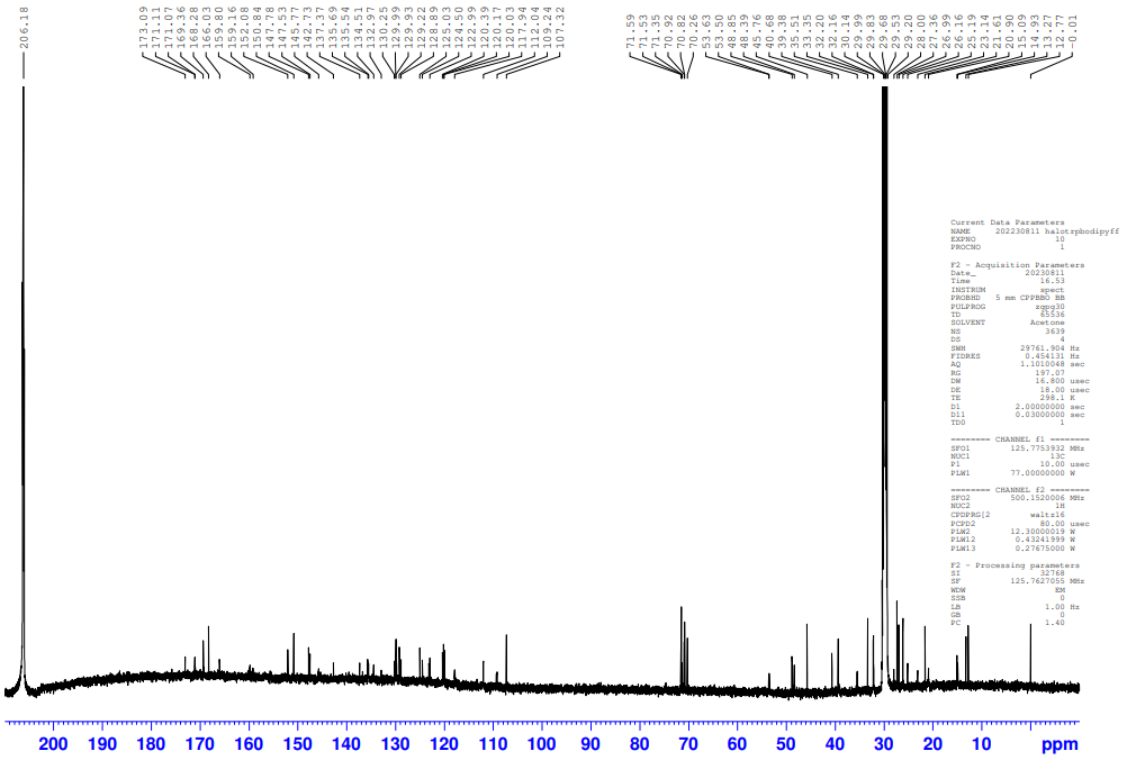

7. References

S1 D. Magde, R. Wong and P. G. Seybold, *Photochem. Photobiol.*, 2002, **75**, 327–334.

S2 L. Casimiro, L. Andreoni, J. Groppi, A. Credi, R. Métivier and S. Silvi, *Photochem. Photobiol. Sci.*, 2022, **21**, 825–833.

S3 K. Torii, Y. Hori and K. Kikuchi, *Anal. Chem.*, 2023, **95**, 8834–8841.

S4 S. Hirayama, Y. Hori, Z. Benedek, T. Suzuki and K. Kikuchi, *Nat. Chem. Biol.*, 2016, **12**, 853–859.

S5 Y. Kamikawa, Y. Hori, K. Yamashita, L. Jin, S. Hirayama, D. M. Standley and K. Kikuchi, *Chem. Sci.*, 2015, **7**, 308–314.

S6 Y. Matsui, Y. Funato, H. Imamura, H. Miki, S. Mizukami and K. Kikuchi, *Chem. Sci.*, 2017, **8**, 8255–8264.

S7 T. Kowada, K. Arai, A. Yoshimura, T. Matsui, K. Kikuchi and S. Mizukami, *Angew. Chem. Int. Ed.*, 2021, **60**, 11378–11383.

S8 S. Mizukami, S. Watanabe, Y. Hori and K. Kikuchi, *J. Am. Chem. Soc.*, 2009, **131**, 5016–5017.

S9 L. Mendive-Tapia, D. Mendive-Tapia, C. Zhao, D. Gordon, S. Benson, M. J. Bromley, W. Wang, J. Wu, A. Kopp, L. Ackermann and M. Vendrell, *Angew. Chem. Int. Ed.*, 2022, **61**, e202117218.

S10 L. Mendive-Tapia, C. Zhao, A. R. Akram, S. Preciado, F. Albericio, M. Lee, A. Serrels, N. Kielland, N. D. Read, R. Lavilla and M. Vendrell, *Nat. Commun.*, 2016, **7**, 10940.

S11 A. Loudet and K. Burgess, *Chem. Rev.*, 2007, **107**, 4891–4932.

S12 N.-S. Cheng, *Ind. Eng. Chem. Res.*, 2008, **47**, 3285–3288.

S13 S. Duwé, E. De Zitter, V. Gielen, B. Moeyaert, W. Vandenberg, T. Grotjohann, K. Clays, S. Jakobs, L. Van Meervelt and P. Dedecker, *ACS Nano*, 2015, **9**, 9528–9541.

S14 R. Ando, H. Mizuno and A. Miyawaki, *Science*, 2004, **306**, 1370–1373.

S15 T. Konen, D. Stumpf, T. Grotjohann, I. Jansen, M. Bossi, M. Weber, N. Jensen, S. W. Hell and S. Jakobs, *ACS Nano*, 2021, **15**, 9509–9521.

S16 G. R. Fulmer, A. J. M. Miller, N. H. Sherden, H. E. Gottlieb, A. Nudelman, B. M. Stoltz, J. E. Bercaw and K. I. Goldberg, *Organometallics*, 2010, **29**, 2176–2179.